NUREG/CR-3788
Vol. 1

Structural Integrity of Light Water Reactor Pressure Boundary Components

Four-Year Plan 1984 - 1988

Materials Engineering Associates, Inc.

Prepared for
U.S. Nuclear Regulatory
Commission

GPO Printed copy price: $4.75

NUREG/CR-3788
MEA-2047
R5, RF
Vol. 1

Structural Integrity of Light Water Reactor Pressure Boundary Components

Four-Year Plan 1984 - 1988

Manuscript Completed: April 1984
Date Published: September 1984

Materials Engineering Associates, Inc.
9700-B George Palmer Highway
Lanham, MD 20706

Prepared for
Division of Engineering Technology
Office of Nuclear Regulatory Research
U.S. Nuclear Regulatory Commission
Washington, D.C. 20555
NRC FIN B8900

TABLE OF CONTENTS

TABLE OF CONTENTS

TABLE OF CONTENTS

TABLE OF CONTENTS

LIST OF FIGURES

LIST OF TABLES

1.0 INTRODUCTION AND OVERVIEW

1.1 Objective of Program Plan Document

This document is the first in a series that is to provide an up-to-date statement of the four-year plan for the program, "Structural Integrity of Light Water Reactor Pressure Boundary Components," which is being conducted by Materials Engineering Associates, Inc. (MEA). The document is intended to be the reference document for management reporting during the current year. The current year for this edition is CY84. The program funding assumptions and the corresponding workscopes are responsive to guidance from the sponsor, the Materials Engineering Branch, Division of Engineering Technology, Office of Nuclear Regulatory Research of the U. S. Nuclear Regulatory Commission (NRC). This document details the program plan to include: Narrative Sections, Milestone Charts and Cost Projections.

This plan is expected to be updated at the beginning of each year. The four years covered by the (current) plan are the current year (CY84), the forthcoming year (FY85), and two out-years (CY86 and CY87). Since a major objective is to provide a reference document for management reporting during the first contract year, that year is highlighted in the milestone charts and is emphasized in the plan-of-action sections. The subsequent years are described in a decreasing level of detail without loss of comprehensive coverage.

1.2 Overview

This program consists of engineering and research in the areas of fracture, fatigue and radiation sensitivity of nuclear structural steels and weldments. The NRC has a continuing need to develop analytical methodologies, test procedures, and data bases relating to these areas for use in the regulatory process. The technical program is formulated in terms of three task areas: Fracture Toughness Criteria (Task 1), Environmentally-Assisted Crack Growth in LWR Materials (Task 2) and Radiation Sensitivity and Postirradiation Properties Recovery (Task 3).

All tasks are integrated to focus on structural integrity of LWR pressure boundary components. The approach centers on an experimental characterization of nuclear grade steels and an assessment of fracture and fatigue behavior under conditions of a nuclear environment where investigation of irradiated materials is a key element of each task. Experimental studies generally involve small laboratory specimens whose behavior forms the basis to develop predictive methods for structural behavior. These studies are supported by analytical models and investigation of the mechanisms responsible for the observed behavior. Data developed in this program will provide the basis for codes and standards, e.g., fatigue and fracture limits for design in the ASME Boiler and Pressure Vessel Code (Sec. III and IX); ASTM test methods, e.g., Plane Strain J_I-R Curve; and revisions to NRC Guides, e.g., Regulatory Guide 1.99.

Task 1 characterizes the fracture toughness of nuclear steels under a variety of conditions. This involves joint programs with ORNL for the characterization of materials from the HSST 4th and 5th irradiations (Subtasks 1d and 1f). A piping fracture mechanics data base will be created (Subtask 1e); correlations between C_v and fracture mechanics tests (K_{Ic}/K_{Jc}) will provide a

more rational interpretation of surveillance data (Subtask 1b); the fracture behavior of stainless steel clad specimens will be investigated in a program which is complementary to that currently underway at ORNL (Subtask 1a); and a combined analytical/experimental program will be undertaken to assess the potential benefit of warm prestress in providing an additional margin of safety during a pressurized thermal shock (Subtask 1c).

Task 2 evaluates environmentally-assisted crack growth under both cyclic and static conditions for a variety of nuclear steels. Thrusts include the development of S-N curves in a PWR environment (Subtask 2a); crack growth rates will be characterized for a variety of plates, welds and HAZ (Subtask 2b); and a "real" crack geometry will be investigated initially in terms of a surface-flawed panel; this task will culminate in the testing of a pipe specimen incorporating a realistic flaw geometry (Subtask 2c). The research with the surface-flawed panel will be extended to include the fatigue behavior of clad plate (Subtask 2d). A mechanisms model will be investigated to explain the observed behavior in environmentally-assisted fatigue crack growth (Subtask 2e). Other innovative tasks include the development of a relation between crack initiation and crack propagation (Subtask 2f) and the investigation of cumulative damage resulting from spectrum loading as seen in service (Subtask 2g).

The focus of Task 3 is on the resolution of questions and uncertainties on radiation sensitivity and on the variables which affect embrittlement relief by postirradiation annealing. The annealing studies represent the interaction of an ongoing effort (IAR program, Subtask 3d) and a new thrust to investigate the effects of high-temperature annealing (Subtask 3a). Two subtasks specifically address the effects of chemical composition on radiation sensitivity (Subtask 3f) and on annealing (Subtask 3b). A mechanisms model will be investigated to provide a basis for the observed behavior on radiation sensitivity and recovery by annealing (Subtask 3c). Finally, a long-term program on dose-rate effects will be continued (Subtask 3e). The results of the latter could bear heavily on the significance of fracture toughness changes measured from accelerated irradiations in test reactors vs. long-term fluence accumulations in a power reactor.

This program is broad in its scope and addresses many of the key questions necessary to resolve uncertainties in the margin of safety that exists in operating nuclear plants. Although the program will not provide definite answers in all areas, its goal is to conduct critical experiments that establish trends to provide answers to engineering questions relating to safety issues facing the NRC.

1.3 Program Organization

The program organization is presented in Fig. 1.1. Each of the three tasks consists of six to eight subtasks. These subtasks are discussed as part of the individual task descriptions and each is presented in terms of an objective statement, a background discussion, a plan of action which includes a flow chart and a milestone chart.

The three program tasks are headed by MEA personnel as shown in Fig. 1.1. Consultants will assist with Subtask 1c "Warm Prestress Under Simulated Loading," Subtask 2f "Total Fatigue Process in PWR Enviroments" and Subtask 2g

"Cumulative Damage Factor for Environmentally-Assisted Fatigue Crack Growth." Much of Subtask 3c "Mechanism Model of Irradiation Damage" will be accomplished through a subcontract with the University of Florida.

Specimen irradiations are performed in the facilities of the Nuclear Science and Technology Facility (NSTF) at the State University of New York (SUNY) at Buffalo. MEA employees perform all mechanical properties characterization of irradiated materials at NSTF. The NSTF irradiation facilities manager (an MEA employee) interacts directly with the Director of NSTF. Overall control is maintained by the MEA program manager.

Progress in this program is formally provided by topical reports (shown in milestone charts for each subtask), annual reports, monthly reports and reports to the NRC Water Reactor Safety Research Information Meeting held in the fall of each year.

Certain subtasks are coordinated with the HSST program activities being conducted at ORNL. The work of Task 2 is discussed at semiannual meetings of the International Cyclic Crack Growth Rate (ICCGR) Group. MEA scientists are active participants on committees of the ASTM and ASME in which the research under the program is discussed in a forum of scientists and engineers representing worldwide participation.

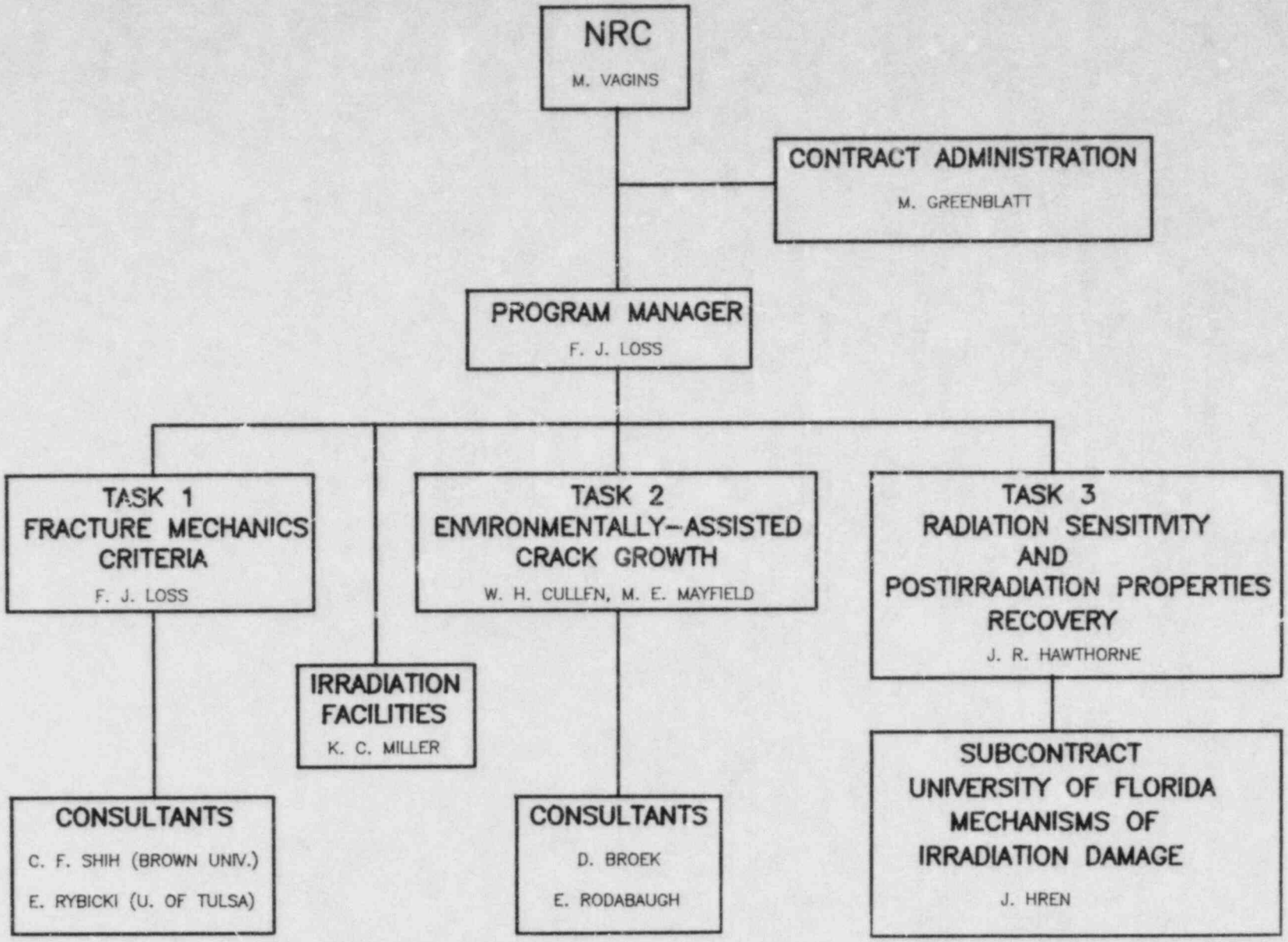

Figure 1.1 Program Organization

2.0 TASK 1 - FRACTURE TOUGHNESS CRITERIA

Characterization of the fracture toughness of nuclear grade steels and weldments is an essential element to quantify the safety margin against fracture in LWR pressure vessels and piping. The objective of the studies described here is to provide the NRC with methodologies and data with which to assess the elastic-plastic fracture behavior of pressure vessel and piping steels in a manner which can have immediate application to the structural integrity assessment of operating plants. Emphasis is placed on the development of test methods, investigation of size effects, and data generation. Investigating the behavior of irradiated materials is a key element of this task.

Task 1 contains six subtasks (Fig. 2.1), each of which addresses different areas vital to the integrity of nuclear vessels and piping. The subtasks are defined such that they are related in terms of approaches and test equipment required so that each subtask can meet its goal in a cost-effective manner. There is also an integration of this task with Tasks 2 and 3 in terms of technical approach, material and data interpretation. Coordination of the work in Task 1 is also achieved with related NRC-sponsored programs at ORNL.

Subtask 1a poses the difficult question of assessing the role of the stainless steel cladding on the toughness of irradiated steel. This subtask will investigate the behavior of a part-through crack in a plate section. This geometry simulates the reactor vessel wall in a simple way to gain insight into the crack behavior which is the key to the safety assessment under PTS conditions. This program will be coordinated with studies of large models under PTS conditions being undertaken by ORNL. Likewise, Subtasks 1d and 1f are coordinated with ORNL in that they involve joint efforts between the two laboratories. Subtask 1d involves the characterization of LEFM fracture behavior of irradiated steels (HSST 5th Irradiation Series) while Subtask 1f centers on elastic-plastic behavior (J-R curve) of vessel steels with irradiation (HSST 4th Irradiation Series). Subtask 1b involves the correlation of C_v and DW-NDT tests with the fracture mechanics quantities K_{Jc} and K_{Ic}. This correlation is essential in order to assess the fracture resistance of reactor vessels which are currently in service and for which only C_v data area available. The objective of Subtask 1e is to establish a piping fracture mechanics data base which involves elastic-plastic behavior (J-R curves). This data base is essential for further analysis of piping integrity by the NRC and its subcontractors. Finally, Subtask 1c will study the phenomenon of warm prestress under PTS conditions. In previous research by MEA scientists, this phonemenon has been shown to be of benefit during a LOCA. This concept was later confirmed by ORNL studies of thermal shock behavior. The previous work of MEA scientists will now be extended to the formulation and verification of a theoretical model which incorprates reloading of the crack after warm prestress. A quantification of this phenomenon would permit advantage to be taken of an apparent higher toughness of the material, thereby providing an extra margin of safety during a PTS accident.

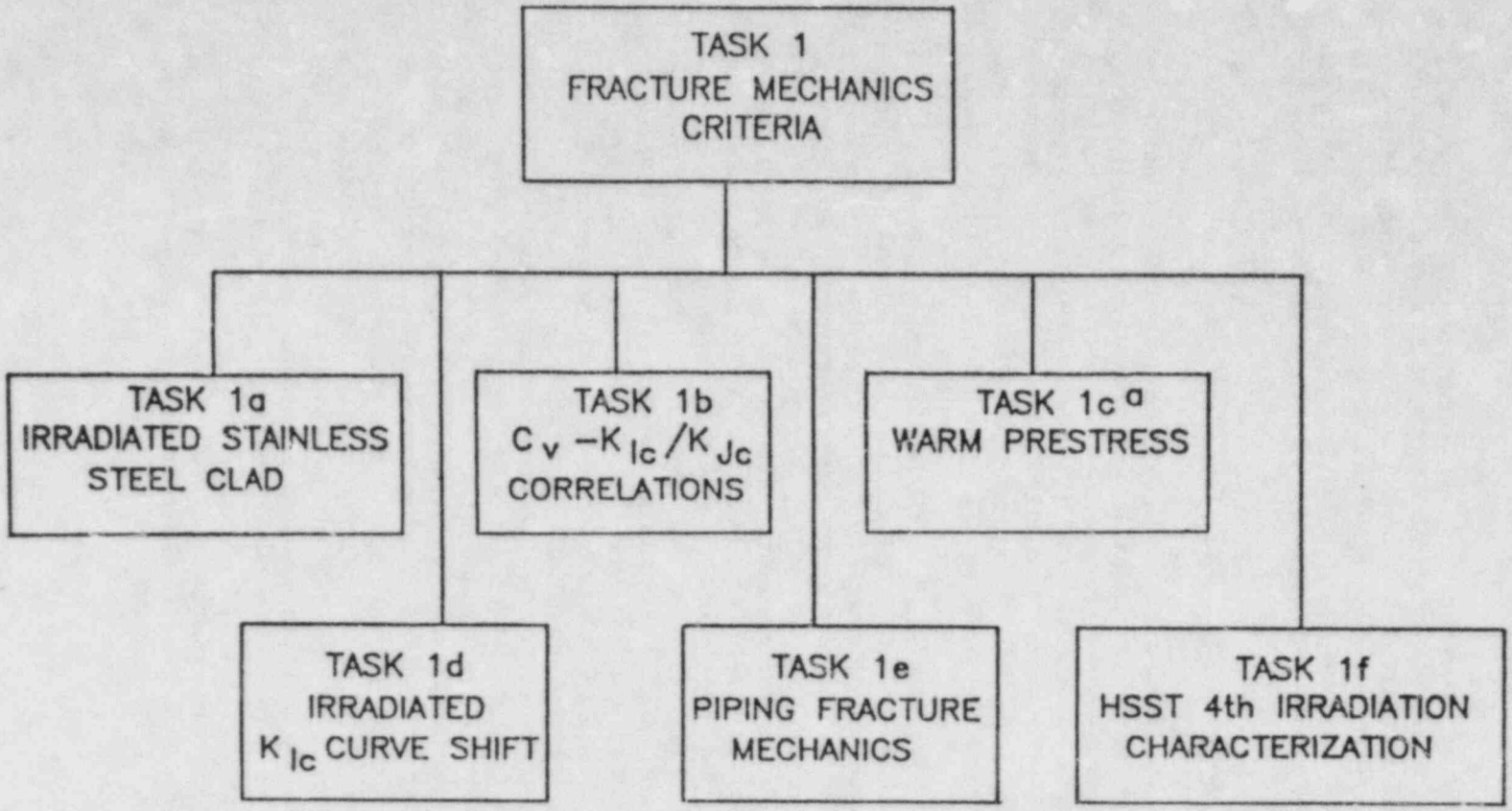

[a] CONSULTANTS: C.F. SHIH, B. ASARO, B.FREUND (BROWN UNIV.)
E. RIBICKI (UNIV OF TULSA)

Figure 2.1 Organization for Task 1: Fracture Toughness Criteria

2.1 Subtask 1a Fracture Resistance of Irradiated Stainless Steel Clad Vessel Steels

2.1.1 Objective

The objective of Subtask 1a is to develop data directly usable in assesing the role played by pressure vessel cladding in enhancing or mitigating crack initiation during a postulated pressurized thermal shock scenario.

2.1.2 Background

The 1978 Rancho Seco accident, among other things, served to illustrate that it was possible for a nuclear pressure vessel subjected to a thermal shock to also experience significant pressure loading. Cheverton and his colleagues (Ref. 2.1) have analyzed a number of pressurized thermal shock (PTS) accident scenarios. One particularly important finding has been the possibility that relatively small flaws, subjected to a PTS accident, could lead to failure of the pressure vessel. This possibility is particularly important since the probability of a flaw being present increases with decreasing flaw size.

Analysis of the potential behavior of relatively small flaws in a nuclear pressure vessel necessarily involves assessing the role played by the stainless steel cladding and to account for the potential effects of irradiation on the cladding. In qualitative terms, the cladding enters the analysis in two ways. First, the thermal conductivity of the cladding, compared to that for the ferritic steel, serves to reduce the through-thickness cooling rate. This, in turn, reduces the peak thermal stresses but also increases the time required for the vessel wall to equilibrate. Second, the presence of cladding enters the analysis due to the differential thermal expansion between the stainless steel cladding and the ferritic steel vessel wall. The net result is that the K_I profile along the crack front in the ferritic steel is different than for an unclad vessel.

The three-dimensional nature of the problem makes a quantitative description of the K_I profile a difficult task. Depending on the flaw geometry (depth and length), the residual stress distribution and the applied loadings (mechanical and thermal), the presence of the cladding may serve to either enhance or mitigate the possibility of crack initiation. Note that for the cladding to be effective in mitigating crack initiation, it must keep the crack from extending in length. Should irradiation damage in the cladding reduce its toughness to the point that the cladding fractures ahead of or along with the base metal, the cladding would surely enhance crack initiation in the base metal.

The general topic of PTS accidents is being considered as a part of the HSST program (see Refs. 2.2, 2.3 and 2.4). The efforts undertaken as part of Subtask 1a have been designed to complement rather than duplicate the HSST program activities.

2.1.3 Plan of Action

The plan of action for Subtask 1a involves testing part-through crack (PTC) specimens, both clad and unclad, with flaw shape, test temperature and irradiation as variables. Figure 2.2 depicts the plan of action for this subtask. The initial clad specimen work performed at ORNL has demonstrated that fabricating and testing specimens taken from clad plate presents some special problems. Thus, a specimen design/test technique development activity has been included as part of this subtask.

The plate material will be clad using a three-wire tandem arc process typical of that used in older vessel construction. The clad plate will be stress relieved using a heat treatment also typical of vessel construction practice. The residual stress distribution will be determined for the clad specimen blanks. This information will be factored into the analysis of surface flawed specimens.

The testing will involve monotonic loading of both clad and unclad specimens in both the irradiated and unirradiated condition. The data to be acquired includes crack shape (using a potential drop measurement technique), crack opening displacement and surface strains as a function of applied load. The test data will be evaluated using the best available K and/or J solutions for the PTC geometry. The effect of the cladding will be assessed in terms of the values of K and/or J at crack initiation as well as the crack shape and changes in crack shape.

2.1.4 Milestones

Figure 2.3 depicts the milestones and anticipated schedule for Subtask 1a.

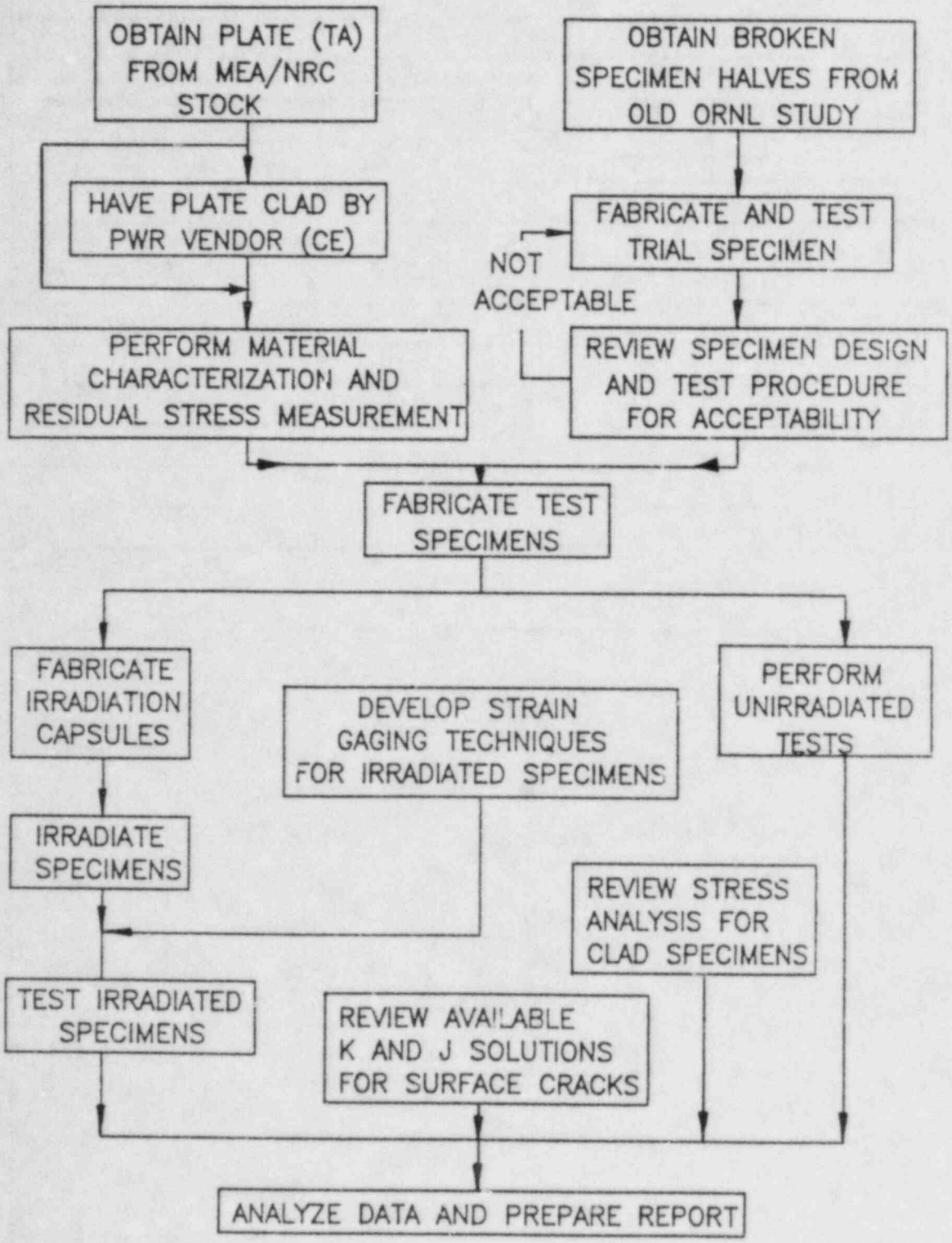

Figure 2.2 Flow Diagram for Subtask 1a: Fracture Resistance of Irradiated Stainless Steel Clad Vessel Steels

MILESTONE STATEMENT AND SCHEDULE

Subtask 1a: Fracture of Irradiated SS Clad Vessel Steels

CY84

MILESTONE	FY84 J	F	M	A	M	J	J	A	S	FY85 O	N	D	2	3	4	FY 86	FY 87	Beyond FY87
1.a.1 Fabrication and Characterization of Test Materials and Specimens																		
a. Complete cladding of plate					▽	△												
b. Complete material characterization							▽	△										
c. Complete residual stress evaluation									▽			△						
d. Complete fabrication of specimens										▽			△					
1.a.2 Complete Specimen Design/Test Technique Development and Prepare Report						▽						△						
1.a.3 Complete Fabrication of Irradiation Assemblies													▽	△				
1.a.4 Perform Unirradiated Specimen Testing and Report													▽			△		
1.a.5 Complete Irradiation of Specimens																▽	△	
1.a.6 Complete Irradiated Specimen Testing and Report																▽		△
REPORT SUMMARY												△				△		△

Figure 2.3 Milestone Statement and Schedule for Subtask 1a

2.2 Subtask 1b Correlation of Dynamic C_v and Static K_{Ic}/K_{Jc} Tests

2.2.1 Objective

The primary objective of this subtask is to establish correlations in transition temperature elevations between notch ductility (C_v) and fracture toughness (K_{Ic}/K_{Jc}) tests. These correlations may depend upon material composition and product form.

2.2.2 Background

Fracture toughness and notch ductility typically are evaluated as a function of temperature. The two major areas of interest are the material toughness/ductility levels on the ductile upper shelf and the temperature at some critical index in the brittle-to-ductile transition region. The effect of irradiation on these two areas is generally to decrease the upper shelf levels, and to increase the brittle-to-ductile transition index temperature. The upper shelf degradation can be visualized as placing limits on pressure levels in a nuclear pressure vessel, while the transition temperature increase would give a lower limit to the temperature at which the pressure vessel could be operated safely under pressure.

Notch ductility as determined by the C_v test is widely used in test and power reactor irradiation effects programs. Unfortunately, the C_v test cannot be interpreted directly in terms of structural performance. Instead, a fracture toughness parameter such as the plane strain stress intensity factor (K) can be related more directly to critical stress/flaw size conditions. However, since fracture toughness specimens (typically compact toughness or CT specimens) are not plentiful in reactor surveillance capsules (in many cases nonexistent), a means of relating C_v transition temperature increase to fracture toughness transition temperature increase would provide a structurally-relevant technique for determining margin of safety in nuclear power plants using C_v trends only.

The ASME K_{IR} reference toughness curve is indexed at the material reference temperature, RT_{NDT}, which is defined in the unirradiated condition based upon drop weight NDT and dynamic C_v tests. Currently, 10CFR50 specifies that the irradiated reference temperature shall be increased by the temperature shift determined at the 41 J level using irradiated C_v specimens. Early work at NRL correlating C_v data with DW-NDT data for the irradiated condition gave confidence to this use. However, recent work at MEA, and earlier at NRL, indicates that C_v data may be an unconservative indication of postirradiation fracture toughness transition behavior, at least for the more radiation sensitive materials (Refs. 2.5 and 2.6). Additionally, significant "flattening" of the C_v curve shape observed in some steels indicates that the linear translation of the K_{IR} curve as specified in 10CFR50 may not be wholly correct.

The studies of Ref. 2.5 involved several pressure vessel materials (plates, welds, forging) irradiated at 288°C to fluences between 0.1 and 4.4×10^{19} n/cm^2. One objective was the comparison of radiation effects on notch ductility (in terms of C_v energy absorption and lateral expansion properties) to dynamic and static fracture toughness (K_{Jd}, K_{Jc}) defined by fatigue precracked Charpy-V (PCC_v) and CT specimen test methods, respectively. The CT specimens were tested using the single specimen compliance method and J-integral

assessment procedures to establish the J-R curve. Representing the dynamic test case, the C_v 41 J and the K_{Jd} 100 MPa$\sqrt{m}$ index temperature (PCC_v) showed comparable transition temperature increases. On the other hand, comparisons of the C_v (PCC_v) results against the static CT test findings showed major differences. In many cases the K_{Jc} 100 MPa$\sqrt{m}$ temperature elevation via the CT specimens was much higher (up to 40°C) than the 41 J or K_{Jd} 100 MPa$\sqrt{m}$ temperature elevations found in the dynamic C_v tests. Wide variability (± 40°C) between 41 J vs. K_{Jc} 100 MPa$\sqrt{m}$ temperature elevations was also described by the data, leading to speculation that metallurgy influences the correlation of the two indices. In terms of importance, a 40°C difference in (projected) elevation of the transition region can amount to three to five years of reactor vessel operation for steels that are particularly radiation sensitive. Unconservatism of C_v surveillance data obviously would have a direct impact on the adjustment of the K_{IR} curve.

A means of minimizing the differences between C_v and CT test data has been postulated recently by Merkle of ORNL using the β_{Ic}-correction technique. Although this technique has only an empirical basis, correction of K_{Jc} data using the β_{Ic}-approach does significantly decrease the differences between C_v and CT data, in some cases resulting in C_v data which appears to be conservative in comparison to similar CT data.

2.2.3 Plan of Action

The plan for investigating the observed differences in C_v and K_{Ic}/K_{Jc} transition temperature shifts is illustrated in Fig. 2.4. Initial work in this area will focus on assimilating data developed in recent years at MEA and NRL into one data base. Besides the C_v and K_{Ic}/K_{Jc}, the K_{Jc} data will be re-evaluated using the β_{Ic}-correction techniques postulated recently by Merkle of ORNL as a successful method of estimating K_{Ic} levels from ASTM E 399 invalid K_{Jc} data. This correction has recently been shown to minimize the differences between C_v and K_{Ic}/K_{Jc} shifts (Ref. 2.6), in some cases decreasing the K_{Ic}/K_{Jc} shifts to levels below the comparable C_v shifts.

Four plates with statistical variations in nickel, copper and phosphorous contents (Table 2.1) will be characterized to add to the data base. C_v, 0.5T-CT (K_{Ic}/K_{Jc}) and tensile specimens from each of the four materials will be irradiated in two separate assemblies at NSTF. In addition, unirradiated DW-NDT and dynamic 0.5T-CT (K_{Jd}) tests will be conducted. The purpose of these additional tests is to provide composition variations not available in the current data. In addition, results from the HSST 4th and 5th Irradiation programs will be assimilated into the data base. The HSST 5th Irradiation will also provide further information on postirradiation DW-NDT behavior, and its relation to the C_v and K_{Ic}/K_{Jc} behavior.

2.2.4 Milestones

The milestones for this subtask are given in the milestone chart (Fig. 2.5). In FY84, the first Test Methods Correlation irradiation assembly (TMC-1) will be constructed and irradiated at NSTF. Testing of the specimens from TMC-1 will be completed by mid-FY85. Once the current data has been assembled and corrected using the β_{Ic} approach, a NUREG report will be issued. This should occur early in FY85. The second TMC assembly (TMC-2) will be constructed in mid-FY85, with testing to be completed by mid-FY86. A NUREG report detailing these results will be prepared by the end of FY86.

Table 2.1 Test Materials for Subtask 1b Investigations

Material	Code No.	Thickness (mm)	Source	Cu	Ni	P	C	Mn	Si	S	Cr	Mo
A 302-B	6A	12.7	Lab Melt	0.28	0.05	0.002	0.23	1.29	0.22	0.013	0.05	0.53
A 533-B	67C	15.9	Lab Melt	0.002	0.70	0.025	0.23	1.31	0.20	0.018	0.05	0.51
A 533-B	68C	15.9	Lab Melt	0.30	0.70	0.028	0.23	1.31	0.22	0.017	0.05	0.52
A 533-B	68A	15.9	Lab Melt	0.30	0.70	0.003	0.23	1.31	0.22	0.017	0.05	0.52

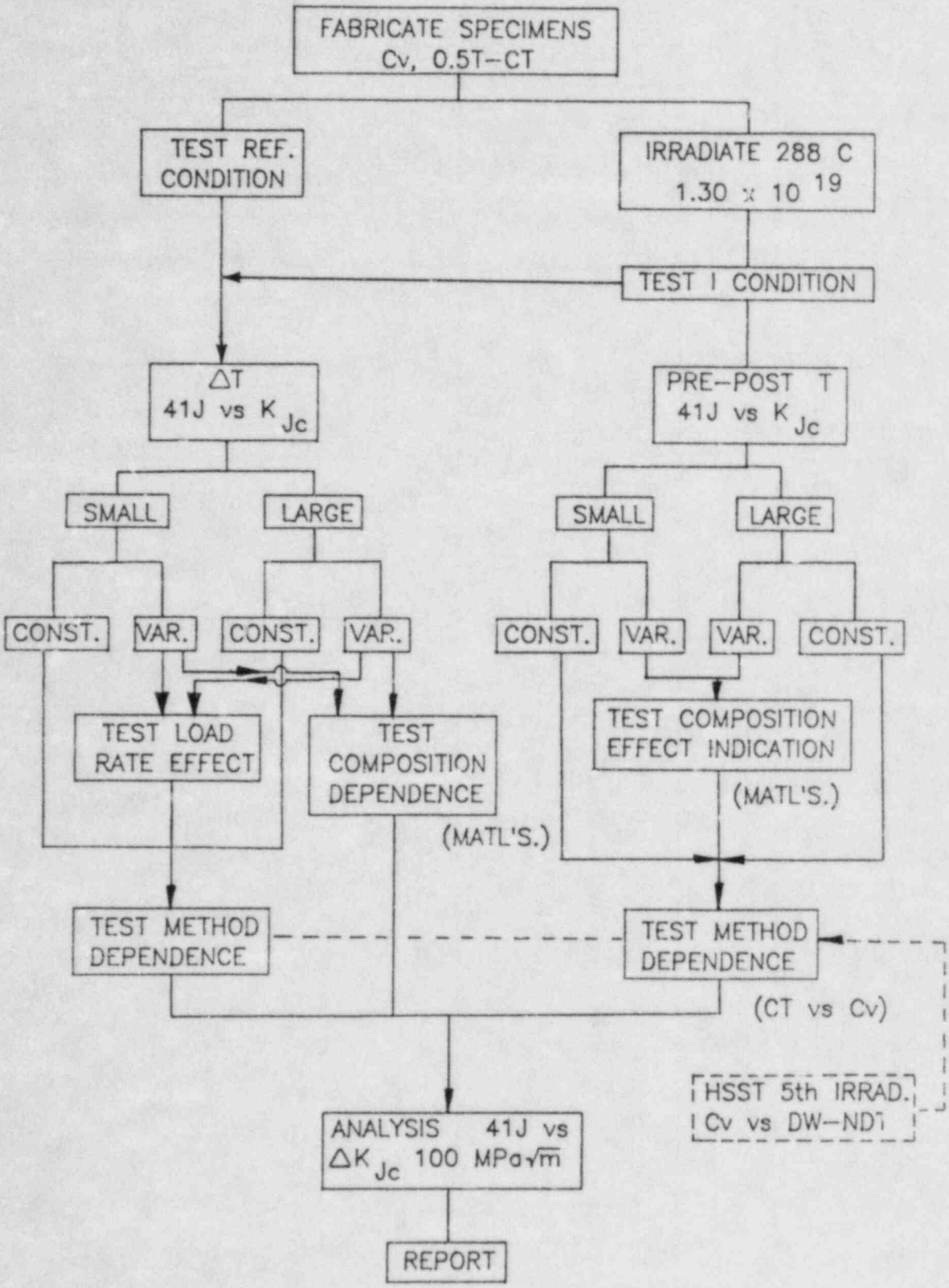

Figure 2.4 Flow Diagram for Subtask 1b: Correlation of Dynamic C_v and Static K_{IC}/K_{JC} Tests

MILESTONE STATEMENT AND SCHEDULE

Subtask 1b: Correlation of Dynamic C_v and Static K_{Ic}/K_{Jc} Tests

CY84

MILESTONE	FY84									FY85						FY 86	FY 87	Beyond FY87
	J	F	M	A	M	J	J	A	S	O	N	D	2	3	4			
1.b.1 Analysis of Data																		
a. Complete analysis of currently available data				▽					△									
b. Report on currently available data									▽	△								
c. Compile new data										▽							△	
1.b.2 Unirradiated Material Characterization																		
a. Complete unirradiated K_{JC} and tensile tests									▽		△							
b. Complete unirradiated K_{JC} and DW tests											▽		△					
1.b.3 Irradiated Material Characterization																		
a. Construct irradiation assembly TMC-1				▽		△												
b. Complete irradiation of TMC-1						▽		△										
c. Complete irradiated testing, TMC-1											▽			△				
d. Construct irradiation assembly, TMC-2													▽		△			
e. Complete irradiation of TMC-2															▽	△		
f. Complete irradiated testing, TMC-2																▽		
g. Report on TMC-1, TMC-2																▽		
1.b.4 Final Report Based on All Data																	▽	
REPORT SUMMARY										△						△	△	

Figure 2.5 Milestone Statement and Schedule for Subtask 1b

2.3 Subtask 1c Warm Prestress Under Simulated Transient Loading

2.3.1 Objective

This subtask will model the crack-tip behavior in a reactor vessel during a simulated pressurized thermal shock (PTS) event. The objective is to formulate and validate a predictive capability to resolve how much of an increase in K_I, with $K_I/K_{Ic} > 1.0$, can be tolerated before the beneficial effects of warm prestress (WPS) are overcome and crack extension initiates.

2.3.2 Background

Warm prestressing is a phenomenon which increases the "apparent" fracture toughness of a cracked body when the latter is loaded under linear elastic fracture mechanics (LEFM) conditions. A typical WPS procedure consists of prestressing a cracked structure at an elevated temperature, which is generally above the brittle-ductile transition region, then unloading and cooling to a lower temperature somewhere below the brittle-ductile transition where LEFM behavior would be anticipated. Upon reloading at the lower temperature the prior WPS would result in the stress intensity at failure K_F exceeding K_{Ic}, provided that the WPS load initially exceeded the level of K_{Ic} at the lower temperature.

Models of the WPS phenomenon have been proposed by Harrison (Ref. 2.7), Harrop (Ref. 2.8), Rice (Ref. 2.9), Chell (Ref. 2.10), Curry (Ref. 2.11) and others. All of these approaches make assumptions which avoid the rigorous analysis and predictive capability that would be required in determining quantitatively the margin of safety in nuclear vessels during a thermal transient. Nevertheless, it can be concluded from these theories that WPS does not, in fact, improve the intrinsic fracture toughness of materials at low temperatures. Instead, the beneficial effects appear to be entirely dependent upon the loading history and the material's reponse to that history. A definitive model of the WPS behavior could be of benefit in quantifying the margin of safety in postulated accidents associated with nuclear reactor vessels.

Experiments conducted by Loss, et al. (Ref. 2.12 and 2.13) have demonstrated the WPS concept for laboratory specimens subjected to a stress history which simulates that seen by the crack-tip region of the vessel wall during a LOCA in which the vessel is unpressurized. The results show a positive benefit of WPS in that K_F always exceeds K_{Ic} when the material has been subject to WPS. It was concluded that for the LOCA event it is impossible for fracture to occur as K_I decreases with time, provided the crack-tip region has been subjected to WPS. The WPS phenomenon has been subsequently demonstrated by Cheverton (Ref. 2.14) at ORNL with intermediate test vessels (unpressurized) which were subject to thermal shock conditions resembling a LOCA.

The postulated PTS accident has been recognized as a potentially more serious accident than the LOCA. During a PTS, the vessel wall is subjected to a thermal shock just as in the case of a LOCA, including the possibility of WPS. A major difference between the two accident scenarios is that the vessel is repressurized in the PTS. In the latter case, the potential benefits of WPS are not as clear as in a LOCA. It has been demonstrated that WPS is effective in a LOCA since the K_I at the crack tip decreases with time after the WPS. Here it is argued on physical grounds, and experimentally

demonstrated by Loss, that fracture will not occur when K_I at the crack decreases even though K_I may exceed K_{Ic}. A similar argument for the PTS event does not exist, because of repressurization. In order to define the benefit from WPS during PTS, it is necessary to know in quantitative terms the degree of reloading permissible in the region where $K_I > K_{Ic}$.

2.3.3 Plan of Action

The planned approach to the investigation of the WPS phenomenon is shown schematically in Fig. 2.6. The thrust of this subtask will be to model the crack-tip behavior during simulated PTS conditions. It is expected that the verification of the model will require numerical simulation as well as an experimental phase.

The initial work on this subtask will be the modelling of the crack-tip behavior during an arbitrary WPS loading which includes reloading such that $K_I > K_{Ic}$. The model will be developed by consultants from Brown University. This effort will include formulation of input for a FEM analysis.

Given this model, investigators from the University of Tulsa will compute the near-field crack-tip behavior (stresses and deformations) under a simple WPS path for a laboratory specimen. This path will involve loading of the crack tip in the ductile regime, partially unloading as occurs in a LOCA, and then reloading at a low temperature, as occurs in a PTS. The objectives will be to predict the failure load. The computations will simply express the K_{Ic} at the crack tip in terms of a far-field load, taking account of residual stresses at the crack tip. The degree to which this far-field load exceeds the load to reach K_{Ic} for a virgin material determines the degree of reloading after WPS that can be achieved. Having performed these computations, the model will be applied to predict the results of Loss, et al., (Ref. 2.12 and 2.13) which involved reloading of the crack tip to varying amounts prior to fracture. MEA will develop flow properites from the steels used in these experiments to support the analysis.

Depending on the degree of success achieved in predicting the experimental results, it may be necessary to refine the model. In any event, additional tests will be undertaken with the same A 533-B steel used in the prior experiments (Ref. 2.13) to test the model under different loading conditions. To further validate the model, one or two materials having different work-hardening characteristics (one steel, one aluminum) will be tested. It is felt that residual stresses are the key to explaining the WPS phenomenon. Since the latter is linked to the strain hardening of the material, the testing of a few different steels is essential to validate the analysis.

The experimental phase of this subtask will be relatively small. In the event that further experiments are required, such as demonstration of the reloading phenomenon with irradiated steels, this work would form the basis for a follow-on effort.

2.3.4 Milestones

Milestones and the anticipated schedule for Subtask 1c are given in Fig. 2.7.

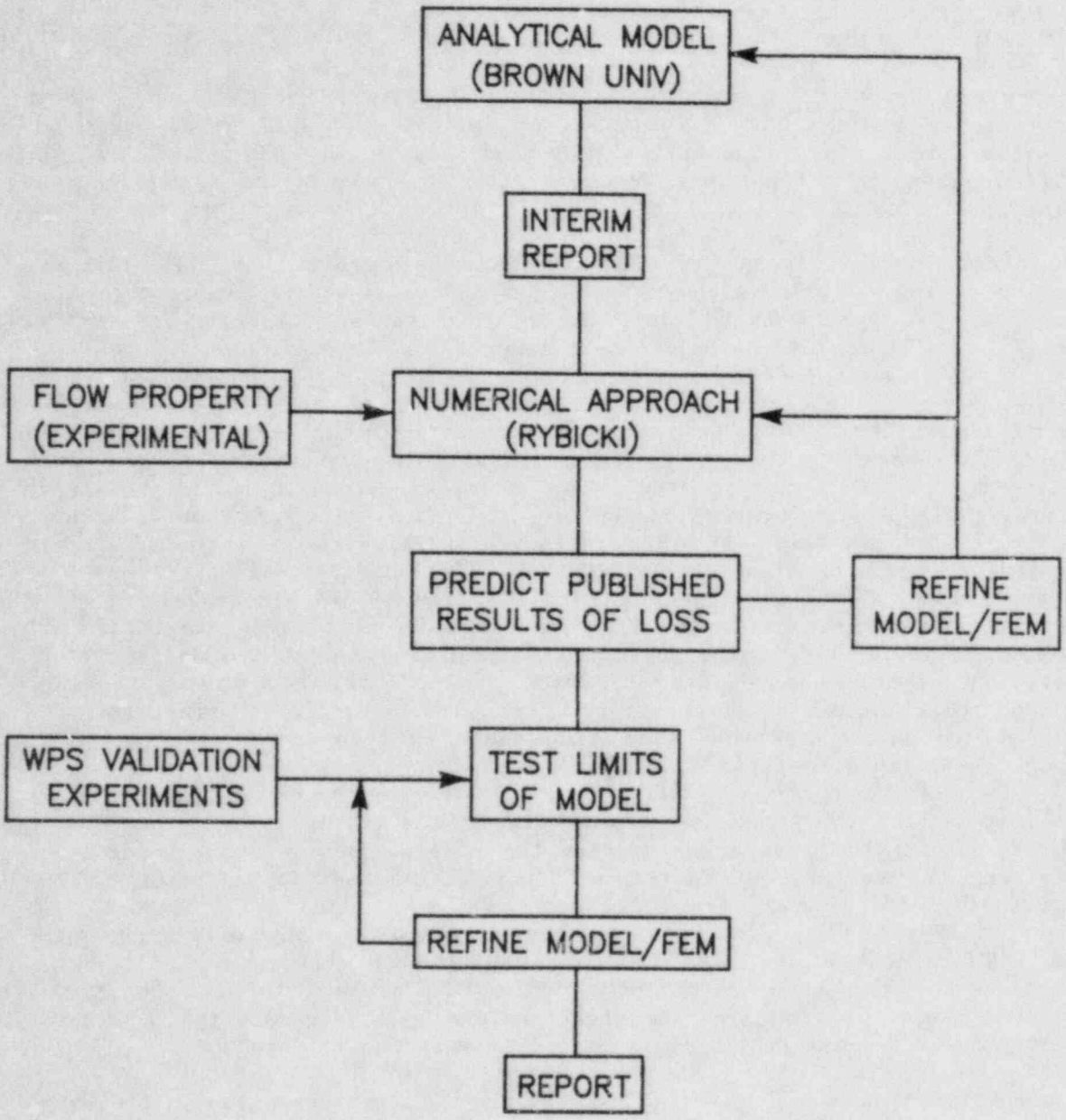

Figure 2.6 Flow Diagram for Subtask 1c: Warm Prestress Under Simulated Transient Loading

MILESTONE STATEMENT AND SCHEDULE

Subtask 1c: Warm Prestress Under Simulated Transient Loading

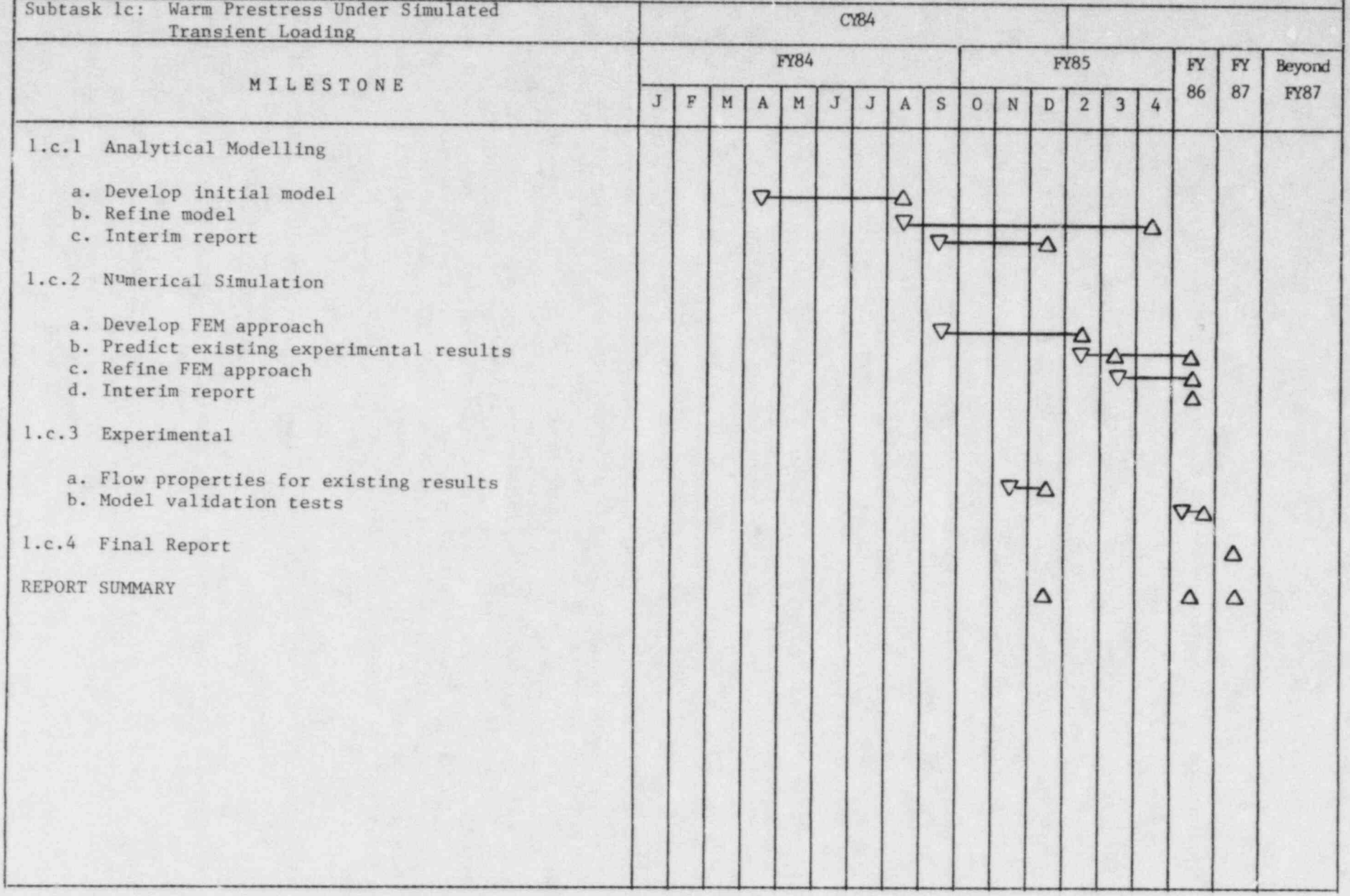

Figure 2.7 Milestone Statement and Schedule for Subtask 1c

2.4 Subtask 1d Irradiation-Induced K_{Ic} Curve Shift

2.4.1 Objective

The primary objective of this subtask is to obtain valid linear elastic fracture toughness (K_{Ic}) curves for two nuclear pressure vessel grade steel welds irradiated at 288°C (550°F) to a target fluence of 1.5×10^{19} n/cm^2 (E > 1 MeV). Secondary objectives are as follows:

- Obtain unirradiated linear elastic and elastic-plastic (K_{Jc}) fracture toughness curves up to about 130 MPa$\sqrt{m}$ (118 ksi$\sqrt{in.}$ as well as irradiated elastic-plastic fracture toughness curves, thus allowing comparison of K_{Ic} and K_{Jc} data.
- Obtain unirradiated and irradiated Charpy (C_v) curves for correlation with the radiation-induced shift of the brittle-to-ductile transition as indicated by the fracture toughness tests.
- Index the nil-ductility transition temperature of both materials with irradiated and unirradiated drop weight tests and obtain tensile properties for both the unirradiated and irradiated condition.
- Test sufficient specimens, as far as practical, to provide a statistical analysis of the results.

2.4.2 Background

This program is being conducted as a cooperative effort between MEA and Oak Ridge National Laboratory (ORNL). It is part of the larger Heavy Section Steel Technology (HSST) program sponsored by the Nuclear Regulatory Commission. This subtask is the fifth in the planned series of HSST irradiation studies and is intended to validate current procedures for estimating the shift and shape change, if any, of the brittle-to-ductile transition K_{Ic} curve with irradiation. Currently, the predicted shift in the K_{Ic} curve is based on the shift of the Charpy toughness curve; it is assumed that the shape of the K_{Ic} curve does not change with irradiation. Validation of this methodology was initiated in the first HSST irradiation study, but insufficient specimens were available to allow statistical analysis.

2.4.3 Plan of Action

Figure 2.8 is a flow chart which describes the general plan of action. ORNL is having 14 meters (216 mm thick) each of the two weldments fabricated having nominal A 533 Gr. B chemical composition with copper contents of 0.23% and 0.32%. These relatively high copper levels assure a significant shift in the transition. To obtain uniform copper distribution in the finished weld, the copper was added to the weld wire melt prior to drawing it into welding wire. The weldments are being fabricated and stress relieved according to current commercial practice. Specimen machining will be performed by ORNL as well as preliminary inspection and characterization of the material which includes: ultrasonic inspection, chemical analysis, metallurgical structure studies, and the preliminary tests of standard tensile, drop weight and C_v specimens. The specimen complement for the program is shown in Table 2.2 on a per material basis.

Specimen testing will be conducted jointly by MEA and ORNL with each laboratory testing about half of the specimens. However, testing of all irradiated 4T-CT and unirradiated 6T-CT and 8T-CT specimens will be conducted by MEA and all tensile and about 75% of the Charpy tests will be done by ORNL. The specimen testing sequence is as follows:

(1) Materials inspection and characterization (ORNL only).

(2) Unirradiated specimen testing

a. C_v tests
b. Tensile tests (ONRL only)
c. J_{Ic} (K_{Jc}) tests of 1T-CT specimens
d. K_{Ic} tests of 1T-CT specimens
e. J_{Ic} (K_{Jc}) tests of 2T-CT specimens
f. K_{Ic} tests of 2T-CT specimens
g. J_{Ic} (K_{Jc}) tests of 4T-CT specimens
h. K_{Ic} tests of 4T-CT specimens
i. K_{Ic} tests of 6T-CT and 8T-CT specimens (MEA only)

(3) Testing of irradiated specimens and remainder of unirradiated specimens

a. C_v tests
b. Tensile tests (ORNL only)
c. Drop-weight tests
d. J_{Ic} (K_{Jc}) tests of 1T-CT specimens
e. K_{Ic} tests of 1T-CT specimens
f. J_{Ic} (K_{Jc}) tests of 2T-CT specimens
g. K_{Ic} tests of 2T-CT specimens
h. K_{Ic} tests of 4T-CT specimens (MEA only).

The testing philosophy resulting in the above sequence is to first conduct those test which will provide guidelines and data input to the larger, more valuable specimen tests. Thus, C_v and tensile testing are conducted first to provide properties needed for compact specimen test data analysis and to provide an indication of where the static brittle-to-ductile transition is located based on the dynamic C_v transition location. Next, the smaller unirradiated compact specimens will be tested. These data in turn will be used to define test temperatures for the larger specimens. Irradiated compact specimen testing will commence after the unirradiated testing is essentially completed. All specimen irradiations will be conducted by ORNL in the Oak Ridge Research Reactor pool-side facility. After completion of all unirradiated large (4T, 6T and 8T) compact testing by MEA, the MEA 550-kip test frame will be moved into the hot cell at the Nuclear Science and Technology Facility at the University of New York at Buffalo in order to test the irradiated 4T-CT specimens.

2.4.4 Milestones

Figure 2.9 illustrates the milestones and anticipated schedule for Subtask 1d.

Table 2.2 Specimen Complement for K_{Ic} Curve Shift Program

SPECIMEN TYPE	PURPOSE	UNIRRADIATED	IRRADIATED	TOTAL PER MATERIAL
1T-CT	K_{Ic}	10	12	22
1T-CT	K_{Jc}	24	24	48
2T-CT	K_{Ic}	4	6	10
2T-CT	K_{Jc}	12	8	20
4T-CT	K_{Ic}	4	8	12
4T-CT	K_{Jc}	8[b]	0	8[b]
6T-CT	K_{Ic}	2	0	2
8T-CT	K_{Ic}	2	0	2
Std. Tensile	Tensile Properties	4	0	4
MT[c]	Tensile Properties	24	12	36
Drop Weight	NDT	12	12	24
Charpy	Transition-Shelf	81	38	119

[a] All entries are on a per material basis

[b] If sufficient material is available

[c] Miniature Charpy-size tensile specimens

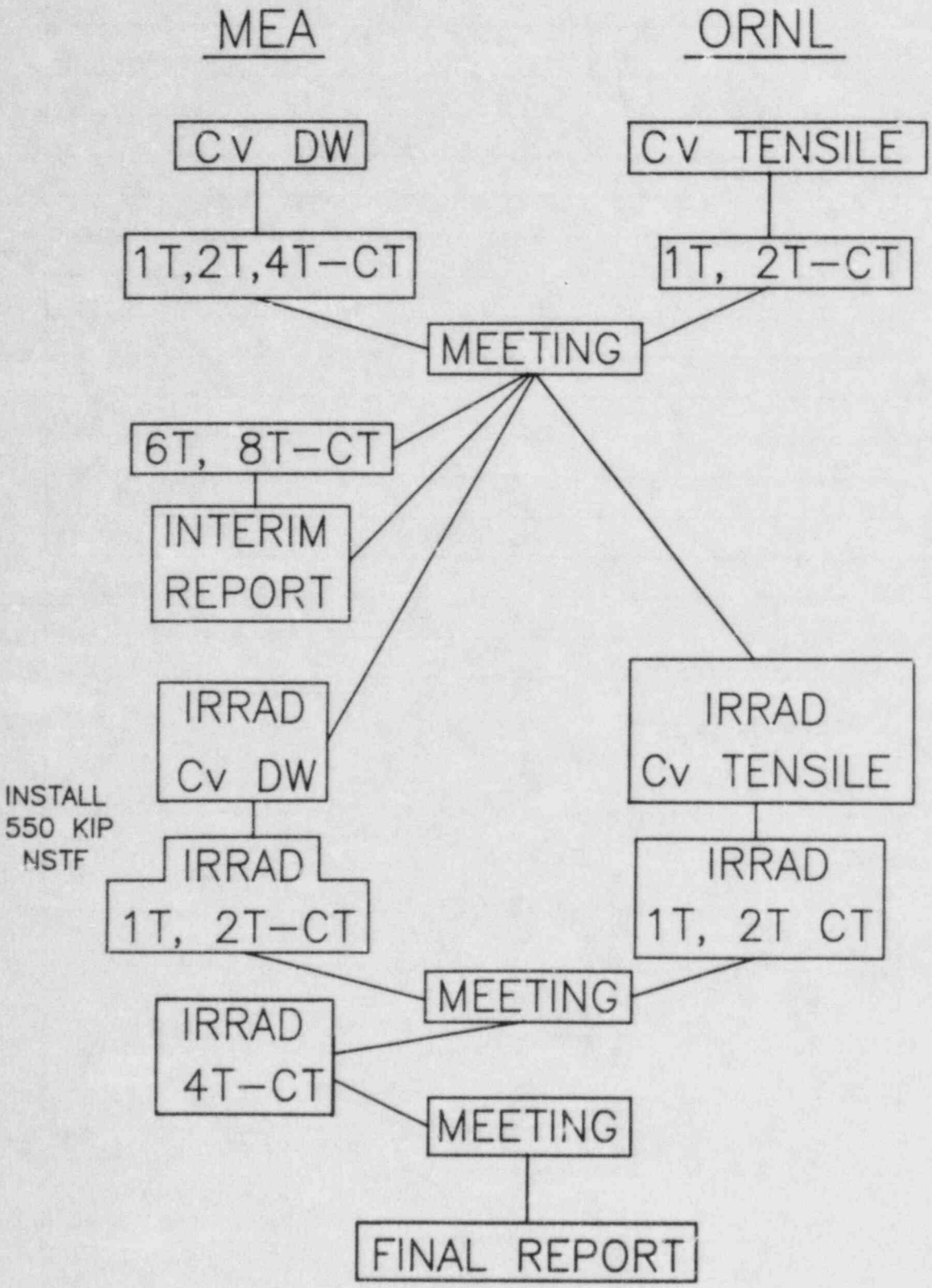

Figure 2.8 Flow Diagram for Subtask 1d: Irradiation-Induced K_{IC} Curve Shift

MILESTONE STATEMENT AND SCHEDULE

Subtask 1d: Irradiation-Induced K_{IC} Curve Shift

MILESTONE	CY84																	
	FY84									FY85						FY 86	FY 87	Beyond FY87
	J	F	M	A	M	J	J	A	S	O	N	D	2	3	4			
1.d.1 Unirradiated Testing																		
a. Receive unirradiated specimens								△										
b. Test DW, Cv, 1T, 2T, 4T-CT specimens									▽				△					
c. Test 6T and 8T-CT specimens														▽△				
d. Interim report															▽△			
1.d.2 Irradiated Tests																		
a. DW, Cv tests														▽	△			
b. Install 550 Kip test machine in NSTF warm well															▽△			
c. Test 1T- and 2T-CT specimens															△			
d. Test 4T-CT specimens															▽△			
1.d.3 Final Joint MEA/ORNL NUREG Report																	▽△	
REPORT SUMMARY															△		△	

Figure 2.9 Milestone Statement and Schedule for Subtask 1d

2.5 Subtask 1e Piping Fracture Mechanics Data Base

2.5.1 Objective

The objectives of this subtask are to develop a comprehensive data base of J-R curves from piping steels commonly used in nuclear power plants, and to establish a numeric data base on a computer system to provide ready access to the data. Data currently available from other laboratories will be supplemented by J-R curve testing at MEA to complete the desired data matrix.

2.5.2 Background

An important consideration in assessing nuclear power plant safety is a determination of the structural integrity of the coolant water piping systems. Besides system-dependent concerns such as loading and flaw distributions, properties of the constituent materials such as tensile strength, fatigue crack growth rates and fracture toughness values are also required. The fracture toughness takes on special significance since it is used in determining whether or not a crack will propagate through thickness under specified loading scenarios, and additionally, whether or not a through-thickness crack will be stable or will result in a large break.

The development of fracture analysis procedures for LWR piping systems has passed through several stages. Currently, J-integral concepts are receiving considerable attention as a suitable technique. Initially, the idea of a critical J value (J_{Ic}) for the initiation of fracture was being applied to many structures, including piping. In general, J_{Ic} was seen as conservative, but perhaps overly conservative, for piping applications. J_{Ic} analyses did not account for the appreciable tearing resistance of very tough materials. In 1979, Paris and coworkers (Ref. 2.15 and 2.16) introduced the tearing instability analysis and applied it to a number of structures including circumferential cracks in pipe. This analysis has gained popularity and is considered by many to provide the best measure of the fracture resistance of a structure.

The essence of the tearing instability analysis is that a material has a tearing (resistance) modulus (T_m), which can be determined from the J resistance, or J-R, curve. For instability of a given crack to occur, T applied to the structure must be greater than T_m and J applied must be greater than J_{Ic}. Both T_m and J_{Ic} come from the J-R curve, which is the primary data for the tearing instability analysis.

Before the tearing instability analysis can be generally applied, a comprehensive data base of J-R curves from pertinent piping materials must be formed. A list of such materials is given in Table 2.3. Unfortunately, little J-R curve data currently exist for these materials. Therefore, additional J-R curve testing will be required to complete the data matrix as best possible.

The immediate task once data are available is to package the data in a format most usable by NRC personnel. This requirement will be best met through a computerized storage and retrieval system.

2.5.3 Plan of Action

The plan for developing the piping data base is given in Fig. 2.10. The list of materials given in Table 2.3 is the target matrix of piping steels for which data is desired. Unfortunately, data are not available for many of the materials on the list. Other laboratories which have characterized piping steels will be contacted in an effort to fill the matrix as much as possible. The data collection efforts will not be restricted to Table 2.3, but rather data from any commonly used materials will be collected.

Concurrent with the data collection effort, sources of pertinent materials (or potential sources) will be solicited in an attempt to procure enough suitable material to provide a reasonable data base. The material collection efforts will be coordinated with Battelle's Columbus Laboratory, the contractor for the NRC's Degraded Piping program.

The data collection and data generation aspects of this subtask will be continuing efforts throughout this contract. On the other hand, implementation of the computerized data base will primarily be a first-year effort, with the following year's work focused on coding new data into the data base.

The data base will be implemented on a mainframe computer, possibly on the NIH computer using the System 2000 Data Base Management System or on another Government-owned system. Prior to the establishment of the data base on the computer, data input forms will be finalized, with some type of instruction manual to the input forms prepared. Additionally, software for processing, plotting and other maintenance operations will have to be developed.

2.5.4 Milestones

The milestones are given in Fig. 2.11. As mentioned previously, the material procurement, data generation and data collection efforts of this subtask will be continuing tasks throughout the contract period. In FY84, the data input forms will be finalized and the instruction manual will be prepared. The initial data collection efforts will be made this year, with actual establishment of the data base by the end of FY84. Coding of the data into system will be initiated shortly thereafter.

Table 2.3 List of Commonly Used Piping Materials to be Included in the Fracture Toughness Data Base

Material Specification	Nominal Diameter (in.)	Wall Thickness (in.)	Typical Application/Comments
SA-516 Gr. 70	30 to 42	2-1/2 to 4-1/2	Straight Pipe and Elbows in Main Coolant Loop/Plate Material formed into Product
SA-106 Gr. C	30 to 42	2-1/2 to 3	Straight Pipe in Main Coolant Loop/Seamless Pipe
SA-351 Gr. CF8M	30 to 32	2 to 2-1/2	Straight Pipe and Safe-ends in Main Coolant Loop/Cent. Cast 316
SA-351 Gr. CF8M	30 to 32	2-1/2 to 3	Elbows in Main Coolan Loop/Cont. Cast 316
SA-351 Gr. CF8A	30 to 32	2 to 2-1/2	Straight Pipe and Safe-ends in Main Coolant Loop Cont. Cast 304
SA-351 Gr. CF8A	30 to 32	2-1/2 to 3	Elbows in Main Coolant Loop/Cent. Cast 304
SA-351 Gr. CF8M	12	Sch. 160	Surge Line and Branch Pipe Safe-ends/Cent. Cast 316
SA-182 F316	30 to 32	2-1/2 to 3	Safe-end in main coolant loop/Forging 316
SA-182 F316	12	Sch. 160	45° and 90° Branch Nozzle in Main Coolant Loop/Forging 316
SA-182 F316	4 to 6	Sch. 80 to 160	Branch Nozzles in Main Coolant Loop/Forging 316
SA-182 F304	30 to 32	2-1/2 to 3	Safe-end in Main Coolant Loop/Forging 304
SA-182 F304	12	Sch. 160	45° to 90° Branch Nozzle in Main Coolant Loop/Forging 304
SA-182 F304	4 to 6	Sch. 80 to 160	Branch Nozzles in Main Coolant Loop/Forging 304
SA-376 Type 316	12	Sch. 160	Surge Line and Branch Line Safe-ends/Seamless Pipe 316
SA-376 Type 316	4 to 6	Sch. 80 to 160	Auxiliary Piping/Seamless Pipe 316
SA-376 Type 304	4 to 12	Sch. 80 to 120	BWR Piping/Seamless Pipe 304
SA-376 Type 304	20 to 24	Sch. 160	BWR Piping/Seamless Pipe 304
SA-358 Gr. 304 Cl.1	4 to 12	Sch. 80 to 120	BWR Piping/Welded Pipe 304
SA-106 Gr. B	4 to 12	Sch. 80 to 120	BWR Piping/Seamless Pipe-Carbon Steel
SA-105 Gr. 2	4 to 12	Sch. 80 to 160	Branch Pipe Nozzles/Carbon Steel Forging
Weld: SA-516 Gr. 70 to SA-516 Gr. 70	30 to 42	2-1/2 to 4-1/2	Pipe to Pipe or Pipe to Elbow Weld in Main Coolant Loop/Field Weld
Weld: SA-106 Gr. C to SA-516 Gr. 70	30 to 42	2-1/2 to 3	Pipe to Elbow Weld in Main Coolant Loop/Field Weld
Weld: SA-106 Gr. C to SA-351 CF8M	30 to 42	2-1/2 to 3	Pipe to Safe-end Dissimilar Metal Weld/Field Weld
Weld: SA-106 Gr. C to SA-182 F316	30 to 42	2-1/2 to 3	Pipe to Safe-end Dissimilar Metal Weld/Field Weld
Weld: SA-376 Type 316 to SA-182 F316	4 to 12	Sch. 80 to 160	Pipe to Safe-end (Forging) Weld/Field Weld
Weld: SA-376 Type 316 to SA-351 Gr. CF8M	4 to 12	Sch. 80 to 160	Pipe to Safe-end (Cent. Cast Pipe) Weld/Field Weld

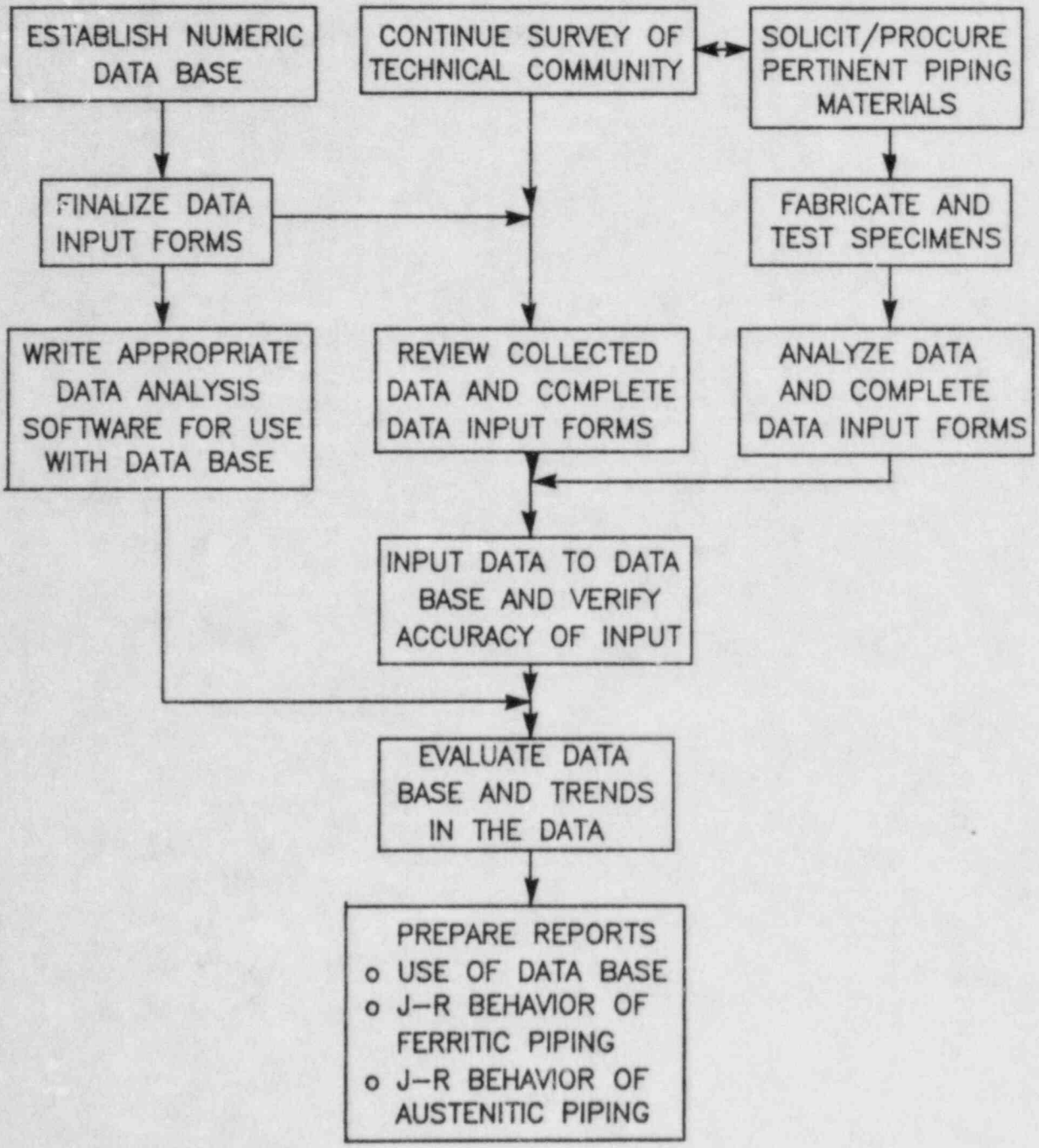

Figure 2.10 Flow Diagram for Subtask 1e: Piping Fracture Mechanics Data Base

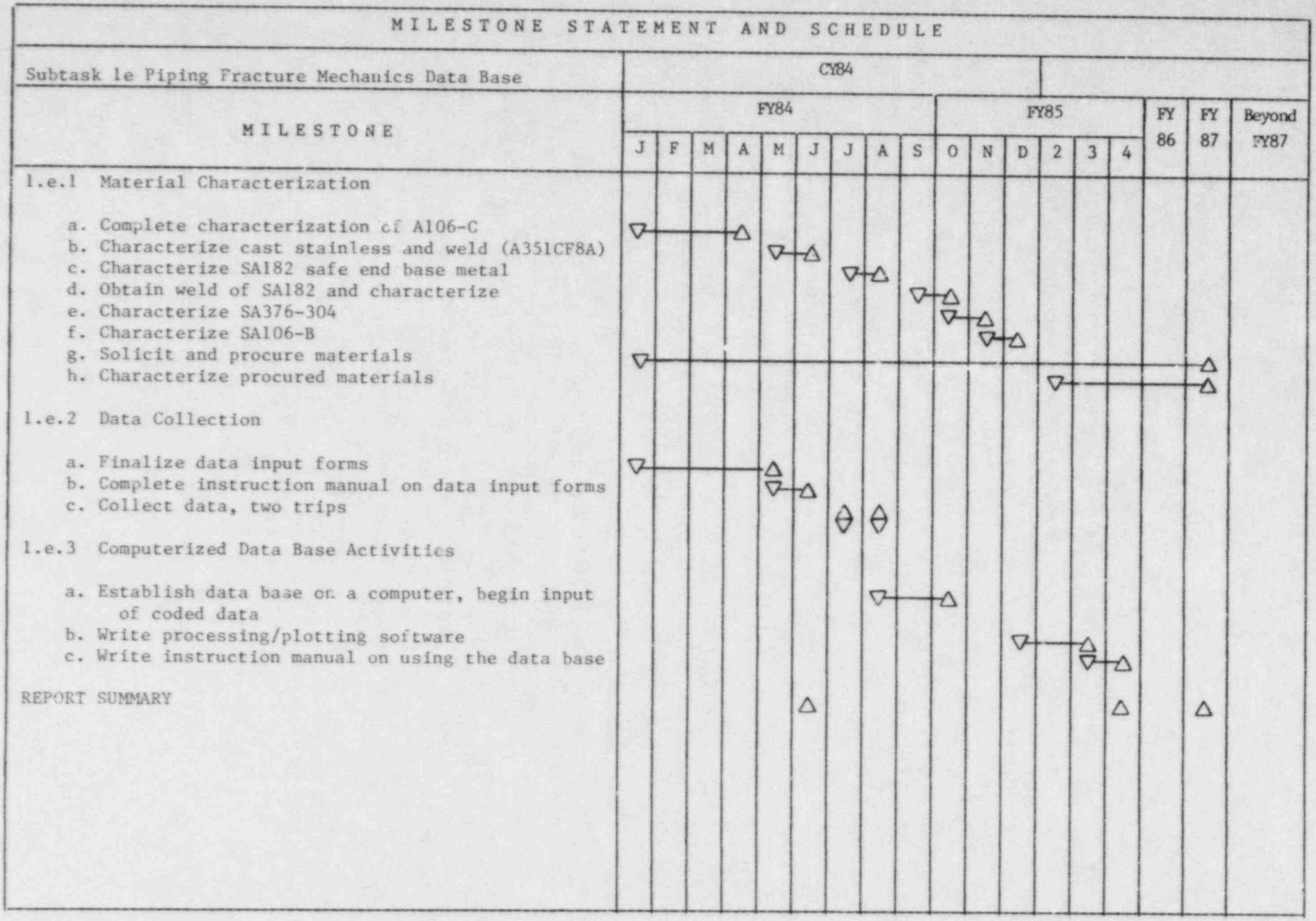

Figure 2.11 Milestone Statement and Schedule for Subtask 1e

2.6 Subtask 1f HSST 4th Irradiation Fracture Toughness

2.6.1 Objective

The primary objective is to characterize the elastic-plastic upper shelf fracture toughness (K_{Jc}) and transition region behavior (K_{Ic}/K_{Jc}) of irradiated steels and welds representing current reactor vessel practice (i.e., low copper impurity level). Sufficient specimens will be tested to provide statistical analysis of the data as far as is practical.

2.6.2 Background

This subtask is part of the larger HSST program sponsored by the Nuclear Regulatory Commission. The HSST 4th Irradiation Program is an ongoing cooperative study between MEA and ORNL with each laboratory testing approximately half of the specimens. Program materials consist of four nominally A 533 Gr. B composition submerged-arc welds having copper contents of 0.04%, 0.046%, 0.056% and 0.12% and one A 533-B plate (HSST Plate 02) with a copper content of 0.14%. From each of these materials specimens were machined and irradiated by ORNL. The specimen complement is shown in Table 2.4.

Currently, all unirradiated specimens and all irradiated Charpy and tensile specimens have been tested. Only the irradiated compact specimens remain to be tested.

2.6.3 Plan of Action

Figure 2.12 is a flow chart which describes the general plan of action. The remaining irradiated compact specimen tests will be tested in the same sequence as the unirradiated compact specimens. First, scoping tests for each material will be conducted to define the transition region temperature range. Temperatures for these tests will be chosen based on the transition shift determined with Charpy specimens. Once the scoping testing and test analysis are complete, test temperatures for the remaining specimens designated for the transition region will be decided jointly by MEA and ORNL. Testing, to define the upper shelf properties will immediately follow completion of the scoping tests; the main matrix transition region tests will then follow these.

A few specimens from each material will be reserved until all main matrix tests are complete. These specimens will be used to fill in areas requiring additional data and to resolve ambiguities that occur.

2.6.4 Milestones

Figure 2.13 illustrates the milestones and anticipated schedule for Subtask 1f.

Table 2.4 Specimen Complement for the 4th HSST Irradiation Program

SPECIMEN TYPE	MATERIAL TYPE	UNIRRADIATED	IRRADIATED	PURPOSE	TOTAL
Charpy[a]	A 533-B Plate	60	50	USE & Trans	110
Charpy[a]	S/A Weld 68W	--	28	USE & Trans	28
Charpy[a]	S/A Weld 69W	50	25	USE & Trans	75
Charpy[a]	S/A Weld 70W	25	33	USE & Trans	58
Charpy[a]	S/A Weld 71W	25	31	USE & Trans	56
Tensile[a]	A 533-B Plate	14	6	Tensile Properites	20
Tensile[a]	S/A Weld 68W	6	5	Tensile Properites	11
Tensile[a]	S/A Weld 69W	12	6	Tensile Properites	18
Tensile[a]	S/A Weld 70W	12	5	Tensile Properites	17
Tensile[a]	S/A Weld 71W	12	5	Tensile Properites	17
1T-CT	A 533-B Plate	52[a]	60	K_{Ic}/K_{Jc}, R Curve	112
1T-CT	S/A Weld 68W	18[a]	30	K_{Ic}/K_{Jc}, R Curve	48
1T-CT	S/A Weld 69W	37[a]	30	K_{Ic}/K_{Jc}, R Curve	67
1T-CT	S/A Weld 70W	21[a]	30	K_{Ic}/K_{Jc}, R Curve	51
1T-CT	S/A Weld 71W	21[a]	30	K_{Ic}/K_{Jc}, R Curve	51

[a] These specimens have been tested.

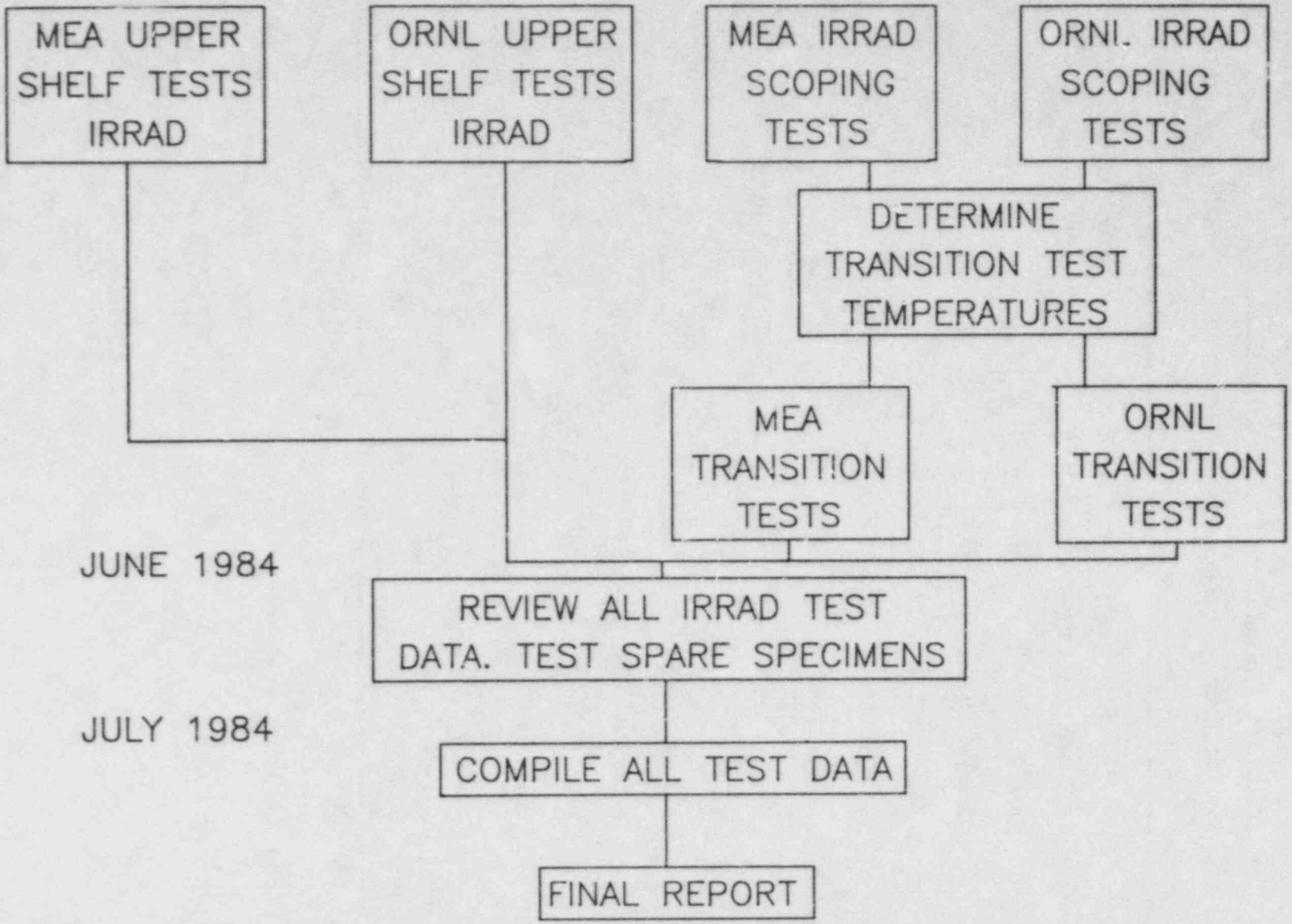

Figure 2.12 Flow Diagram for Subtask 1f: HSST 4th Irradiation Fracture Toughness

MILESTONE STATEMENT AND SCHEDULE

Subtask 1f: HSST 4th Irradiation Fracture Toughness

MILESTONE	CY84															FY 86	FY 87	Beyond FY87
	FY84									FY85								
	J	F	M	A	M	J	J	A	S	O	N	D	2	3	4			
1.f.1 Unirradiated Testing			▲															
1.f.2 Irradiated Testing																		
a. Scoping tests				▽	△													
b. Main matrix					▽	△												
1.f.3 Complete Remaining Unirradiated and Irradiated Tests						▽	△											
1.f.4 Joint MEA/ORNL NUREG										▽		△						
REPORT SUMMARY												△						

Figure 2.13 Milestone Statement and Schedule for Subtask 1f

2.7 REFERENCES

2.1 R. D. Cheverton, et al., "PWR Pressure Vessel Integrity During Overcooling Accidents: A Parametric Analysis," USNRC Report NUREG/CR-2895, February 1983.

2.2 "Heavy-Section Steel Technology Program, Quarterly Progress Report for July-September 1981," USNRC Report NUREG/CR-2141, Vol. 3, 1981.

2.3 "Heavy-Section Steel Technology Program, Quarterly Progress Report for January-March 1982," USNRC Report NUREG/CR-2751, Vol. 1, 1982.

2.4 "Heavy-Section Steel Technology Program, Quarterly Progress Report for April-June 1982," USNRC Report NUREG/CR-2751, Vol. 2, 1982.

2.5 "Evaluation and Prediction of Neutron Embrittlement in Reactor Pressure Vessel Materials," EPRI NP-2782, Final Report, J. R. Hawthorne, ed., Electric Power Research Institute, Palo Alto, CA, Dec. 1982.

2.6 J. R. Hawthorne, B. H. Menke and A. L. Hiser, "Notch Ductility and Fracture Toughness Degradation of A 302-B and A 533-B Reference Plates from PSF Simulated Surveillance and Through-Wall Irradiation Capsules," USNRC Report NUREG/CR-3295, MEA-2017, in press.

2.7 T. C. Harrison and G. D. Fearnehough, "The Influence of Warm Prestressing on the Brittle Fracture of Structures Containing Sharpy Defects," Trans. ASME, J. Basic Engrg., Vol. 94, June 1972, pp. 373-376.

2.8 L. P. Harrop, "Warm Prestressing During Severe Thermal Shock Loading of a Pressure Vessel," Int. J. of Pressure Vessels and Piping, Vol. 7(6), Nov. 1979, p. 463.

2.9 J. R. Rice, "Mechanics of Crack Tip Deformation," ASTM STP 415, 1967, p. 247.

2.10 G. G. Chell, "A Fracture Mechanics Approach to Predicting the Effects of Warm Prestressing and its Application to Pressure Vessels," Fifth Int. Conf. on Structural Mechanics in Reactor Technology, Paper 99/6, Berlin, Aug. 1979.

2.11 D. A. Curry, "A Micromechanistic Approah to the Warm Prestressing of Ferritic Steels," CERL Lab Note RD/L/N103/79, Sept. 1979.

2.12 F. J. Loss, R. A. Gray and J. R. Hawthorne, "Significance of Warm Prestress to Crack Initiation During Thermal Shock," NRL Report 8165, Naval Research Laboratory, Sept. 1977.

2.13 F. J. Loss, R. A. Gray and J. R. Hawthorne, "Investigation of Warm Prestress for the Case of Small T During a Reactor Loss-of-Coolant Accident," NRL Report 8198, Naval Research Laboratory, Mar. 9, 1978.

2.14 R. D. Cheverton, "Thermal Shock Investigations, Heavy Section Steel Technology Program, Quarterly Progress Report for July-September 1980," USNRC Report NUREG/CR-1806, Dec. 1980, pp. 31-52.

2.15 P. C. Paris, H. Tada, A. Zahoor and H. Ernst, "The Theory of Instability of the Tearing Mode of Elastic-Plastic Crack Growth," Elastic-Plastic Fracture, ASTM STP 668, 1979.

2.16 J. W. Hutchison and P. C. Paris, "Stability Analysis of J-Controlled Crack Growth," Elastic-Plastic Fracture, ASTM STP 668, 1979.

3.0 TASK 2 - ENVIRONMENTALLY-ASSISTED CRACK GROWTH IN LWR MATERIALS

In developing crack initiation and growth data for nuclear reactor safety applications, the complex combinations of environment, materials, stress, and structural geometry must be considered. Characterization of the environments can be made on the basis of either the boiling water or pressurized water reactor designs. Reference 3.1 gives the basic chemistry for each of these. Since transients in the chemistry do occur, they are a legitimate concern in understanding the relationship of the laboratory data to the operating reactor situation. Itemization of the materials shows that there are more than thirty iron-base alloys, exclusive of the welds, used in the primary system of common light water reactors (Ref. 3.2). Characterization of the stress varies with the reactor design and operational characteristics, but the basic transients have been identified and evaluated. A reasonably condensed, comprehensive analysis of these load spectra is available (Ref. 3.3). Largely due to improved computational techniques, the influence of structural geometry, including far-field stresses and the redistribution of stresses with growing cracks, is becoming more understandable.

The recognition that fatigue criteria should be incorporated in the ASME Boiler and Pressure Vessel Code (BPVC) came in the mid-1950's. Primarily through the experimental work of Coffin and colleagues (Ref. 3.4), and the design analysis procedures suggested by Langer (Ref. 3.5), a design curve for thermally-induced stresses was derived. In its original version, this method incorporated a Goodman diagram to account for mean stress effects, Miner's rule for evaluating the cumulative effect of various stresses, and maximum shear theory to calculate the combined stress levels.

During the intervening years, some work has been completed on the environmentally-degraded fatigue life of both smooth and notched fatigue specimens. Much of this work has been carried out in boiling water reactor environments and shows a band of data which uses up essentially the safety margins incorporated into the Code. Matching results for the PWR environment are not available, but will be generated as part of the present study.

Whereas development of the ASME-BPVC Section III (Ref. 3.6) design curves was concluded in the mid-1950's, the research leading to development of the ASME-BPVC Section XI - Appendix A reference curves (Ref. 3.7) for fatigue crack growth was just beginning about that time, with the first successful results published during 1971-1972. Results for BWR environments were described by Kondo (Ref. 3.8), and by a team from the Nuclear Technology Division at General Electric in San Jose, California (Ref. 3.9). Results for both BWR and PWR environments were generated by a group of scientists at Westinghouse Nuclear Technology Division, as part of the HSST program (Ref. 3.10). In spite of the technological shortcomings of the research equipment (as judged by today's standards), these data have withstood the test of time and reside within the currently known band of data which describes the fatigue crack growth rate response in each of the two environments.

In formulating the technical approach to this task, every attempt has been made to build on the significant body of knowledge and data presently available. The task is composed of seven subtasks that span the phenomena of crack nucleation and growth. (An eighth subtask provides for participation in the activities of the International Cyclic Crack Growth Rate (ICCGR) Group.)

Completion of these various subtasks will provide, for the first time, a comprehensive picture of the development and growth of an environmentally-assisted flaw in a nuclear reactor component. It is most important that each of the seven sections is considered in the context of the entire Task 2 program.

These subtasks interact with one another in a scientific way -- in that data from one supplies input to another -- and in a management way -- in that some subtasks cannot start until others have ended. Figure 3.1 is a block diagram of these subtasks showing how these investigations link together and how data and findings for some subtasks will feed other subtasks. This global view shows that all phases of environmental degradation are considered in this proposed work. Cracks will be studied from their development in unflawed specimens and piping specimens and monitored for their two-dimensional growth characteristics as they progress from small to large. Task 2 will explore also the application of these findings to reactor component materials, geometries and environmental situations.

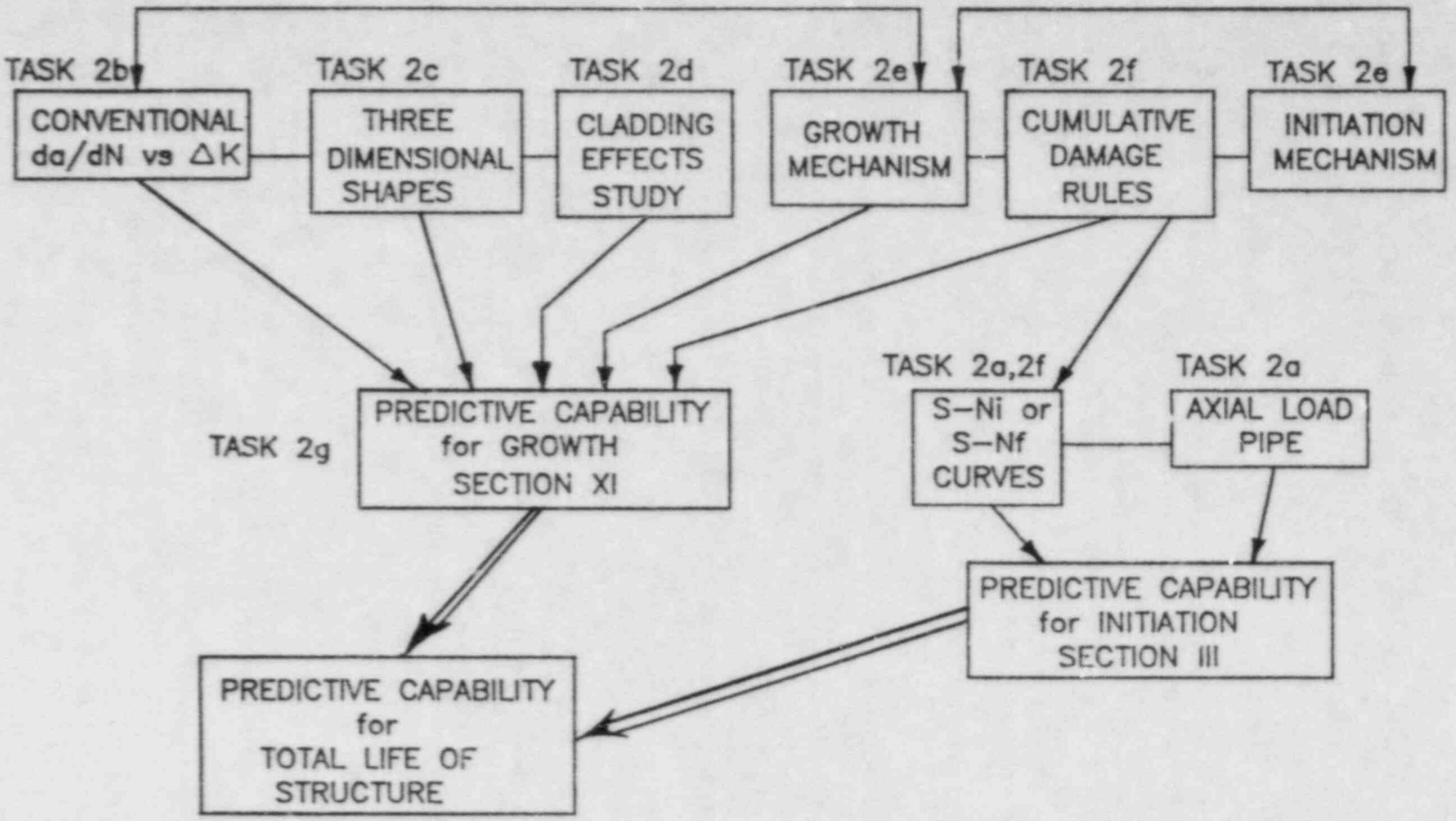

Figure 3.1 Subtask Interactions for Task 2: Environmentally-Assisted Crack Growth In LWR Materials

3.1 Subtask 2a S-N Curves for Nuclear Grade Steels in PWR Environments

3.1.1 Objective

The objectives of this subtask are to (a) evaluate the effects of a simulated PWR environment on the stress vs. life curves for a typical LWR material and (b) develop data to support potential modifications to the ASME S-N design curves.

3.1.2 Background

The experimental work of Coffin and colleagues (Ref. 3.4), and the design work of Langer (Ref. 3.5) formed the basis for the introduction of fatigue design curves to Section III of the ASME Code. These curves give an estimate of cyclic life as a function of extrapolated elastic stress for the material in question. Different curves have been developed for the basic classes of materials which are found in pressure vessel and piping systems: stainless steels, low-alloy steels, non-ferrous alloys (Inconel, etc.) and bolting steels. The stress values to be used in the application of these fatigue design curves comes from a tabulation of pressure-, moment-, and thermal-induced loads, together with a set of piping system analysis rules which are found in Section NB-3600 of the Code.

The structural applicability of the Code stress analysis rules and the design curve data was "verified", in the mid 1960's by a series of structural tests of pressure vessels (Ref. 3.11). However, some recent tests by General Electric (Ref. 3.12) have suggested that inadequacies in the stress analysis procedures, coupled with the presence of a BWR environment (i.e., 0.2 ppm dissolved oxygen in 288°C water) can result in non-conservative life estimates. The potential problems with the analysis procedures are being examined as part of the Section III Committee effort. However, the potential for the environment to significantly reduce the margin of safety is being explored further as part of this program.

MEA will carry out an effort, somewhat parallel to the General Electric effort, to examine the effects of the low-dissolved oxygen, PWR environment on cyclic life and crack initiation. The early work seeks to evaluate the possible effect of the PWR environment in the context of smooth specimens. Presuming that a significant effect is found, the balance of the effort is devoted to developing a data base which could be used in formulating Code revisions.

3.1.3 Plan of Action

Figure 3.2 is a flow chart which describes the general plan of action and shows the major blocks of effort. The first phases of testing under this subtask will be to determine the smooth specimen design curve for a low-carbon piping steel (A 333 Gr. 6) in an air environment at 288°C (550°F), and to determine the effects of test frequency on cyclic life in pressurized, high-temperature (288°C) water. In the latter case, tests will be conducted over a frequency range of 1 Hz to 17 mHz, with cyclic life targets of 10 to 10^5 cycles. Pending the results of the frequency sensitivity study, the size of the balance of the test matrix can be determined. The matrix will be extended to cover load-ratio (mean stress) effects, and notch geometries in smooth specimens of base metal and weld metal specimens.

The culmination of the program is the testing of 0.65 m-long sections of 102 mm-diameter (4-inch nominal pipe diameter), girth-welded A 106 Gr. B pipe. These tests will be conducted in the autoclaves which have been dedicated to multispecimen tests during the forerunner of this program. It is anticipated that tests will be run covering a stress ratio range including 0.05, 0.50 and 0.80, in the aqueous environment for specific cyclic life targets, and a full cyclic life series, at a stress ratio of 0.05, for air environment tests.

3.1.4 Milestones

The milestone charts for this subtask are shown in Fig. 3.3. This subtask constitutes a major portion of the program in the environmentally-assisted crack growth task area. The program spans all four years of the contract period, and at its peak, in the latter part of the third year, will require three autoclave units for small specimen testing, and two autoclaves for the pipe tests.

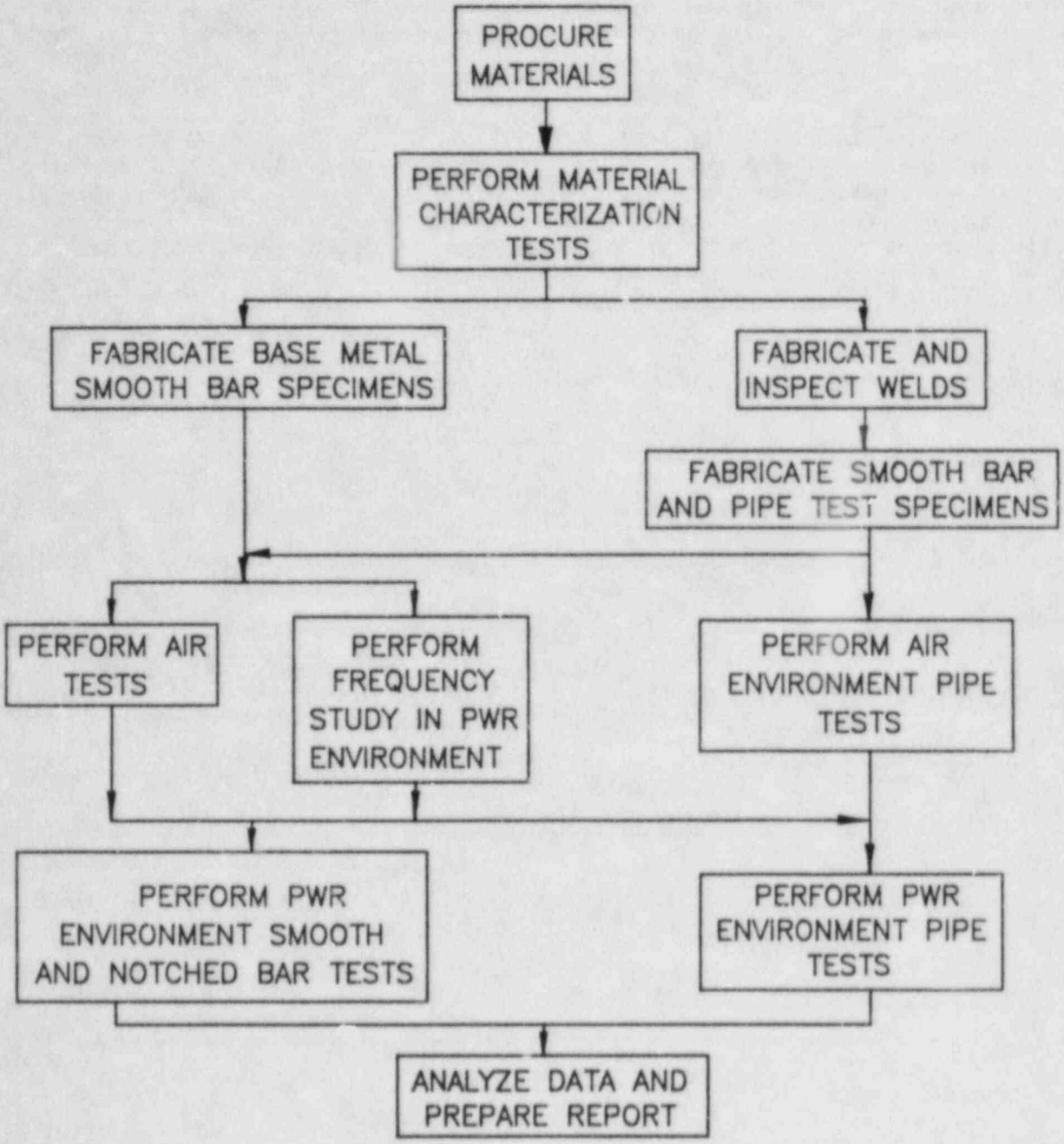

Figure 3.2 Flow Diagram for Subtask 2a: S-N Curves for Nuclear Grade Steels In PWR Environments

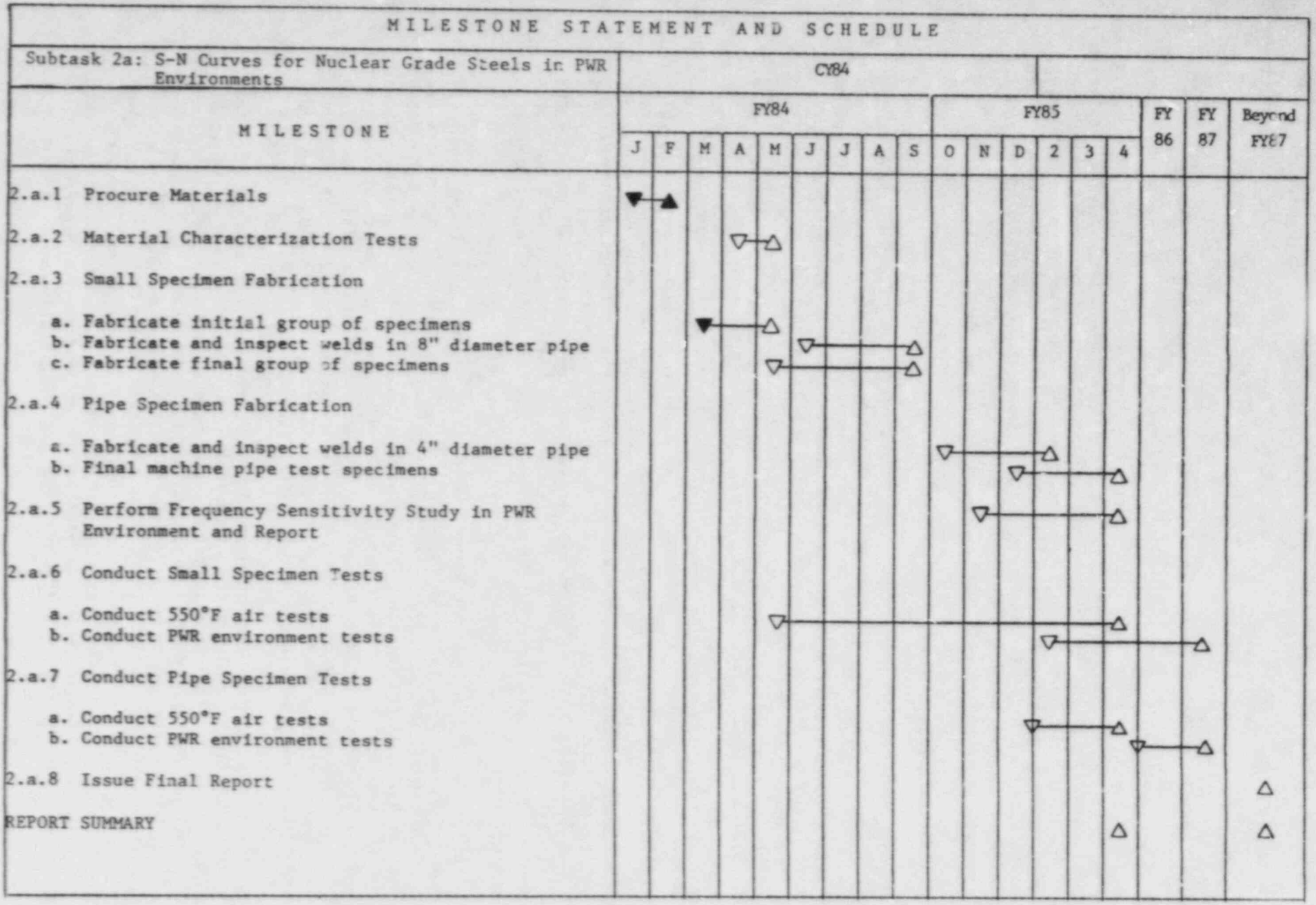

Figure 3.3 Milestone Statement and Schedule for Subtask 2a

3.2 Subtask 2b Environmentally-Assisted Fatigue Crack Growth

3.2.1 Objective

The objective of this subtask is to continue an on-going program aimed at the development of da/dN vs. ΔK data for a wide variety of pressure vessel and piping materials. The emphasis is on extending the range of selected variables for the materials being tested. To this end, the load ratio range to be investigated will be increased to 0.95. Orientation studies and material chemistry studies will be expanded to cover more materials. Stainless, low-alloy and low-carbon steels are part of this test matrix.

3.2.2 Background

Fatigue crack growth rate (FCGR) and stress-corrosion cracking (SCC) tests, utilizing conventional fracture mechanics specimens [Compact Tension (CT) and Wedge-Opening Load (WOL)] have been the backbone of the NRC-sponsored program on environmental effects since its inception in the mid-1970's. These specimens were used for two primary reasons: (1) they are very conservatively sized, making the most of a given volume of material, and (2) the strong functional dependence of crack length on compliance makes it relatively easy and accurate to calculate crack extension.

Use of these specimens in several programs with various test parameter matrices has resulted in recognition of several critical variables which determine crack growth rates in pressurized, high-temperature reactor-grade water. One of the first recognized trends was that sinusoidal waveforms consistently produced higher crack growth rates than "linearized" waveforms, such as ramp-and-hold, or sawtooth profiles (Ref. 3.13). Subsequent research showed at first that a 17 mHz sinusoidal waveform seemed to maximize the growth rate, but some very recent work seems to indicate that this maximization might also be a function of load ratio and possibly material chemistry (Ref. 3.14).

Shortly after the above conclusion was reached, allowing a large amount of data to be sorted out, it was realized that sulfur content in these pressure vessel steels had a major influence on fatigue crack growth rates (Ref. 3.15). Older pressure vessel steels, usually with a higher sulfur content, were exhibiting crack growth rates which exceeded the reference line found in Appendix A of the 1974 edition of Section XI of the ASME Code. Even before the connection with sulfur chemistry had been directly proven, the code was amended (Winter 1980 Addendum) with new reference lines which had a bilinear shape and incorporated a load ratio rule.

Other variables were investigated and found to have varying degrees of effect on fatigue crack growth rates. Irradiation was found to have a negligible effect (Ref. 3.16) for three types of vessel steel A 508-2, A 533B, and a heat of submerged-arc weld metal. Researchers in the UK (Ref. 3.17) showed that temperature has a significant effect, with a distinct minimum in growth rates at temperatures of about 200°C. This is in direct contrast to earlier, Japanese results for the BWR environment (Ref. 3.18) which showed a maximum in growth rates at about the same temperature. Current interpretations of this difference take into account the significant effects of the higher level of dissolved oxygen content in the two (PWR and BWR) environments. Additional

work shows that there are orientation effects (Ref. 3.15), as well as other microstructurally-related effects (Refs. 3.19).

3.2.3 Plan of Action

Figure 3.4 is a flow chart which describes the general plan of action and shows the major blocks of effort. The effort under this subtask will be phased out during the term of this contract period, with testing to terminate toward the end of the third year. The general plan is to extend the range of investigation into the known critical variables, and to continue to incorporate new heats of pressure vessel and piping steel into the program. Use of bolt-loaded specimens to investigate stress-corrosion cracking susceptibility will continue under this program.

Specifically, tests will be carried out at load ratios of 0.85 and 0.95, principally on piping steels, to complete the series of tests already conducted at load ratios of 0.2 and 0.7. Axial and circumferential orientations will be included in the test plan. A more complete orientation study will be conducted on pressure vessel steels, in support of work on part-through cracks in Subtask 2c.

3.2.4 Milestones

The milestone charts for this subtask are shown in Fig. 3.5. This subtask will be phased out over the first three years of the contract period.

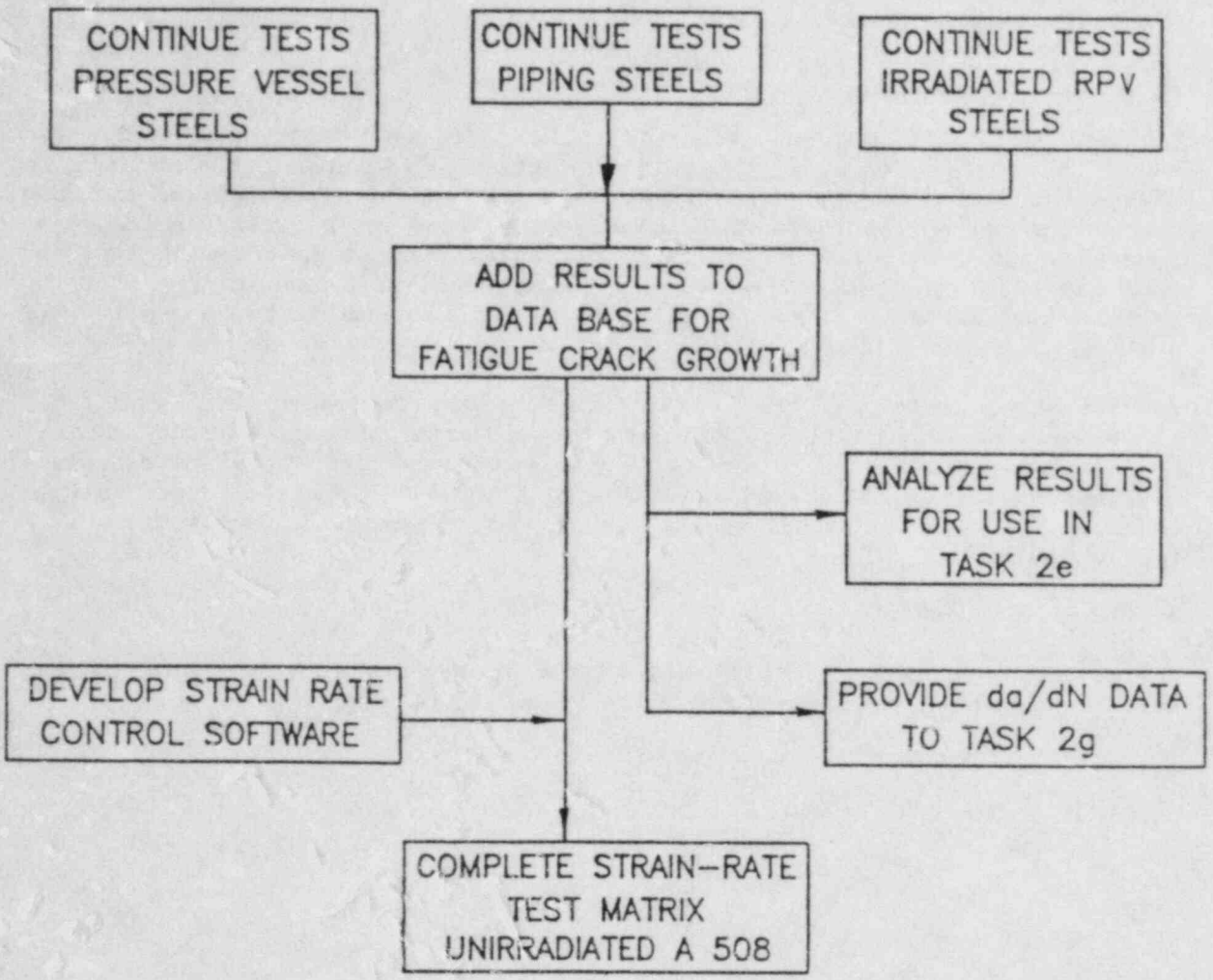

Figure 3.4 Flow Diagram for Subtask 2b: Environmentally-Assisted Fatigue Crack Growth

MILESTONE STATEMENT AND SCHEDULE

Subtask 2b: Environmentally-Assisted Fatigue Crack Growth

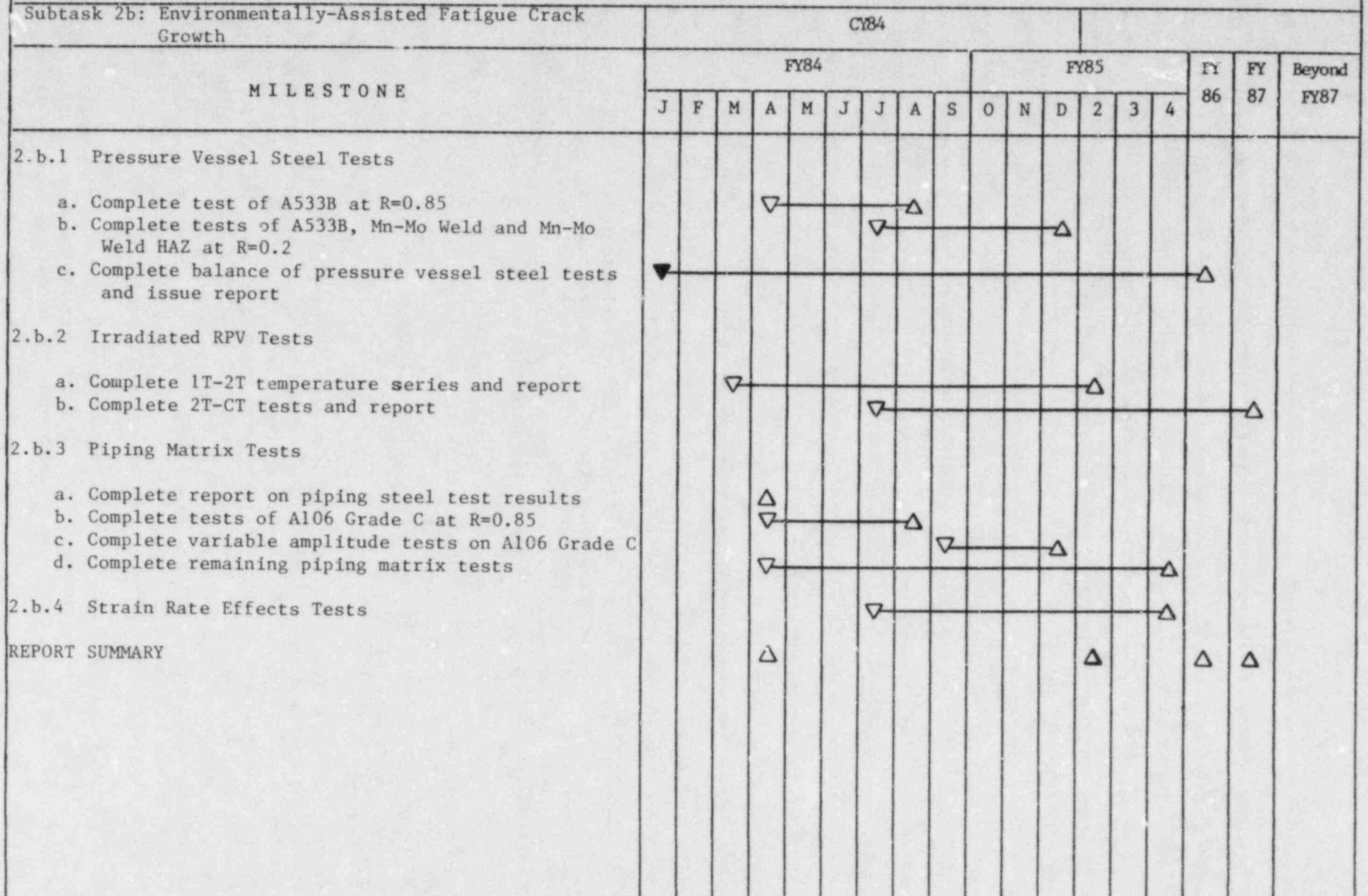

Figure 3.5 Milestone Statement and Schedule for Subtask 2b

3.3 Subtask 2c Effect of Crack Geometry on Environmentally-Assisted Fatigue Crack Growth

3.3.1 Objective

The objective of this subtask is to evaluate the usefulness of CT specimen fatigue crack growth rate data in evaluating/predicting the growth of cracks in "real" structures exposed to "real" environments and 3D constraints.

3.3.2 Background

As indicated in the previous section, testing with through-cracked specimens, principally of the compact tension design, has been the backbone of the data base development of fatigue crack growth data for pressure vessel and piping steels in reactor-grade water environments. However, it has been long recognized that the one-dimensional flaw geometry is not typical of in-service cracks, which are semi-circular, or semi-elliptical when still in the early stages of development. It has been assumed generally that the CT specimen design does provide conservative data. However, as the technology has developed, a number of questions have arisen concerning the potential for the CT specimen to be non-conservative.

There are three major differences (mechanical, metallurgical and environmental) between one- and two-dimensional cracks:

(1) Mechanical: The mechanical component relates to the varying stress intensity factor (K), along the crack front.

(2) Metallurgical: The metallurgical component relates to the inhomogeneous nature of structural materials as a result of thermomechanical processing. It has been shown that orientation effects can cause a difference in fatigue crack growth rates, and it follows that the eccentricity of two-dimensional flaws will be reflected in these different growth rates.

(3) Environmental: The environmental component relates to the potential changes in the environment with crack depth, due to the decreased crack mouth opening with load. This results in less effective "pumping" of the environment, and decreased access of the environment through the crack mouth.

3.3.3 Plan of Action

Figure 3.6 is a flow chart which describes the general plan of action and shows the major blocks of effort. The general plan for this subtask calls for testing CT specimens and PTC specimens from materials typical of LWR pressure boundary components. Four materials have been selected for study, i.e., A 533-B with a "low" sulfur content, an A 533-B with a "medium" sulfur content, an A 106 Grade B pipe and a Type 304 stainless steel plate. For the purpose of fabricating PTC specimens from the A 106 Grade B pipe, rings of pipe will be flattened and stress relieved. Both CT and PTC specimens will be fabricated from the flattened and stress relieved material.

As a parallel, yet separate activity, a facility will be constructed for the purpose of testing pipe specimens subjected to a cyclic pressure loading. The planned facility will be capable of testing using either an inert environment

or a simulated PWR environment. However, the present plan of action includes inert environment tests only.

The data generated from the pipe tests will be contrasted to data generated using CT specimens taken from the as-received pipe.

3.3.4 Milestones

Figure 3.7 shows the milestone schedule for this subtask. The CT and PTC specimen testing will be conducted during the first three years of the program. Construction of the pipe test facility will begin during the third year with the inert environment tests being performed in the last year of the program.

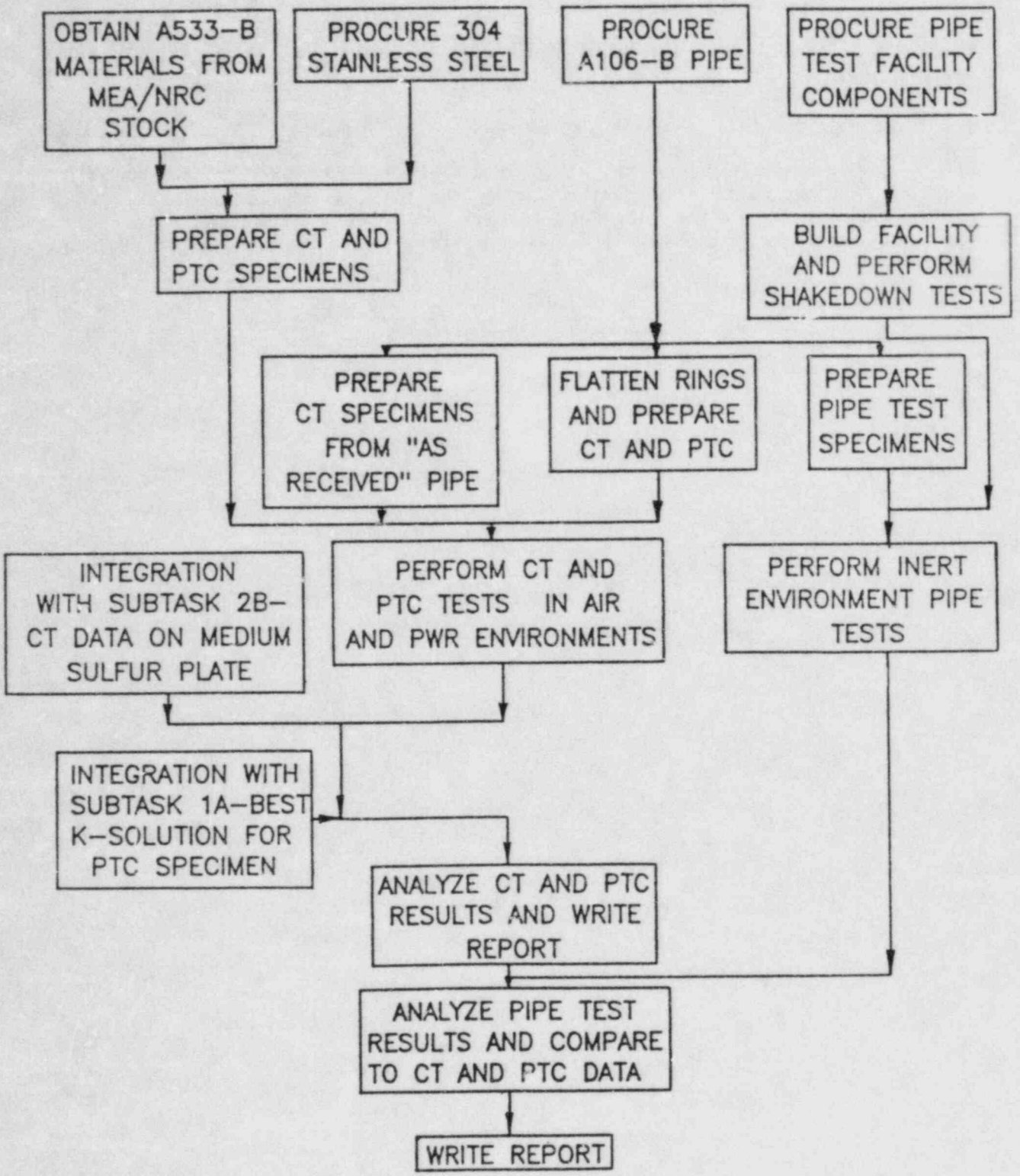

Figure 3.6 Flow Diagram for Subtask 2c: Effect of Crack Geometry on Environmentally-Assisted Fatigue Crack Growth

MILESTONE STATEMENT AND SCHEDULE

Subtask 2c: Effect of Crack Geometry on Environmentally-Assisted Fatigue Crack Growth

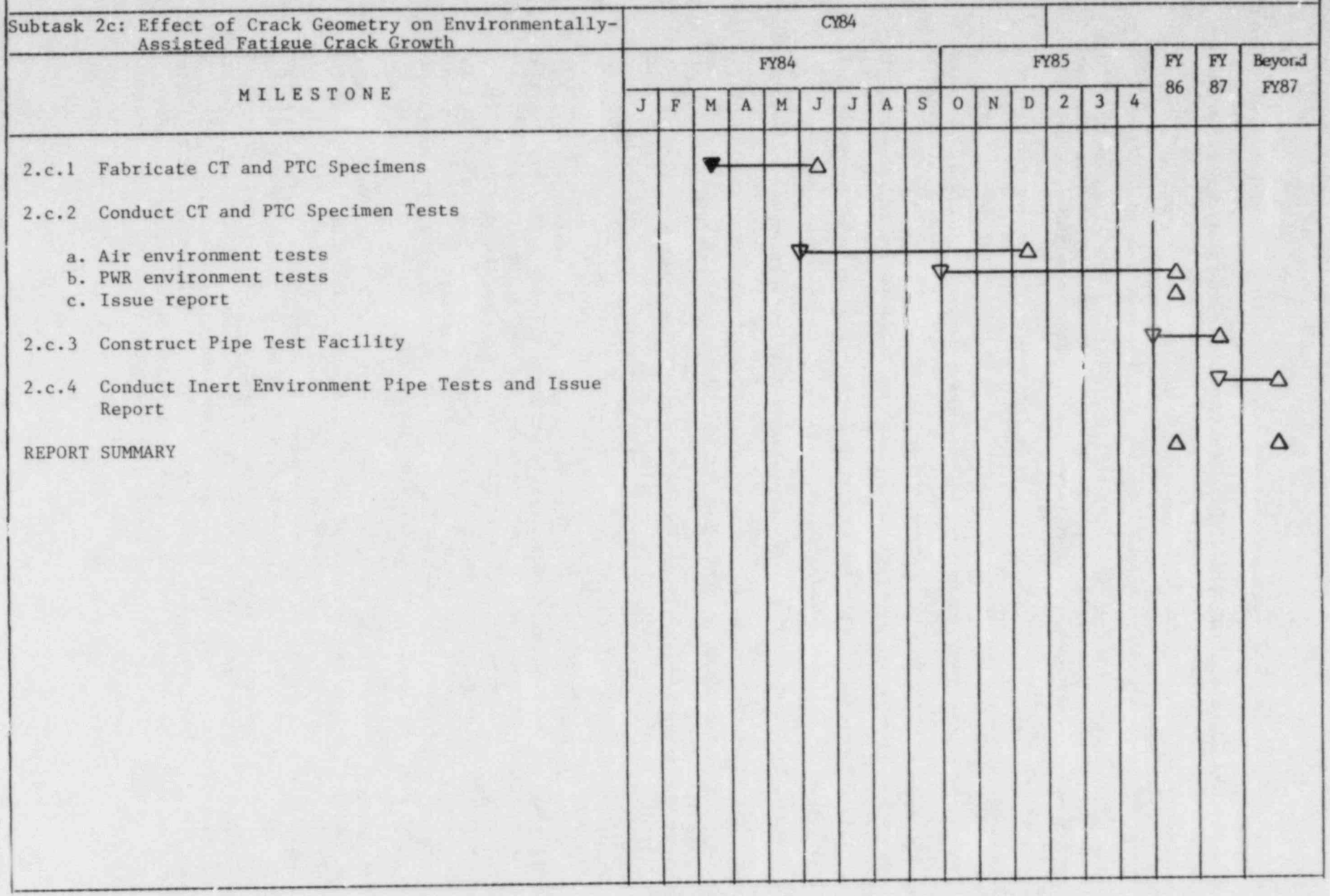

Figure 3.7 Milestone Statement and Schedule for Subtask 2c

3.4 Subtask 2d Effect of Cladding on Environmentally-Assisted Fatigue Crack Growth

3.4 1 Objective

The objective of this subtask is similar to that of Subtask 2c, except that the plates will be clad with stainless weld. Tests will be conducted in both air and water environments. Crack shape and crack growth rates will be compared with those generated in Subtask 2c.

3.4.2 Background

As our understanding of the general fatigue crack growth process has improved, it is appropriate that research advance to the more sophisticated problems of "real" crack growth, and the potential effects of cladding on that growth. In formulating a technical approach to the problem it is important to review the manner in which cladding might influence the growth of "real" cracks. As in the review of Subtask 2c, the differences can be considered in three main respects:

(1) Mechanical: Although the vessel is stress relieved after the cladding is applied, the difference in thermal expansion between the cladding and baseplate results in the cladding being left in tension when the vessel is maintained within the normal operating range of temperatures. If the vessel were to contain a through clad crack, the K_I profile along the crack front would be altered compared to that for an unclad vessel. This altered K_I profile will modify the strains and strain rates along the crack front (compared with the unclad case) and will tend to change the shape of the crack and the crack opening.

(2) Metallurgical: The cladding process results in a heat-affected, diluted-metal zone at the base metal and clad interface. Crack growth rates for this alloyed region are not known, and there is no way of knowing whether this material would be more or less sensitive to environmentally-assisted fatigue crack growth. There is some evidence that fatigue crack growth in cast stainless steel, an alloy similar to clad, is about a factor of two slower than growth rates in low-alloy pressure vessel steel. Hence, crack propagation in the clad may "lag" that in the underlying base plate.

(3) Environmental: There are two possible differences in the mechanisms of environmental influence in the clad case, as opposed to the unclad case. The first is the possible electrochemical effect due to the small difference in potential between the clad and base. Most researchers assume that the difference (probably less than 150 millivolts) is not enough to change the reaction kinetics in a measurable way. The second possible environmental effect is a consequence of the crack shape change which may occur. If the crack in the base does "tunnel" under the clad, due to the expected slower growth rates in the clad, then the environment would be more effectively trapped in the crack enclave. In most cases, the stagnated environment would achieve a lower pH character, and this in turn may increase crack growth rates through a variety of micromechanisms.

3.4.3 Plan of Action

Figure 3.8 is a flow chart which describes the general plan of action and the major blocks of effort. The clad specimens for this subtask will be fabricated, stress relieved and machined along with those in Subtask 1a. The residual stress determinations provided in the context of Subtask 1a will be incorporated in this subtask also. Tests will be conducted in air and water environments, for load ratios of 0.2 and 0.7, and for aspect ratios of 0.5 and 0.1. Tests in air will conducted at two temperatures in order to determine empirically if the thermal expansion contribution to the residual stress distribution has a significant effect on crack shape. Tests in air will be conducted at 10 Hz, while tests in water will be conducted at 17 mHz, in order to maximize the contribution of environmental effects. Direct current potential drop techniques with multiple probes along the mouth of the crack will be used to monitor crack extension and crack shape changes. In addition, beachmarks along the crack front will be used as input to a post-test correction of the two-dimensional crack growth rates.

3.4.4 Milestones

The milestone charts for this subtask are shown in Fig. 3.9. Tests in air environment will be conducted first in order to work out the experimental difficulties associated with the bimetal character of the clad, low-alloy steel. Tests in the PWR environment will commence in the third year.

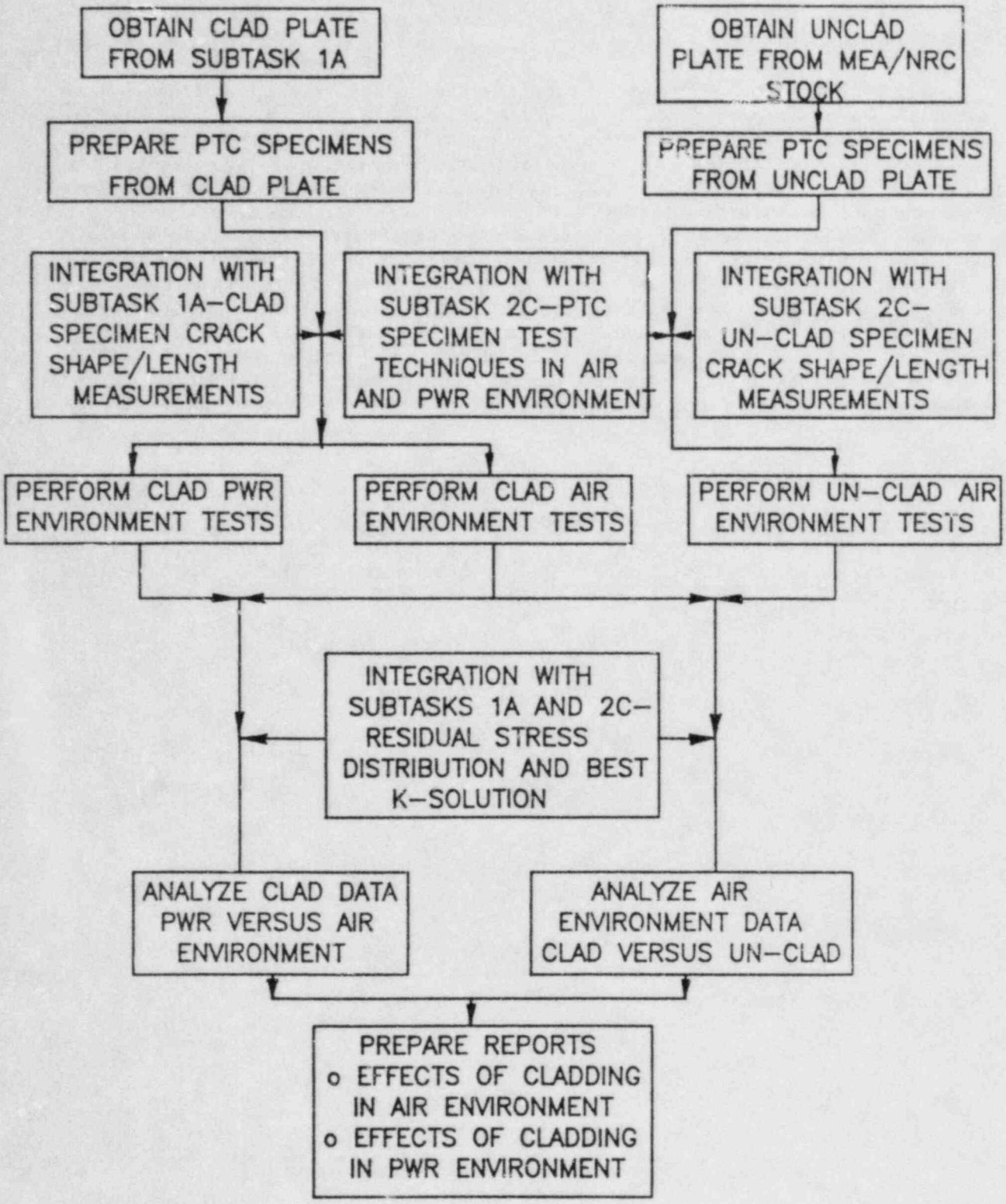

Figure 3.8 Flow Diagram for Subtask 2d: Effect of Cladding on Environmentally-Assisted Fatigue Crack Growth

MILESTONE STATEMENT AND SCHEDULE

Subtask 2d: Effect of Cladding on Environmentally-Assisted Fatigue Crack Growth

CY84

MILESTONE	FY84									FY85						FY 86	FY 87	Beyond FY87
	J	F	M	A	M	J	J	A	S	O	N	D	2	3	4			
2.d.1 Fabrication of Test Materials and Specimens																		
a. Complete cladding and stress relief of plate - see Subtask 1a also					▽	△												
b. Fabricate clad and unclad specimens					▽							△						
c. Characterize microstructure of plate and cladding							▽		△									
2.d.2 Conduct Tests																		
a. Conduct air environment tests and report												▽			△			
b. Conduct PWR environment tests and report															▽			△
REPORT SUMMARY															△			△

Figure 3.9 Milestone Statement and Schedule for Subtask 2d

3.5 Subtask 2e Mechanism Models for Environmentally-Assisted Fatigue Crack Growth

3.5.1 Objective

The objective of this subtask is to identify, describe and refine the micromechanistic model which best explains the characteristics of environmentally-assisted fatigue crack growth in LWR pressure vessel and piping steels.

3.5.2 Background

There are two primary schools of thought about the micromechanism of environmentally-enhanced fatigue crack growth (Refs. 3.13, 3.20-3.22). One espouses a theory of active path (anodic) dissolution, and the other suggests that cracking is hydrogen assisted. While hydrogen assistance is a clearly accepted phenomenon at low and ambient temperatures, it was popularly believed until about 1980, that the diffusion rates of hydrogen in steel at temperatures of about 200°C and higher were so rapid that hydrogen would not accumulate in the plastic zone at the tip of the crack in an amount which would cause a significant amount of "hydrogen embrittlement" as it was then called. Hence, the explanation of the environmental assistance which is observed in tests of pressure vessel and piping steels was based on the theories of anodic dissolution. However, it is difficult to rationalize that the essentially oxygen-free chemistry of the PWR environment would allow the degree of anodic dissolution required to account for the increase in fatigue crack growth rates. Also, in the early 1980's, it was found that fatigue fracture surfaces of pressure vessel steels tested in pressurized, high-temperature water were characterized by brittle-like features, including brittle striations, fan-shaped cleavage-like facets, and microcracking — all features which were principally associated with hydrogen-assisted cracking (Ref. 3.13). Since that time, several investigators have suggested that, temperature notwithstanding, hydrogen-assisted cracking might be a viable candidate for interpretation of reactor environment cracking.

Both parties to this discussion agree that in the electrochemical corrosion reaction, there is an oxidation/ reduction balance, and that atomistic hydrogen is produced as well as a surface oxide. Therefore, the rate-determining steps for both reactions are the same, and it will be difficult to construct a critical experiment which will unequivocally show that one or the other is responsible for the environmental enhancement of fatigue crack growth. Resolution of the dilemma is likely to come about through observation of the external variables (such as water chemistry, temperature, and material chemistry) which affect crack growth rates, and metallographic and fractographic analysis of fatigue and fracture surfaces. There is considerable research currently being carried out in these areas.

Because in-service cracking in BWR plants has been a costly industry problem, and the focus of attention in a number of research laboratories, the investigations into the mechanisms of cracking in PWR water has not proceeded apace. Interest in the problem has resulted recently in the funding of several research programs which do address the PWR situation, and some of these results and conclusions are now becoming available.

3.5.3 Plan of Action

Figure 3.10 is a flow chart which describes the general plan of action and shows the major blocks of effort. The first segment within the subtask is to assemble a document which will review the present state-of-the-art in environmentally-assisted cracking in the PWR environment. This review will also present an interpretation of the mechanisms which seem to prevail, and will suggest a series of laboratory experiments which would help to clarify the mechanism or its kinetics. These experiments might involve, but not be limited to, the following:

(1) Continue fractographic and metallographic observations of post-test fatigue fracture surfaces.

(2) Conduct tests with "poisoned" water chemistry, which would alter the kinetics, in a known way, of one or more of the micromechanistic processes of corrosion.

(3) Conduct tests in hydrogen-bearing environments, such as hydrogen gas, hydrogen sulfide gas, or bicarbonate or biphosphate solutions, to see if the additional hydrogen, beyond that produced by hydrolysis, further increases the hydrogen assistance.

(4) Tests with a "backfed" specimen, tested in an inert atmosphere, or vacuum, in which the hydrogen is provided, by hydrolysis, to the straining plastic zone behind the crack tip. If the fractographic features continue to appear to have brittle-like character, then the source of the hydrogen input to the plastic zone is not the question, and the absence of any possibility of oxidation (i.e., no aqueous environment) will preclude the oxidation reaction at the crack tip.

(5) Tests with specimens in which the environment is fed, via capillary tubes, directly to the crack tip. By forcibly refreshing the environment at the crack tip and canceling out stagnation of the environment in the enclave, the concomitant increase in pH and increase in oxygenation should alter the crack growth kinetics in some proportion to the chemistry of the pumped environment.

3.5.4 Milestones

The milestone charts for this subtask are shown in Fig. 3.11. Compilation of the review document is expected to take most of the first year of the program, with the experimental effort to follow afterward.

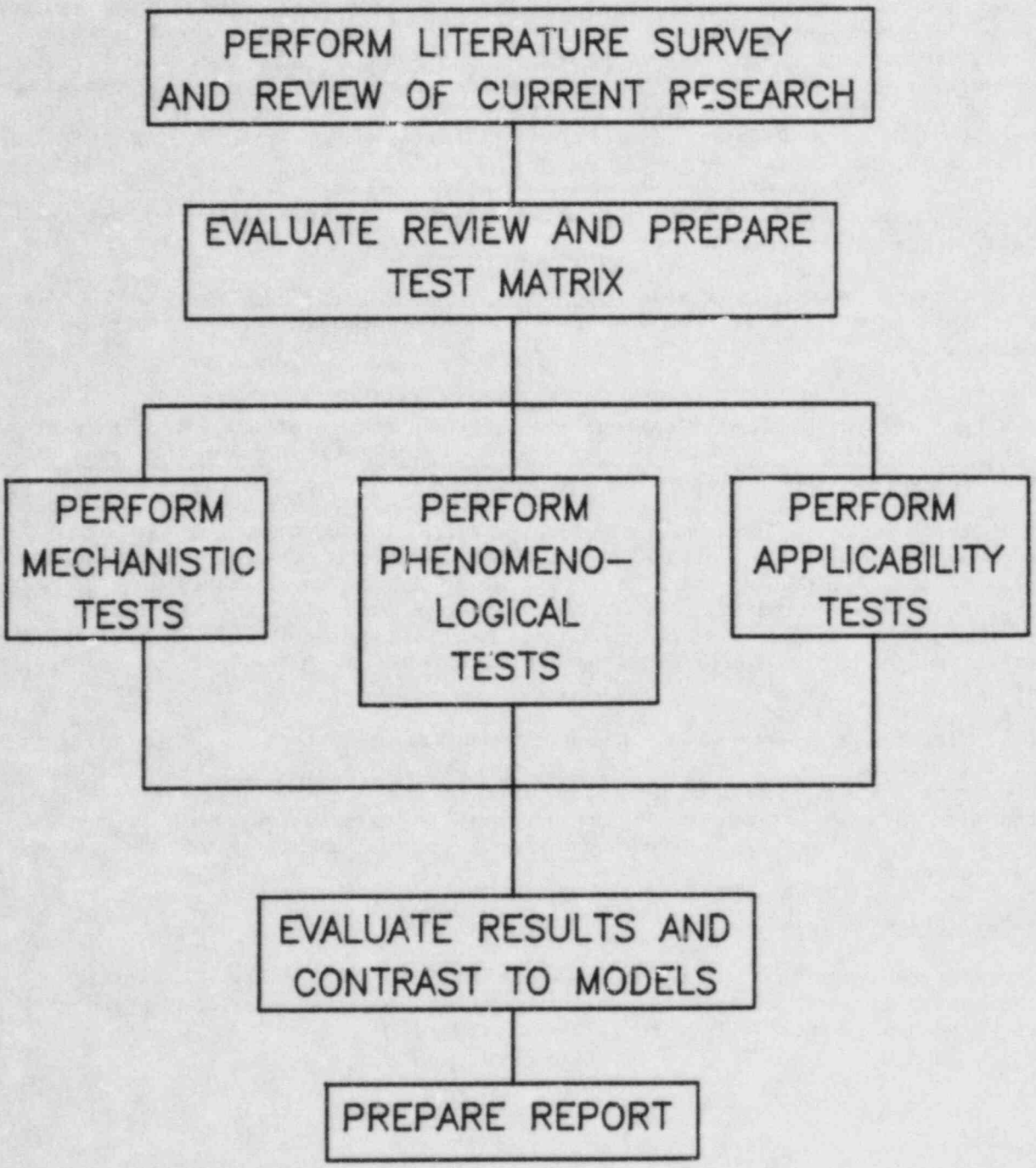

Figure 3.10 Flow Diagram for Subtask 2e: Mechanism Models for Environmentally-Assisted Fatigue Crack Growth

MILESTONE STATEMENT AND SCHEDULE

Subtask 2e: Mechanism Models for Environmentally-Assisted Fatigue Crack Growth

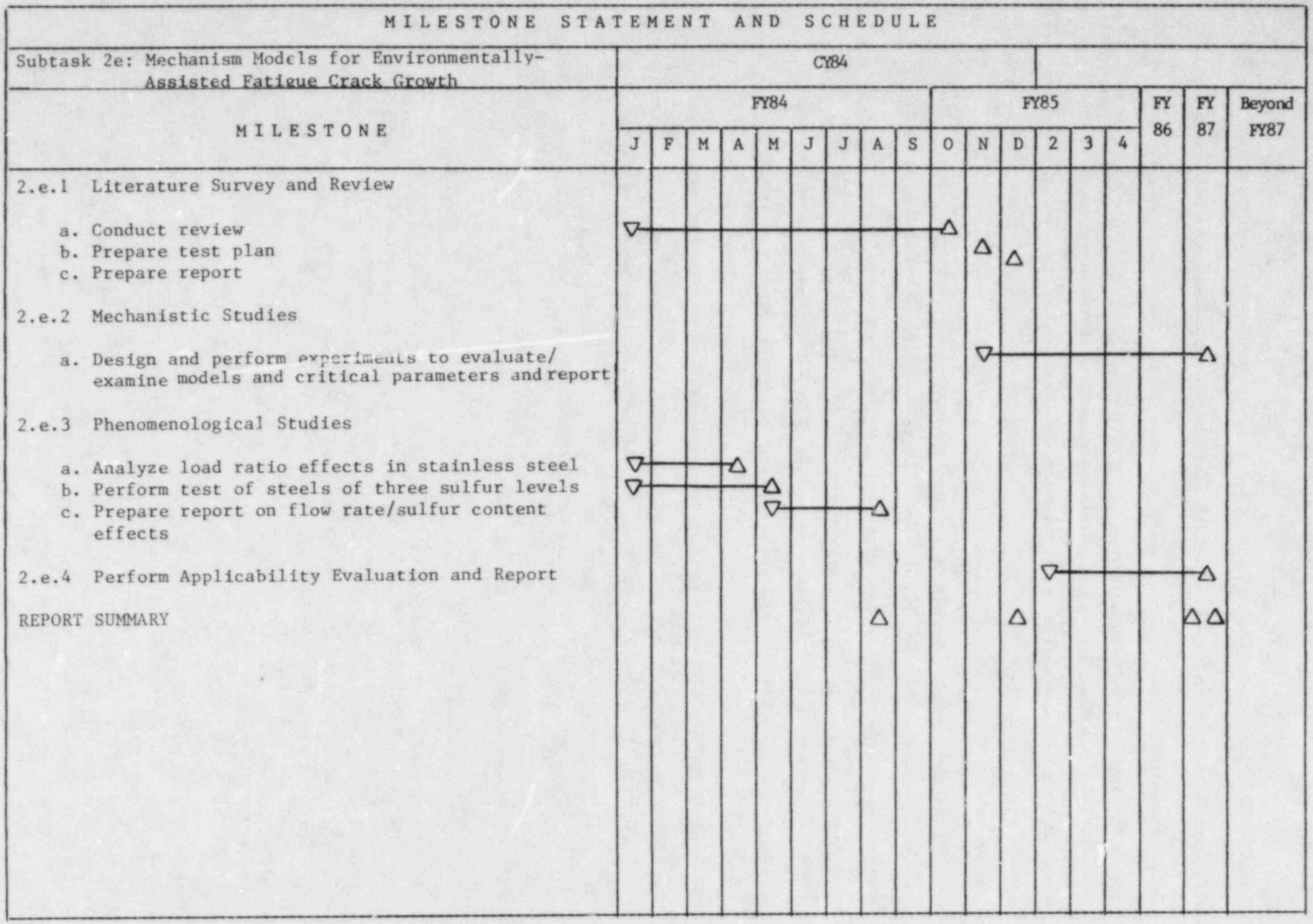

Figure 3.11 Milestone Statement and Schedule for Subtask 2e

3.6 Subtask 2f Total Fatigue Process in PWR Environments

3.6.1 Objective

The objective of this subtask is to provide a unified interpretation of component lifetime encompassing both fatigue crack nucleation and growth. Subtasks 2a, 2b and 2c will all "feed" results to this task, but some explicit experiments will be conducted to address specifically this objective.

3.6.2 Background

In the research world, the subject of fatigue has been customarily divided into two, essentially separate fields of study: (1) fatigue life, utilizing the testing of smooth or blunt notched specimens, with analysis in terms of stress or strain, and (2) fatigue crack growth, utilizing the testing of cracked specimens, with analysis in terms of linear elastic fracture mechanics and the stress intensity factor, K. However, in the real world many cracks do nucleate on smooth surfaces and grow from essentially nothing to visibly sized flaws. This results in a situation which can be analyzed in terms of applied stress being changed to a situation requiring fracture mechanics, and eventually, elastic-plastic methodologies. The boundaries between these analysis regimes are extremely difficult to define.

In the very early stages of nucleation and growth, a microcrack may appear by means of slip-step formation, or extrusion-intrusion mechanisms. Once the microcrack has become a "short crack", in the currently popular parlance, its crack growth rate can be defined, but is often found to be significantly different from that measured for large cracks in a similar ΔK range. At this point, it is obvious that applied ΔK is not an adequate similitude parameter because the local field is still of great influence. Eventually, the flaw grows to a size such that similitude of K does pertain and, assuming the stress field is accurately defined, crack growth rate calculations and life predictions can be performed with reasonable confidence.

3.6.3 Plan of Action

Figure 3.12 is a flow chart which describes the general plan of action and shows the major blocks of effort. While there is a large data base, particularly from aircraft industry-sponsored research on this subject, there is little background for nuclear structure/material/environment combinations. We anticipate that measurements performed on instrumented S-N specimens from Subtask 2a will return some data on crack nucleation and environmental effects relationships. Similarly, data on materials effects will be provided by Subtask 2b and data on the behavior of two-dimensional cracks will come from Subtask 2c.

MEA will attempt to use plastic strain range parameters to link the two processes of nucleation and growth. During nucleation and early growth, the strain range is dominated by the notch field (be it a structural notch or perhaps a particle or inclusion in the material), while during later growth the strain range is dominated by the crack tip field. Although in both cases the strain range can be evaluated, the changeover is uncertain. Thus, we propose to approach the changeover from either end to determine where that match occurs and how. This phenomenological approach has to be taken to define the problem.

In order to provide some experimental data which directly address the elements of this subtask, a limited number of tests using center-notched specimens will be conducted. These specimens will have specific notch geometries, with selected K_t factors, and will be instrumented with potential drop probes so that initiation and propagation evaluations can be carried out. These tests will be conducted in both air and water environments, and will be subjected to the plastic-strain-range analysis indicated above.

3.6.4 Milestones

The milestone charts for this subtask are shown in Fig. 3.13. This is a small effort compared to the other subtasks, with much of the work being on the analytical side, rather than the experimental side. The testing in autoclaves will be carried out toward the end of the third year of the contract.

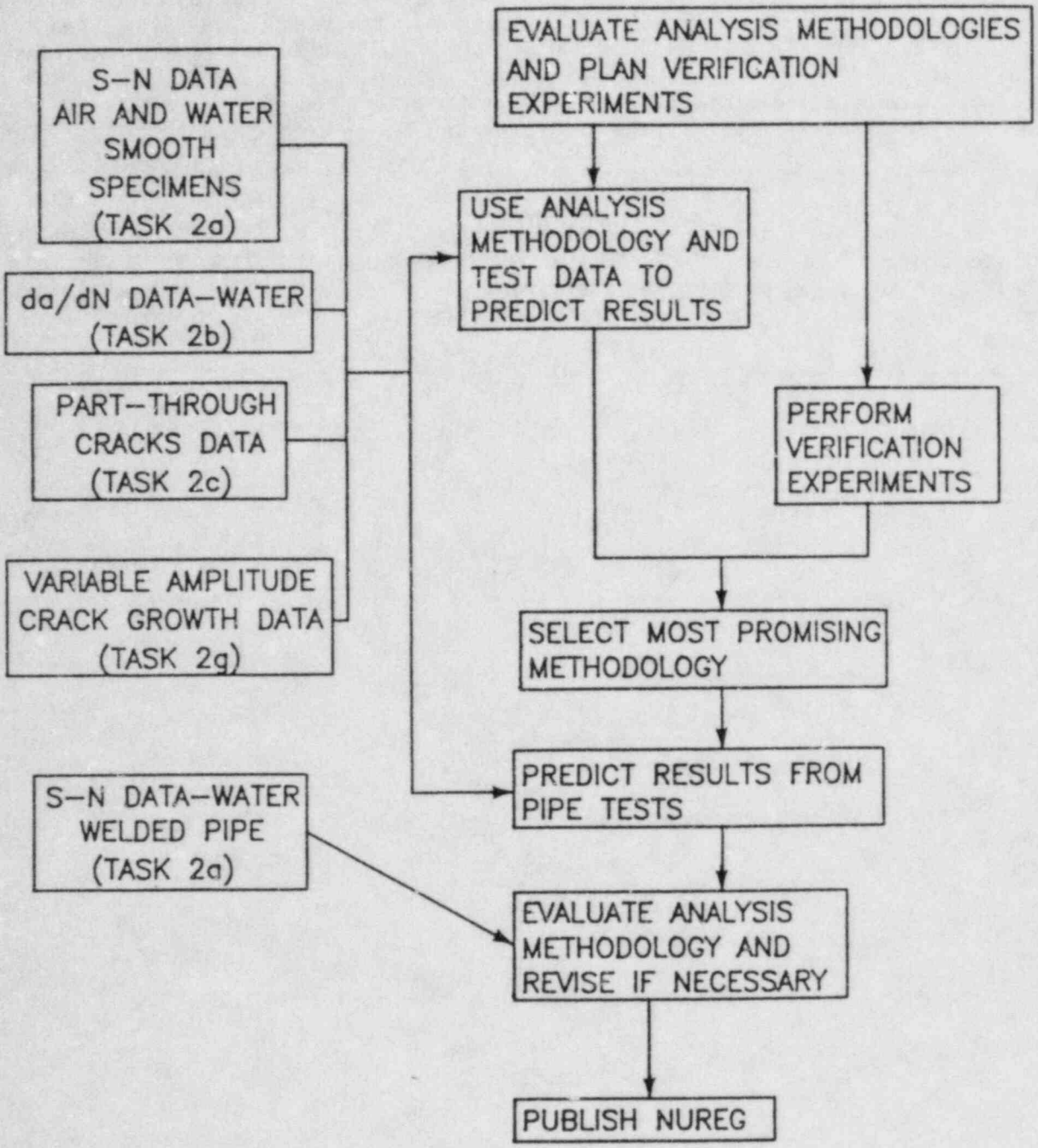

Figure 3.12 Flow Diagram for Subtask 2f: Total Fatigue Process in PWR Environments

MILESTONE STATEMENT AND SCHEDULE

Subtask 2f: Total Fatigue Process in PWR Environments

CY84

MILESTONE	FY84									FY85						FY 86	FY 87	Beyond FY87
	J	F	M	A	M	J	J	A	S	O	N	D	2	3	4			
2.f.1 Initial Analytical Effort																		
a. Evaluate existing methodologies													▽			△		
b. Evaluate plastic strain range model														▽		△		
c. Plan verification experiments															▽	△		
2.f.2 Perform Air Environment Verification Experiments																▽△		
2.f.3 Review and Revise Analysis Methodologies - Preliminary																▽	△	
2.f.4 Perform PWR Environment Verification Experiments																	▽△	
2.f.5 Review and Revise Analysis Methodologies - Final																	▽△	
2.f.6 Evaluate Analysis Methodologies Against Pipe Test Results																	▽△	
2.f.7 Prepare Final Report																		▽△
REPORT SUMMARY																		△

Figure 3.13 Milestone Statement and Schedule for Subtask 2f

3.7 Subtask 2g Cumulative Damage Factor for Environmentally-Assisted Fatigue Crack Growth

3.7.1 Objective

The objective of this subtask is to perform fatigue crack growth rate tests in pressurized, high-temperature water, using loading waveforms with simple overload spectra, and to attempt to develop a predictive capability for determination of growth rates incorporating the combined effects of environment and loading spectra.

3.7.2 Background

Serious research on fatigue crack growth rate effects began in the early 1960's. By the time Paris and Erdogan proposed to correlate crack growth on the basis of ΔK in 1965, the qualitative effects of load interaction, particularly retardation, were already well known. The first explanations of retardation were based on residual stress due to reversed yielding, and the early models, due to Wheeler and Willenborg (Refs. 3.23 and 3.24) using this consideration have achieved a rather lasting popularity. This is due in part to incorporation of such models in the Military Aircraft Damage Tolerance requirement (MIL-A-8344). Later research indicated that crack tip closure loads, due to plastic zones in the wake of the crack tip contributed to the crack tip opening, and a new generation of interaction models was born (Ref. 3.25). Because most of these models were directed for use in the aircraft and aerospace industries, none of them account for environmental-assistance effects. In fact, even qualitative models for load interaction including environmental effects are not available. It can be supposed generally that environmental effects will mollify the beneficial effects of load retardation due to overloads, but the degree of synergism between the acceleration due to underloads and the enhancement to growth rates due to environmental effects is an unknown quantity.

3.7.3 Plan of Action

Figure 3.14 is a flow chart which describes the general plan of action and shows the major blocks of effort. In view of the number of unknowns bearing on the research of this subtask, a very fundamental test and analysis plan has been proposed. This plan consists of a series of tests, using compact specimens, conducted using simple loading spectra. The spectra basically involve constant amplitude fatigue crack growth rate tests, with occasional applications of single overloads, or underloads, followed by careful monitoring of the subsequent crack extension. These tests will be conducted in both air and pressurized, high-temperature water environments, in order to compare the magnitude of the effects, and to separate out the environmental contribution. Later tests will involve applications of multiple overload or underload cycles. Testing will be conducted in multispecimen daisy chains with a variety of steels of differing known susceptibility to environmentally-assisted fatigue crack growth.

Analysis of these effects will be carried out with help of all the above interaction models, including the reversed plasticity model which is currently undergoing additional refinement. The first exercise of the model will be carried out to determine the sensitivity of the calculations to load history

input, including sequencing of the loads, and incorporation of the known effects of cyclic frequency. The second phase of the analytical effort will be calibration of the model to incorporate the environmental effects. Lastly, fatigue crack growth rate tests will be conducted using the reactor stress history profile suggested by Scott (Ref. 3.26), and the calibrated model will be used in an attempt to "predict" the measured growth rate response.

3.7.4 Milestones

The milestone chart for this subtask is shown in Fig. 3.15. This subtask will involve testing in air environments and calibration of the computer models for the first two years, with testing and modeling in the PWR environment taking place in the last two years of the contract period.

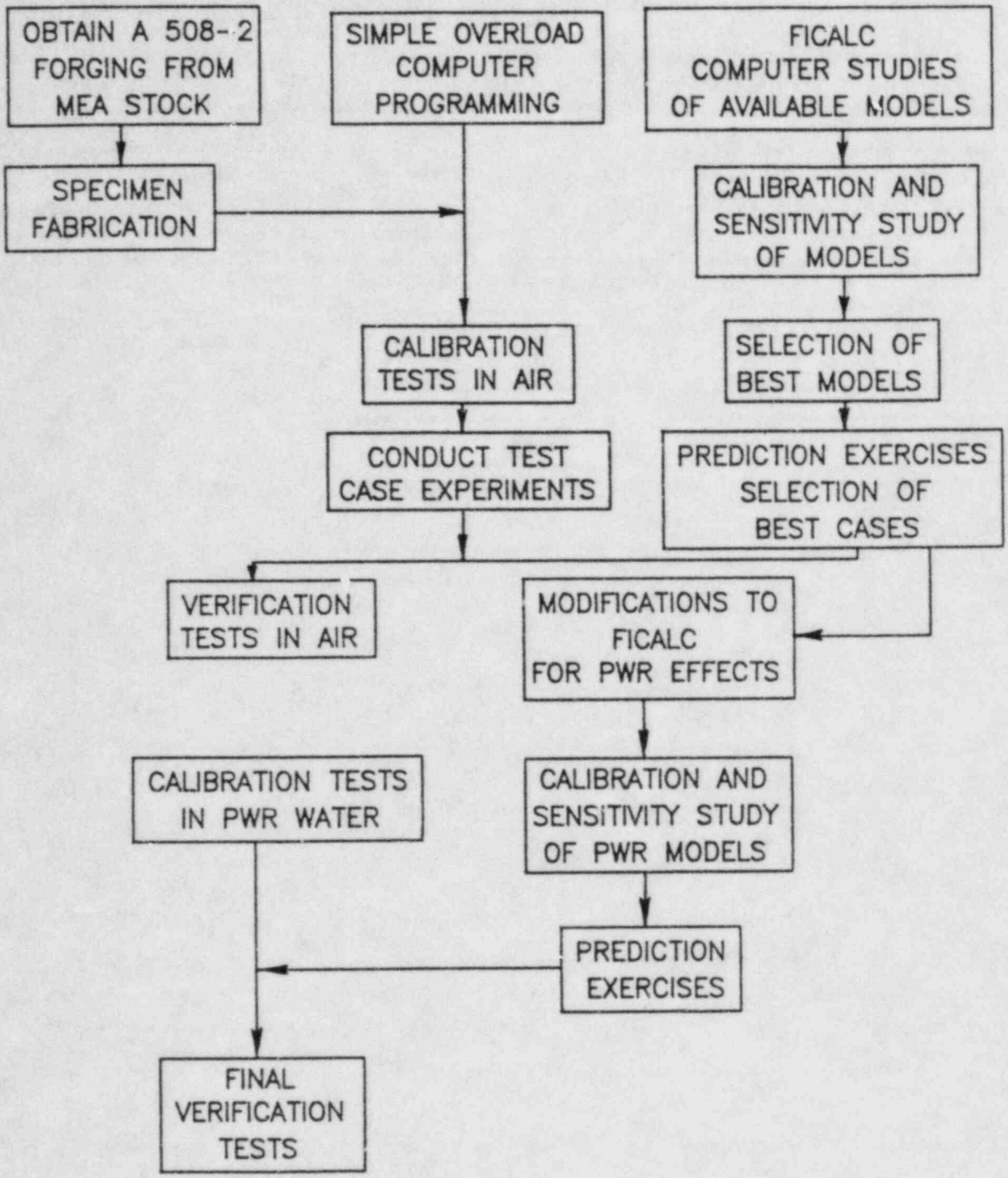

Figure 3.14 Flow Diagram for Subtask 2g: Cumulative Damage Factor for Environmentally-Assisted Fatigue Crack Growth

MILESTONE STATEMENT AND SCHEDULE

Subtask 2g: Cumulative Damage Factor for Environmentally-Assisted Fatigue Crack Growth

MILESTONE	CY84																	
	FY84									FY85						FY 86	FY 87	Beyond FY87
	J	F	M	A	M	J	J	A	S	O	N	D	2	3	4			
2.g.1 Model Development																		
a. Perform calculation sensitivity study												▽			△			
b. Calculate calibration										▽					△			
c. Complete model development and check against experimental results												▽				△		
d. Issue report																△		
2.g.2 Calibration and Verification Experiments																		
a. Perform simple overload tests and calibration tests										▽					△			
b. Perform verification experiments in air and PWR environment																▽	△	
2.g.3 Issue Final Report																	△	
REPORT SUMMARY																△	△	

Figure 3.15 Milestone Statement and Schedule for Subtask 2g

3.8 Subtask 2h International Cyclic Crack Growth Rate Group

3.8.1 Objective

The objective of this task is to participate in the ICCGR group, to contribute to round robin tests and data base development sponsored by the group, and to help author codes and standards developed within the ASME and ASTM society structures.

3.8.2 Background

The International Cyclic Crack Growth Rate (ICCGR) Group was founded in 1977 with the support of both the NRC and EPRI. It has grown today to include members from 41 sponsoring or research organizations, representing 11 nations. Comprehensive reviews of the Group, its history, and activities have been authored by Slama and Jones (Ref. 3.27) and Cullen (Ref. 3.28). The most important activities can be described as follows:

- 1977 - ICCGR Group was formed. In summary form, the charter states that the specific objectives of the Group were to provide a forum for the timely interchange of information, to perform cooperative research programs, to develop consensus test data and internationally accepted standards, and to recommend test procedures and applications techniques. The Group's semiannual meetings continue to be marked by a free and open exchange of ideas on techniques and the interpretation of the most recent data.

- 1978 - Completion of a round robin on data reduction and processing showed that a variety of computational techniques and stress intensity factor formulae led to an intolerably wide scatter band in the final results. This, in turn, led to a recommendation, completed in 1983, of a standard procedure for data acquisition, processing and presentation.

- 1981 - First round robin test was completed by the initial selection of laboratories. The very wide scatter in results led, in part, to new conclusions about the effects of dissolved oxygen content.

- 1981 - The ICCGR, with the sponsorship of the International Atomic Energy Agency (IAEA), organized a two-day specialists' meeting in Freiburg, West Germany. MEA authors contributed three papers to NRC Conference Proceeding NUREG/CP-0044 (Ref. 3.29) which was assembled and edited at MEA.

- 1982-1983 - A second round robin was initiated, with tightened constraints, in order to eliminate many of the interpretation problems associated with the first round robin. The basic parameters for the second round robin are R = 0.7, 17 mHz sinusoidal waveform, 288°C (550°F) and 1000 ppm boron as boric acid will be dissolved in the water.

3.8.3 Plan of Action

The plan of action for this subtask is simply to attend the various meetings (hosting the Fall 1985 meeting) and to present the results of the Task 2 effort to the group. Interaction with the international community involved with related research will have a positive impact on the Task 2 research in terms of building on the positive results of others or being guided by their false starts.

3.8.4 Milestones

Figure 3.16 shows the milestone schedule for this subtask.

MILESTONE STATEMENT AND SCHEDULE

Subtask 2h: International Cyclic Crack Growth Rate Group

MILESTONE	CY84																	
	FY84									FY85						FY 86	FY 87	Beyond FY87
	J	F	M	A	M	J	J	A	S	O	N	D	2	3	4			
2.h.1 Attend ICCGR Meeting at Risley					△													
2.h.2 Attend ICCGR Meeting in U.S.A.										△								
2.h.3 Attend ICCGR Meeting in Europe														△				
2.h.4 Host ICCGR Meeting																△		
2.h.5 Attend ICCGR Meeting in Europe																△		
2.h.6 Attend ICCGR Meetings in U.S.A.																	△	
2.h.7 Attend ICCGR Meetings in Europe																	△	

Figure 3.16 Milestone Statement and Schedule for Subtask 2h

3.9 REFERENCES

3.1 "Investigation and Evaluation of Stress-Corrosion Cracking in Piping of Light Water Reactor Plants," Reprot of the Pipe Crack Study Group, USNRC Report NUREG/CR-0351, U. S. Nuclear Regulatory Commission, Washington, D. C., 20555.

3.2 W. H. Bamford, "A Review of Fatigue Crack Growth Studies of Light Water Reactor Pressure Boundary Steel," in Time and Load Dependent Degradation of Pressure Boundary Materials, IWG-RRPC-79/2, IAEA, Innsbruck, Austria, 1978, pp. 5-15.

3.3 M. E. Mayfield, et al., "Cold Leg Integrity Evaluation," USNRC Report NUREG/CR-1319, U. S. Nuclear Regulatory Commission, Washington, D.C. 20555.

3.4 L. F. Coffin and J. F. Tavernelli, "The Cyclic Straining and Fatigue of Metals," Trans. Met. Soc., Vol. 215, AIME, 1959, pp. 794-807.

3.5 B. F. Langer, "Design of Pressure Vessels for Low-Cycle Fatigue," J. Basic Engineering, Trans. ASME, Series D, Vol. 88, 1962, pp. 389-402.

3.6 ASME Boiler and Pressure Vessel Code, Section III, Rules for Construction of Nuclear Power Plant Components, American Society of Mechanical Engineers, New York, NY, 10017, issued annually.

3.7 ASME Boiler and Pressure Vessel Code, Section XI, Rules for In-service Inspection of Nuclear Power Plant Components, American Society of Mechanical Engineers, New York, NY, 10017, issued annually.

3.8 T. Kondo, T. Kikuyama, H. Nakajima and M. Shindo, "Fatigue of Low-Alloy Steels in Aqueous Environment at Elevated Temperatures, Procedures of the 1971 International Conference on Mechanical Behavior of Materials, Vol. III, 1972, pp. 319-327.

3.9 T. L. Gerber, J. D. Heald and E. Kiss, "Fatigue Crack Growth in SA 508-C12 Steel in a High Temperature, High Purity Water Environment," Trans. ASME, Ser. H., J. Eng. Mat. and Technology, Vol. 96, 1974, pp. 255-261.

3.10 T. R. Mager and V. J. McLoughlin, "The Effect of an Environment of High Temperature Primary Grade Nuclear Reactor Water on the Fatigue Crack Growth Characteristics of A 533 Grade B Class 1 Plate and Weldment Material," Heavy Section Steel Technology Program Technical Report No. 16, WCAP-7776, Westinghouse Electric Corporation, Pittsburgh, PA, Oct. 1971.

3.11 A. G. Pickett, S. C. Grigory, "Prediction of the Low Cycle Fatigue Life of Pressure Vessels," Transactions of the ASME, J. Basic Engineering, 1967, pp. 858-870.

3.12 T. A. Prather and L. F. Coffin, "Part-Through and Compact Tension Corrosion Fatigue Crack Growth Behavior of Carbon Steel in High-Temperature Water," Report No. 81CRD159, General Electric Corporate Research and Development, 1981.

3.13 W. H. Cullen, et al., "Fatigue Crack Growth of A 508-2 Steel in High-Temperature, Pressurized Reactor-Grade Water," USNRC Report NUREG/CR-0969, 1979.

3.14 W. A. van der Sluys and R. H. Emanuelson, "Corrosion Fatigue Behavior of Pressure Vessel Steels in Light Water Reactor Environments," Paper #171, Corrosion '84, New Orleans, LA, 1984.

3.15 W. H. Bamford, "Environmentally-Assisted Crack Growth Studies," in Heavy Section Steel Technology Program Quarterly Report for October-December 1982, USNRC Report NUREG/CR-2751, ORNL/TM-8369/V4, 1983.

3.16 W. H. Cullen, et al., "Fatigue Crack Growth Rates of Irradiated Pressure Vessel Steels in Simulated Nuclear Coolant Environment," J. Nuclear Materials, Vol. 96, 1980, pp. 261-268.

3.17 J. D. Atkinson, S. T. Cole and J. E. Forrest, "Corrosion Fatigue Mechanisms in Ferritic Pressure Vessel Steels Exposed to Simulated PWR Environments", in Proceedings of Specialists' Meeting on Subcritical Crack Growth, May 13-15, 1981, International Atomic Energy Agency, 1981, pp. 459-483.

3.18 T. Kondo, et al., "Corrosion Fatigue of ASTM A 302-B Steel in High Temperature Water : The Simulated Nuclear Reactor Environment" in Corrosion Fatigue: Chemisry, Mechanics and Microstructure, NACE-2, eds. O. Devereux, et al., National Association of Corrosion Engineers, Houston, TX, 1973, pp. 539-556.

3.19 K. Torronen and M. Kemppainen, "Fractography and Mechanisms of Environmentally-Enchanced Fatigue Crack Propagation of a Reactor Pressure Vessel Steel," in Corrosion Fatigue: Mechanics, Metallurgy, Electrochemistry and Engineering, ASTM STP 801, eds., T Crooker and B. N. Leis, American Society for Testing and Materials, 1983, pp. 287-318.

3.20 W. H. Bamford and D. M. Moon, "Some Mechanistic Observations on the Crack Growth Characterisitcs of Pressure Vessel and Piping Steel in PWR Environment," Corrosion, Vol. 36(6), 1980, pp. 289-298.

3.21 B. Tompkins, "Role of Mechanics in Corrosion Fatigue," Metal Science, Vol. 13, 1979, pp. 387-395.

3.22 W. H. Cullen, V. Provenzano and K. Torronen, "A Hydrogen Assisted Fatigue Crack Growth Model for PWR Environments," Report of NRL Progress, 1979, pp. 9-15.

3.23 O. E. Wheeler, Spectrum Loading and Crack Growth," J. Basic Engrg., Transactions ASME, Vol. 94, Series D, No. 1, 1972, pp. 181-186.

3.24 J. Willenborg, R. M. Engle, and H. A. Wood, "A Crack Growth Retardation Model Using an Effective Stress Concept," AFFDL-TM-71-1 FBR, 1971.

3.25 P. D. Bell and M. Creager, "Crack Growth Analysis for Arbitrary Spectrum Loading," AFFDL-TR-74-129, 1974.

3.26 P. M. Scott, "Proposed Spectrum Load Sequence for Corrosion Fatigue Experiments in PWR Primary Water," working document to ICCGR, AERE, 1982.

3.27 G. Slama and R. Jones, "International Cooperative Group on Cyclic Crack Growth Rate" in Structural Integrity of Light Water Reactor Components, Applied Science Publishers, 1982, pp. 261-274.

3.28 W. H. Cullen "Work of the ICCGR on Environmentally-Affected Crack Growth," in Proceedings of the USNRC Tenth Water Reactor Safety Research Information Meeting, Vol. 4, USNRC Conference Proceeding NUREG/CP-0041, 1983.

3.29 Proceedings of the International Atomic Energy Agency Specialists' Meeting on Subcritical Crack Growth, USNRC Conference Proceeding NUREG/CP-0044, in two volumes, W. H. Cullen, ed., 1983.

4.0 TASK 3 RADIATION SENSITIVITY AND POSTIRRADIATION PROPERTIES RECOVERY

Task 3 is designed to advance the technology and expand the data base on the deleterious effects of neutron radiation on the fracture resistance of structural steels. Emphasis is placed on exploring postirradiation heat treatment (annealing) as a method for alleviating neutron effects periodically during service. These research thrusts build on knowledge gained by previous studies on pressure vessel steels and respectively seek information permitting future refinements to NRC Regulatory Guide 1.99 and information defining the benefits and governing variables of embrittlement relief by annealing. Common to the studies is the development and better understanding of underlying radiation effects mechanisms.

The Task 3 effort consists of six primary subtasks. The interaction of these subtasks is illustrated in Fig. 4.1. These, in most cases, are closely integrated in the interests of maximum research payoff and efficiency in investigating process variables. Two subtasks focus on the variable radiation embrittlement sensitivity of steels and deal with uncertainties over the correlation of test vs. power reactor environments from the view of damage producing capability and with metallurgical factors responsible for differences among steels in resistance to radiation-induced embrittlement at the service temperature. Three subtasks focus on embrittlement relief by annealing for nonimproved (older vessel) steel compositions. They are exploring the merits and limitations of high temperature (454°C) and intermediate temperature (400°C) annealing, the composition effects on annealing response, and fracture resistance changes under cyclic annealing and reirradiation. Consistent with NRC priorities, a distinct subtask was undertaken for the isolation and definition of radiation mechanisms attributable to composition effects and interactions. This subtask will be pursued through subcontract with the University of Florida (Gainesville).

Task 3 is restricted to the investigation of low-alloy vessel steels, including types representative of old and new reactor vessel construction. Projected information from this task will have significant benefit to Tasks 1 and 2 since several research materials, especially weld deposits and laboratory melted plates, are being shared with these tasks.

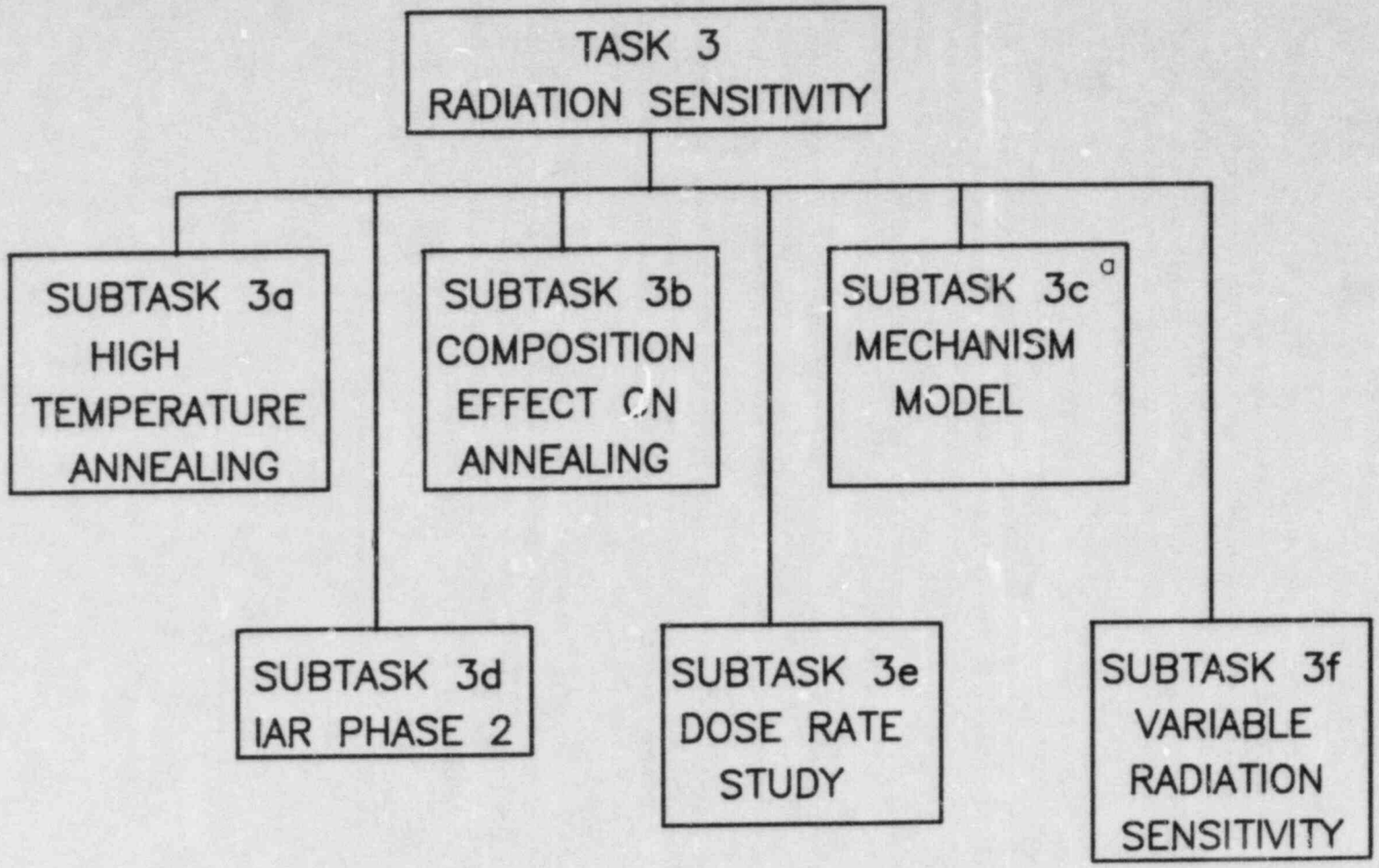

[a] SUBCONTRACT: UNIV. OF FLORIDA

Figure 4.1 Subtask Interactions in Task 3: Radiation Sensitivity and Postirradiation Properties Recovery.

4.1 Subtask 3a High Temperature Annealing

4.1.1 Objective

The objectives include experimental verification of high (> 80%) notch ductility recovery with 454°C annealing, verification of the superiority of 454°C-168 hr annealing response over 400°C-168 hr annealing, examination of the dependency on welding flux of 454°C vs. 400°C annealing recovery and exploration of reembrittlement rates for 454°C vs. 400°C annealing. An additional objective is to establish if embrittlement saturation occurs, or alternatively, the fluence level at which embrittlement of annealed and reirradiated material begins to surpass the embrittlement level preceding the anneal.

4.1.2 Background

This subtask represents one of several systematic investigations being carried out for full qualification of the annealing method for embrittlement relief of reactor vessels in service. The subtask builds on prior MEA investigations for the NRC and others and has two key elements: embrittlement relief by postirradiation heat treatment and reembrittlement behavior upon resumption of the irradiation exposure. Tests of irradiated (I), annealed (IA) and reirradiated (IAR) material thus are implicit to this study. Information gained here will be maximized through correlation with other Subtasks 3b and 3c described below.

Studies to date have shown that recoveries in notch ductility as high as 70 to 75% are possible with 400°C annealing. For 454°C annealing, exploratory data developed by MEA in tests of wrought materials suggest that notch ductility recovery is dependent, in part, on material composition or type. For example, results for plates irradiated at vessel service temperatures (~ 288°C) describe equivalent recovery (< 100%) for 454°C-168 hr annealing vs. 400°C-168 hr annealing in some cases but large differences in recovery for other plates. A parallel test for welds is one thrust of this subtask. A critical test of welding flux type vs. recovery will be possible with the materials chosen for study.

Studies of the IAR condition likewise have revealed a promise of the annealing method for minimizing radiation embrittlement build-up in service. The results in combination with those cited above are encouraging, but raise the question of a steel's reembrittlement path. Reports by one laboratory, moreover, indicate that embrittlement after 454°C annealing is at a slower rate than the (initial) embrittlement of virgin material. This indication is a direct contrast to MEA findings with another set of materials and with 400°C intermediate annealing. Research objectives listed in 4.1.1 above stem from the several current uncertainties over IAR (and IA) behavior.

4.1.3 Plan of Action

The planned approach to the resolution of the subject question is shown schematically in Fig. 4.2. The activities focus on the behavior of weld deposits, recognizing that this component appears to be the most problematic with regard to old production vessels now in service. The welds of interest have in common a high (> 0.30%) copper content. Primary differences are in nickel content (high or low) and the as-fabricated C_v upper shelf energy level

(high or low) resulting from the choice of welding flux. Welds representing three of the four types are on hand for Subtask 3a and were fabricated with Linde 80 flux (low upper shelf) or with Linde 0091 and Linde 124 (high upper shelf). The version lacking (low nickel, Linde 80 flux) will be made by a commercial reactor vessel manufacturer for the task in CY 84 (subelement 4.1.3.1). Base plate will be provided by MEA.

Starting in CY85, sets of standard C_v and tensile specimens will be irradiated at 288°C to ~ 1.2×10^{19} n/cm^2 (E > 1 MeV), annealed at 400°C-168 hr or at 454°C-168 hr, and reirradiated to 0.3×10^{19} n/cm^2 and to 0.7×10^{19} n/cm^2. One additional set of specimens will be irradiated at 288°C to 0.7×10^{19} and tested in the I condition only. Irradiation operations will be completed in CY86. Additional sets of specimens (controls) will be thermally conditioned out of reactor to simulate IAR thermal histories.

The irradiations, identified as the High Temperature Annealing (HTA) Series, will proceed in two phases. Phase 1 (subelement 3.a.2) will investigate I and IA response only to assess variability in recovery for 454°C vs. 400°C annealing. Phase 2 (subelement 3.a.3) will investigate IAR behavior following annealing at 454°C vs. 400°C. (Phase 1 provides the necessary I, IA reference data for Phase 2.) The test of the I condition at 0.7×10^{19} also falls within Phase 2.

In both Phase 1 and Phase 2 the primary analysis will be based on observed C_v 41 J transition temperature change and 24°C yield strength change. Other notch ductility and tension properties will be determined, but are not expected to be drivers in the analysis. For example, essentially full C_v upper shelf recovery is anticipated with 400°C-168 hr and 454°C-168 hr heat treatments.

4.1.4 Milestones

Milestones and the anticipated schedule for Subtask 3a are given in Fig. 4.3.

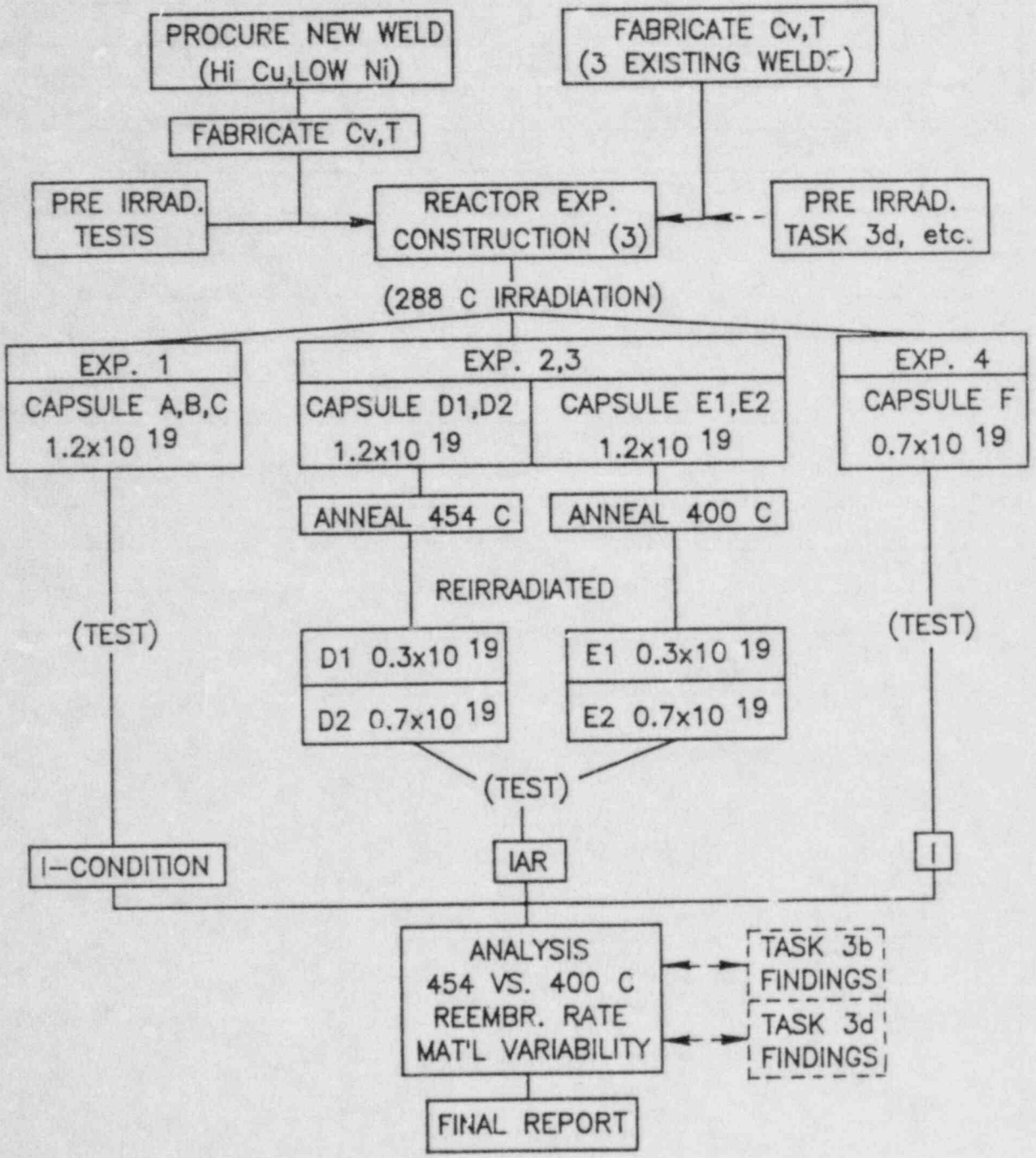

Figure 4.2 Flow Diagram for Subtask 3a: High Temperature (454°C) Annealing. Capsule Irradiations in this subtask are designated High Temperature Annealing (HTA) Series.

MILESTONE STATEMENT AND SCHEDULE

Subtask 3a High Temperature Annealing

CY84

MILESTONE	FY84 J	F	M	A	M	J	J	A	S	FY85 O	N	D	2	3	4	FY 86	FY 87	Beyond FY87
3.a.1 Procure high Cu, low Ni S/A weld (Linde 80)																		
a. Complete weld fabrication					▽						△							
b. Complete weld tests/qualification											▽	△						
3.a.2 Phase One irradiation-anneal study																		
a. Cut/machine specimens (welds 1,2, and 4)							▽		△									
b. Cut/machine specimens (weld 3)											▽		△					
c. Construct HTA Series assembly 1													▽					
d. Complete irradiation, HTA-1														△				
e. Test specimens of HTA-1 (I,IA conditions)															▽	△		
f. Analyze specimen/dosimetry results																▽		
g. Interim report																△		
3.a.3 Phase Two reirradiation investigations																		
a. Cut/machine specimens															▽	△		
b. Construct HTA Series assemblies 2,3,4																▽	△	
c. Complete I exposure, HTA-4																	▽	△
d. Complete IAR exposures, HTA-2 and HTA-3																	▽	△
e. Test specimens of HTA-2, HTA-3, HTA-4																	▽	△
f. Analyze specimen/dosimetry results																	▽	△
3.a.4 Final report, Subtask 3a																	▽	△
REPORT SUMMARY																△		△

Figure 4.3 Milestone Statement and Schedule for Subtask 3a

4.2. Subtask 3b Composition Effect on Annealing

4.2.1 Objective

Objectives of this subtask are a general assessment of the influence of steel composition on notch ductility recovery produced by postirradiation annealing and development of specific qualifications of the individual and combined influences of copper, nickel and phosphorus on recovery by a 400°C-168 hr heat treatment.

4.2.2 Background

Studies of heat treatment capabilities for mitigating radiation-induced embrittlement are providing increasing evidence of an effect of steel (or weld) composition on observed recovery. The description of Subtask 3a gave one example. Surveys of percentage recovery of transition temperature by annealing at a given temperature likewise have revealed large material-to-material variability. These constitute a clear indication of a composition dependence of some type. Accordingly, composition must be considered as a critical metallurgical factor potentially influencing both recovery rate and the degree of embrittlement remaining after heat treatment. Metallurgical influences on the anneal process have not been investigated in detail but obviously form a prerequisite to NRC's evaluation of commercial reactor annealing applications.

Unfortunately, reactor vessel surveillance programs are very limited in scope and in the number of materials assessed. Typically, only one plate (or forging), one weld and one weld heat-affected zone are selected for the program. The numbers of specimens and capsules clearly are too few to probe material annealing behavior. By default, laboratory tests must be relied upon for the bulk of needed information on metallurgical effects on annealing response, including those of composition. Studies with split laboratory melts have had singular success in the isolation of composition influences on radiation sensitivity level. It is logical then to apply this same approach for assessing the relationship of composition variables to annealing behavior. That is, laboratory melts are a convenient way to eliminate metallurgical guesswork and to obtain composition variations (statistical arrays) as needed.

The technology suggests that the magnitude and direction of individual element influences on annealing response will vary for the simple reason that more than one radiation embrittlement mechanism appears to be operating in the embrittlement process. Copper and phosphorus, having known contributions to radiation sensitivity development, were selected for the Subtask 3b study on the basis of their difference in (suspect) mechanism. Nickel was included because of its recently proven reinforcement of the copper influence in radiation sensitivity level. The choice of annealing temperature for studies of this type, on the other hand, appears optional. Strong interest currently exists in both 400°C and 454°C annealing capabilities and trends. Subtask 3b will employ 400°C annealing, in part, to enable the large band of existing annealing data for this temperature to be used in the final analysis and for making correlations. In contrast, data for 454°C annealing are sparse. Also, long term time-at-temperature effects are a distinct possibility with this temperature.

4.2.3 Plan of Action

The overall subtask will evolve as shown in Fig. 4.4. Irradiations of this subtask are identified as the Composition Effects on Annealing (CEA) series. The first group of materials (Investigation 1, subelement 3.b.1) will be irradiated in CY84, and results reported in the Fall of 1985. The second group (Investigation 2, subelement 3.b.2) will be irradiated in CY86. Full analysis of subtask findings is expected in mid 1987. Research materials (plates) for the study are being supplied by Subtask 3f below, and another MEA study. The referenced studies will provide the bulk of required information on I-condition behavior also.

A total of eight plates have been selected for investigation which together provide statistical variations in copper, nickel and phosphorus content. For example, plates in investigation 1 have a high-nickel content (0.70% Ni) and depict high/low copper contents and high/low phosphorus contents. The primary composition variables for plates of investigation 2 are copper and nickel content. In each case, C_v specimens will be irradiated to a target fluence of 2×10^{19} n/cm^2 (E > 1 MeV). The bulk of the specimens will then be annealed at 400°C for 168 hr and tested to establish transition temperature recovery and upper shelf recovery. The balance of the specimens will be used to verify the estimates of I-condition properties derived from earlier findings on the materials. As a precaution, out-of-reactor thermal conditioning tests are also planned for this subtask. As with Subtask 3a, the effects of irradiation time-at-temperature and that of the irradiation plus annealing temperature cycle will be assessed individually, using two sets of samples.

4.2.4 Milestones

Milestones and the schedule for their accomplishment are shown in Fig. 4.5.

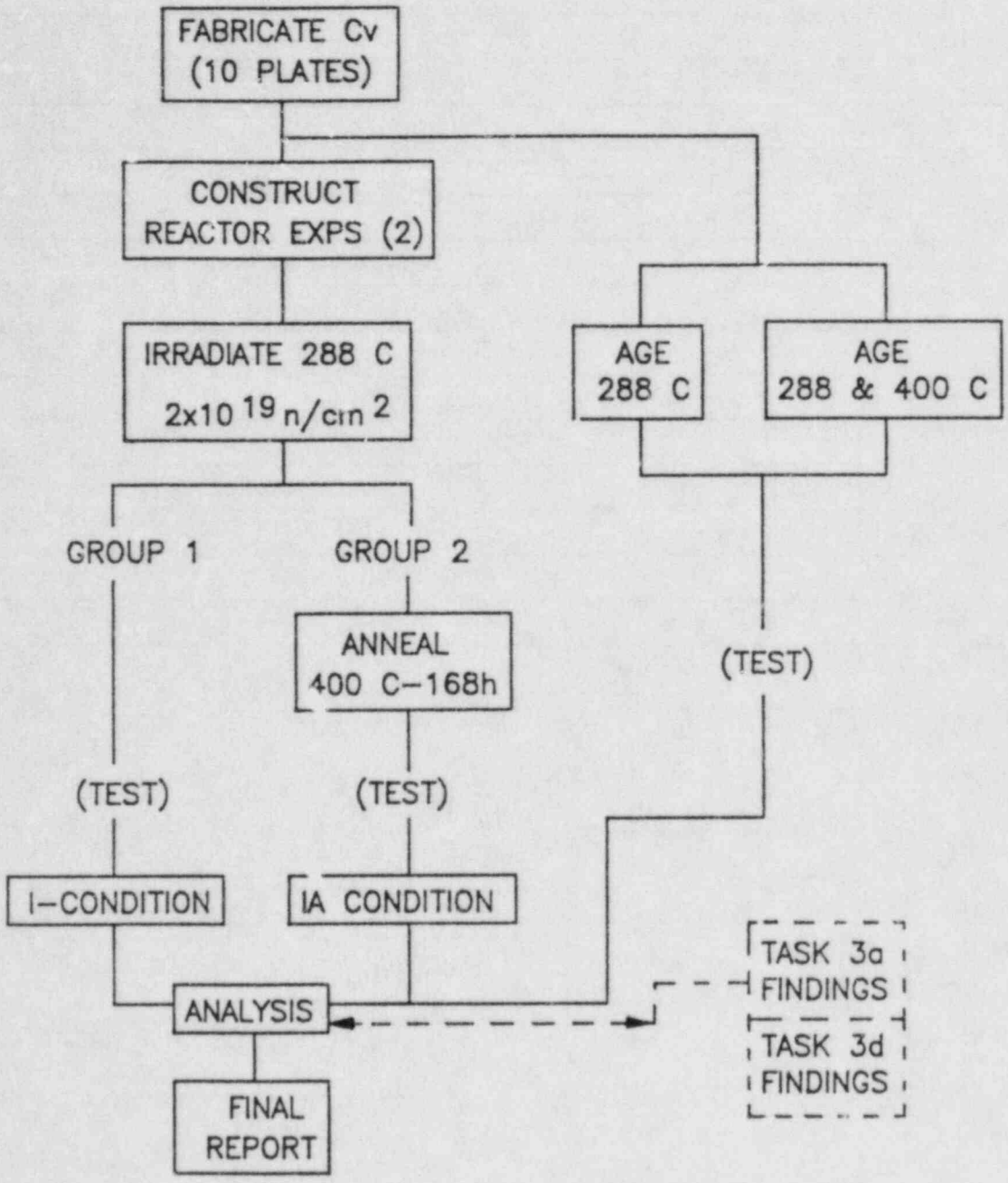

Figure 4.4 Flow Diagram for Subtask 3b: Composition Effect on Annealing Response. Capsule Irradiations in this subtask are designated as Composition Effects on Annealing (CEA) Series.

MILESTONE STATEMENT AND SCHEDULE

Subtask 3b Composition Effect on Annealing

MILESTONE	CY84																	
	FY84									FY85						FY 86	FY 87	Beyond FY87
	J	F	M	A	M	J	J	A	S	O	N	D	2	3	4			
3.b.1 Investigation 1																		
a. Cut/machine specimens (4 plates)				▽		△												
b. Construct reactor assembly, CEA-1						▽		△										
c. Complete irradiation, CEA-1										▽	△							
d. Complete thermal aging, control specimen sets												▽	△					
e. Test thermally aged specimens														▽	△			
f. Test specimens of CEA-1 (I, IA conditions)															▽	△		
g. Analyze specimen/dosimetry results																		
h. Interim report, CEA-1 findings																		
3.b.2 Investigation 2																		
a. Cut/machine specimens													▽	△				
b. Construct reactor assembly, CEA-2																▽ △		
c. Complete irradiation, CEA-2																▽ △		
d. Complete thermal aging, control speciman sets																▽	△	
e. Test thermally aged specimens																	▽ △	
f. Test specimens of CEA-2, (I, IA conditions)																	▽ △	
g. Analyze specimen/dosimetry results																	▽ △	
3.b.3 Final report																	▽ △	
REPORT SUMMARY																△	△	

Figure 4.5 Milestone Statement and Schedule for Subtask 3b

4.3 Subtask 3c Mechanism Model of Irradiation Damage

4.3.1 Objective

Objectives of this subtask are to confirm the basic mechanism of the copper contribution to radiation sensitivity development, to define the mechanism(s) by which nickel alloying reinforces the copper content to sensitivity level and to isolate the mechanism responsible for the phosphorus contribution to radiation sensitivity development. The subtask will also assess the dependence of the respective mechanisms on the ambient radiation flux level (high vs. low). The major portion of the research activities will be carried out by a subcontractor to MEA.

4.3.2 Background

Radiation damage to pressure vessel steels typically is associated with changes wrought in the metal lattice by high energy neutrons colliding with the atoms of the alloy. In this simplistic view, the collision process produces lattice displacements (or displacement cascades) which result in metal hardening and, in turn, the elevation of the brittle/ ductile transition temperature found in postirradiation notch ductility and fracture toughness tests. Steels, however, are complex materials at the microscale and, as might be expected, show that radiation damage mechanisms extend well beyond the simple displacement cascade and displacement spike models. Cases in point are the harmful effects of copper and phosphorus impurities on 288°C radiation resistance and the recently confirmed interaction between nickel and copper which magnifies the effect of the latter on sensitivity.

In 1972, Smidt and Sprague (Ref. 4.1) reported evidence that the copper mechanism is different from that of phosphorus and that nickel content does not enhance directly, the radiation sensitivity of iron, at least for compositions up to 0.3 atom percent nickel. Their observations with binary iron alloys and low alloy pressure vessel steels indicate that the probable mechanism for the copper influence is the promotion by copper atoms or atom clusters of inhomogeneous nucleation of vacancy defects, i.e., small dislocation loops. These provide the barriers to dislocation motion responsible for the enhanced yield strength elevation by irradiation. Because a different yield strength dependence with fluence was observed for the iron-phosphorus binary, they concluded that the mechanism for the phosphorus contribution must be different from that of copper. Separately, it has been proposed that the phosphorus mechanism is similar to that of temper embrittlement and derives from radiation-enhanced diffusion of phosphorus to ferrite-carbide interfaces.

A review of the present (1984) state of the fundamental understanding of radiation sensitivity provides the following picture: (a) more than one mechanism at the microscale generally is responsible for observed embrittlement by 288°C irradiation, (b) the mechanism for the copper influence still lacks confirmation even though it has been studied for several years and has been modeled based on abundant empirical data, (c) the form of the interaction between nickel and copper content in sensitivity development is not known, neither is the reason for the greater level of interaction seen in welds compared to plates, and (d) the mechanism for the phosphorus effect remains elusive, partly because of past microscopy limitations. Relative to (d), investigations by Subtask 3f recently revealed an interaction between

phosphorus and copper such that a greater phosphorus effect arises if the copper level is low. Observation (d) clearly shows the merits of a statistically based materials matrix when investigating sensitivity variables (approach taken by this subtask and Subtask 3f).

4.3.3 Plan of Action

A unified, systematic investigation into operating mechanisms is planned. In addition, a two-pronged approach using laboratory-melted binary and ternary iron alloys and A 302-B and A 533-B steel alloys is felt necessary (see Fig. 4.6).

Iron alloys (iron-copper, iron-copper-nickel) to be melted by October 1984, will be used in studies of defect production aimed at confirming the copper mechanisms and identifying how the mechanism is altered by nickel. TEM and more advanced microscopy techniques will be applied in this thrust. The approach to the isolation of the phosphorus mechanism assumes it reduces the fracture stress through a weakening of carbide interfaces. Fracture surface analyses of plates from Subtask 3f and of welds previously irradiated in the form of C_v specimens will comprise the primary (initial) thrust for phosphorus. If results prove negative, plans are to explore other possible mechanisms compatible with observed the copper-phosphorus interaction.

Efforts by the subcontractor (University of Florida at Gainesville) are to begin October 1984. In advance of this date, MEA will supply necessary research materials to the subcontractor. Planned research involving new melts (e.g., iron binaries) from subelement 3.c.3; those involving materials from Subtask 3f and other MEA investigations constitute subelement 3.c.4. Irradiations required by the former will be carried out piggyback fashion in reactor assemblies serving other subtasks such as 1b. The subcontractor has at his disposal state-of-the-art equipment for direct detection and measurement of local concentrations of copper, nickel and phosphorus and for lattice imaging and analysis.

4.3.4 Milestones

Milestones and anticipated completion dates for this subtask are identified in Fig. 4.7.

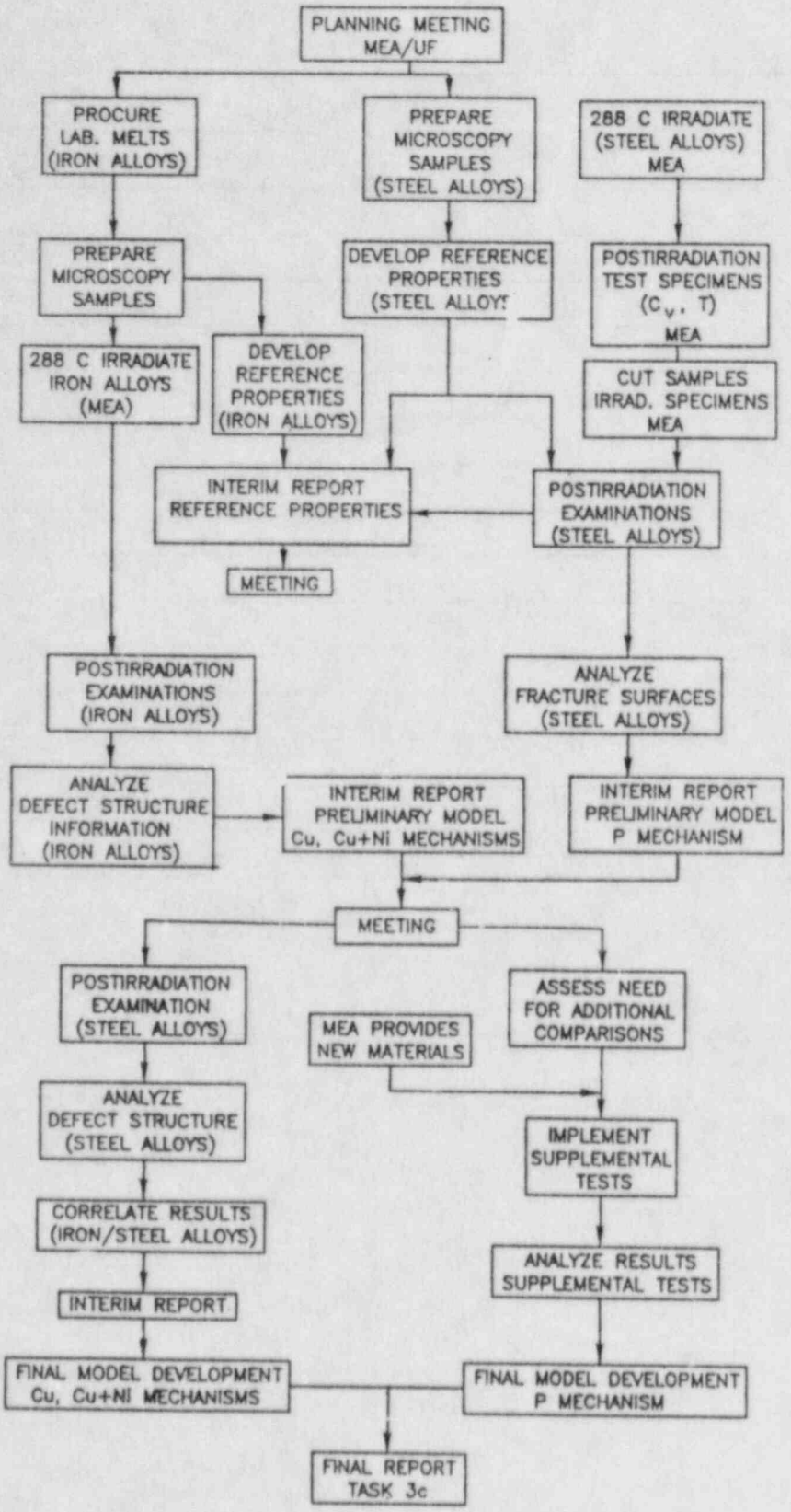

Figure 4.6 Flow Diagram for Subtask 3c: Mechanism Model of Irradiation Damage

MILESTONE STATEMENT AND SCHEDULE

Subtask 3c Mechanism Model of Irradiation Damage

CY84

MILESTONE	FY84									FY85						FY 86	FY 87	Beyond FY87
	J	F	M	A	M	J	J	A	S	O	N	D	2	3	4			
3.c.1 Initial task planning with subcontractor				▽	△													
3.c.2 Material acquisition and preparation (MEA)																		
a. Procure lab melts - Iron alloys						▽				△								
b. Specimen preparation - unirrad alloy steels								▽		△								
c. Specimen preparation - irrad alloy steels								▽			△							
d. Conduct irradiation - Iron alloys														▽	△			
Subcontractor Efforts(University of Florida)										▽							△	
3.c.3 Cu, Cu+Ni (defect microstructure studies)																		
a. Develop ref. properties - iron alloys													▽		△			
b. Interim report, ref. properties															▽ △			
c. Postirradiation examine - iron alloys															▽	△		
d. Analyze pre-post defect structures																▽ △		
e. Develop preliminary models																▽ △		
f. Interim report, preliminary models																▽ △		
g. Develop ref. properties - steel alloys																▽	△	
h. Postirradiation examine - steel alloys																	▽ △	
i. Correlate observations - alloy steel/iron alloy																	▽ △	
j. Complete model development																	▽ △	
3.c.4 Phosphorus investigations(fracture surface chem.)																		
a. Develop initial ref. properties - alloy steels											▽	△						
b. Interim report, ref. properties															▽	△		
c. Postirradiation examine - alloy steels													▽			△		
d. Analyze pre-post surface chemistry															▽	△		
e. Develop preliminary model																▽ △		
f. Interim report, preliminary model																▽ △		
g. Conduct and analyze supplemental tests																	▽ △	
h. Complete model development																	▽ △	
3.c.5 Final Report																	▽ △	
REPORT SUMMARY														△		△	△	

Figure 4.7 Milestone Statement and Schedule for Subtask 3c

4.4 Subtask 3d IAR Phase 2

4.4.1 Objective

Objectives of this subtask are to complete an irradiation-anneal-reirradiation investigation designed to explore reembrittlement path after 288°C irradiation and 399°C annealing. The investigation employs two submerged-arc weld deposits and C_v test determinations. The welds were fabricated with different flux types but shared the same lot of filler wire (high copper, high nickel composition).

4.4.2 Background

The NRC's irradiation (I)-anneal(A)-reirradiation(R) program represents a systematic effort to qualify the annealing method for the control of radiation-induced embrittlement to commercial vessel materials. IAR behavior is being assessed both from the standpoint of transition temperature elevation and from the standpoint of upper shelf toughness reduction.

The first phase investigation, reported by MEA investigators in 1978, employed two commercially produced submerged-arc welds (nozzle cutouts) containing 0.35% copper and ~ 0.65% nickel but which differed in welding flux type. One flux type (Linde 80) typically produces a low as-fabricated C_v upper shelf level; the second flux type (Linde 124) yields a high as-fabricated upper shelf level. Irradiations at 288°C to ~ 1.3×10^{19} n/cm^2 were used for the first cycle exposure; reirradiation fluences were less. This investigation revealed that 399°C-168 hr annealing, but not 343°C-168 hr annealing, has a high potential for reducing radiation effects build-up in service. The Phase 2 investigations builds on this finding. Subtasks 3a and 3b, in turn, build on the Phase 2 study which is now nearing completion.

Additional observations of Phase 1 were (a) a greater rate of embrittlement in heat-treated material compared to nonheat-treated material and (b) a significant difference between upper shelf and transition temperature responses to heat treatment. The first was the primary motivation for the Phase 2 study. Its goal is to explore the reembrittlement path after annealing. This follow-on investigation, additionally, is testing the significance of welding flux type to IA and IAR performance, noting that considerable differences in as-fabricated transition temperature and upper shelf properties can result from the flux choice.

The investigations of IAR Phase 2 center on C_v assessments with some supporting information derived from companion tensile tests. Compact tension tests for J_{Ic} properties of I vs. IAR conditions at a fluence of 1.5×10^{19} n/cm^2 have been conducted; results generally agree with the C_v observations to date. Remaining experimental C_v assessments involve fluences of $> 2 \times 10^{19}$ n/cm^2, i.e., significantly higher than that of the J_{Ic} test comparisons.

4.4.3 Plan of Action

Figure 4.8 shows the sequence of experimental operations planned in completion of this subtask. Test materials are two welds produced from the same lot of filler metal but different welding flux types (Linde 80 and Linde 0091). Qualification tests of these welds indicated significantly different preirradiation C_v properties consistent with these flux types.

Completion of the IAR (Phase 2) Series involves 288°C irradiation, 399°C-168 hr intermediate annealing and 288°C reirradiation of C_v and tensile specimen sets of both welds. Objectives are to establish I- and IA-condition properties after a (total) fluence of 2.5×10^{19} n/cm^2 (E > 1 MeV) and to establish IAR-condition properties for a first cycle exposure of 2.0×10^{19} at 288°C followed by 399°C-168 hr annealing and 288°C reirradiation to second cycle fluences of 0.25×10^{19} and 0.50×10^{19} n/cm^2. These operations are scheduled for completion in CY84. Findings on notch-ductility changes will be intercompared to identify the reembrittlement path with fluence, the effect of weld flux type on the IAR trend, and through comparison with previously reported findings on these welds, the significance of the first cycle fluence level (high vs. low) to subsequent IA and IAR property changes.

Results from this subtask are to be closely integrated with the observations of Subtasks 3a and 3b.

4.4.4 Milestones

Milestones and the schedule for their completion are shown in Fig. 4.9.

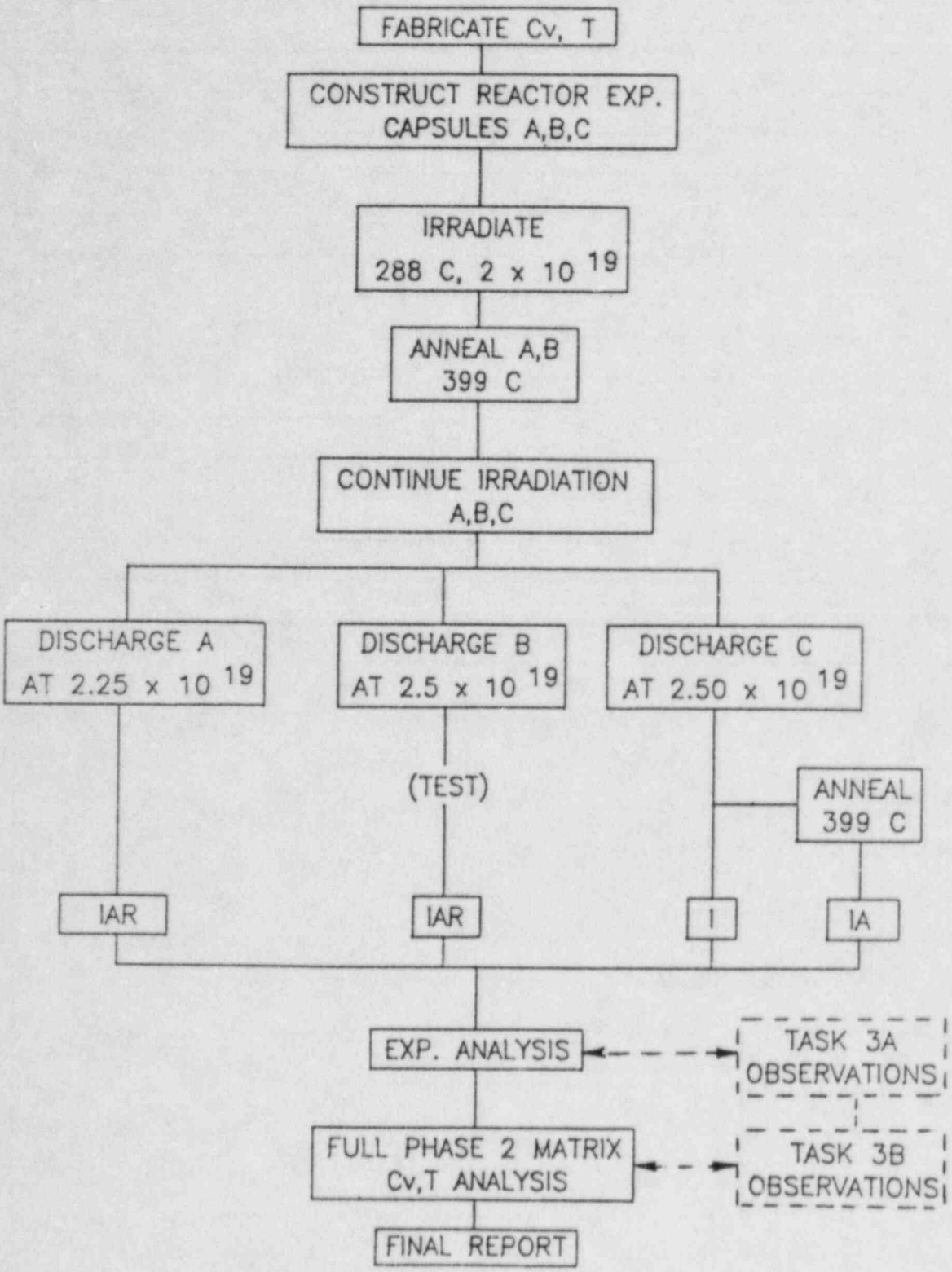

Figure 4.8 Flow Diagram for Subtask 3d: IAR Phase 2. Capsule Irradiations in this subtask are designated as Irradiation-Anneal-Reirradiation (IAR) Series.

MILESTONE STATEMENT AND SCHEDULE

Subtask 3d IAR Phase 2

CY84

MILESTONE	FY84 J	F	M	A	M	J	J	A	S	FY85 O	N	D	2	3	4	FY 86	FY 87	Beyond FY87
3.d.1 IAR Series Assembly 6																		
a. Complete irradiation/reirradiation operations	▽	—	△															
b. Test Cv specimens (I, IA, IAR conditions) and tensile specimens (I, IAR conditions)								▽	—	△								
c. Analyze specimen/dosimetry results								▽	—	—	△							
d. Interim report, IAR-6 findings												▽	—	△				
3.d.2 Final Report, Subtask 3d													▽	—	△			
REPORT SUMMARY													△	△				

Figure 4.9 Milestone Statement and Schedule for Subtask 3d

4.5 Subtask 3e Dose Rate Effects

4.5.1 Objective

The main objective is to demonstrate experimentally, using closely controlled test conditions, the relative effects of long-term vs. short-term irradiation exposures on the mechanical properties of reactor vessel steels. Neutron flux levels employed are representative of power reactor and test reactor environments; the temperature of irradiation (288°C) is typical of reactor vessel service.

4.5.2 Background

Reactor vessel surveillance programs have been highly beneficial not only for confirming radiation embrittlement trends established in test reactor experiments but also for verifying the high radiation sensitivity of materials having a high copper and a high nickel content. A historical objective of such programs, additionally, was to ascertain the combined effects of long-term irradiation and elevated temperature. Comparison data now evolving from long vs. short-term neutron exposures provide some evidence of a time-at-temperature dependence of the embrittlement process. Specifically, embrittlement levels observed for power reactor irradiations at low fluxes appear to be lower than those found in test reactor irradiations, especially for the case of fluences typical of vessel end-of-life.

Because of the major import to vessel operations, both in terms of allowable lifetimes and startup/shutdown procedures that are safe yet most economical, the flux dependence uncertainty bears examination and confirmation for NRC regulatory decisions. Also, out of necessity, it is fully expected that test reactor data will continue to be a key element in the analysis of the power reactor case. The former represents a major portion of the available information and, from a practical standpoint, test reactor experiments are the only means by which metallurgical and annealing variables can be studied and qualified within a reasonable (short) time frame.

Subtask 3e and the Dose Rate Effects (DRE) Series of experiments were established to provide a critical test of the flux effects issue. The irradiations are being conducted in the UBR test reactor, which is light-water-cooled and has a low enrichment. This vehicle was chosen because of the high degree of control which can be exercised over fluence levels (for fluence matching) and exposure temperatures (positive temperature control and continuous temperature monitoring are possible). In turn, this capability avoids the primary uncertainties found in power reactor specimen irradiations.

4.5.3 Plan of Action

The irradiation matrix calls for the exposure of A 302-B and A 533-B reference plates (one each) and A 533-B weld materials (one each of Linde 80 flux and Linde 0091 flux) at three neutron flux levels: 7-8 x 10^{10}, 4-5 x 10^{11} and 8-9 x 10^{12} n/cm^2-sec^{-1}. Requisite flux levels are being obtained using two reflector (in-pool) locations and one in-core location in the UBR. The reflector region locations are identified here as standpipe (SP) and core-edge (CE) locations, respectively. The majority of required irradiations have been in progress since 1983. Figure 4.10 shows schematically the general plan for

the relationship of remaining research efforts regarding Subtask 3e. Subelements 3.e.1, 3.e.2 and 3.e.3 refer to operations in the standpipe, core-edge and in-core (IC) facilities, respectively.

Specimen types being irradiated include C_v specimens for notch ducility determinations, fatigue precracked C_v specimens for dynamic fracture toughness (K_{Jd}) determinations, 0.5T-CT specimens for static fracture toughness tests, and tensile specimens. The irradiation temperature is controlled at 288°C in all three locations. Target fluences for the two higher flux levels are 0.5×10^{19}, 1.0×10^{19} and 2.0×10^{19} n/cm^2. Specimen sets irradiated at the lowest flux are to receive 0.5×10^{19} n/cm^2 (E > 1 MeV) only. Irradiation tests of the A 302-B plate and the Linde 80 weld will be made at each matrix point; tests of the A 533-B plate and the Linde 0091 weld will be made at the lowest fluence only because of program size and time constraints.

The initial comparison for testing flux effects is not expected until July 1986. The results from one of the DRS assemblies [Core-edge (CE) Assembly 1] will be available in 1984, however, and data for the A 302-B plate could be compared against existing in-core data trends for this material. Likewise, some in-core data will become available from Subtask 3a for the Linde 80 weld. Thus, preliminary comparisons of the effects of core-edge vs. in-core locations should be possible before mid 1986. A special neutron spectrum calculation will be made in CY86 for core-edge and in-pool locations to aid overall comparisons (subelement 3.e.4). A spectrum calculation already exists for the in-core locations.

In addition to the main objective, test method correlations will be investigated using data supplied by the C_v and CT specimen tests. Accordingly, this portion of the effort will reinforce the efforts of Subtask 1b above.

4.5.4 Milestones

Milestones and target completion dates for Subtask 3e are given in Fig. 4.11.

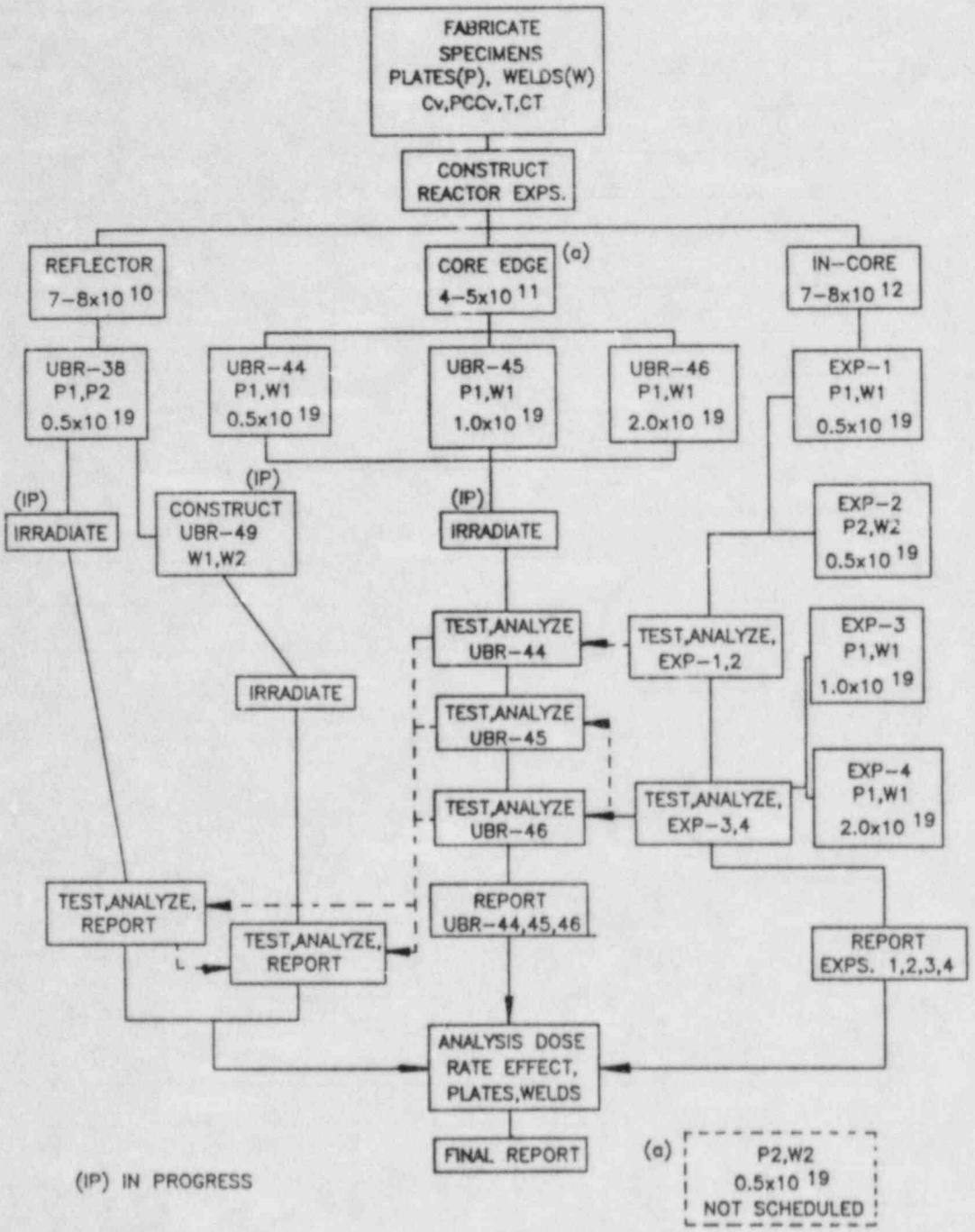

Figure 4.10 Flow Diagram for Subtask 3e: Dose Rate Effects. Capsule Irradiations in this subtask are designated as Dose Rate Effects (DRE) Series.

MILESTONE STATEMENT AND SCHEDULE

Subtask 3e Dose Rate Effects

CY84

MILESTONE	FY84 J	F	M	A	M	J	J	A	S	FY85 O	N	D	2	3	4	FY 86	FY 87	Beyond FY87
3.e.1 Low flux irradiation assessments																		
a. Construct DRE-In Pool (IP) facility no. 2															▽	△		
b. Construct DRE-IP assembly no. 2 (welds)															▽	△		
c. Complete irradiation, DRE-IP-1 (plates)															▽			△
d. Complete irradiation, DRE-IP-2	▽															△		
e. Test specimens of DRE-IP-2																	▽△	
f. Analyze specimen/dosimetry results																	▽△	
g. Interim report, DRE-IP-1 findings																	▽△	
3.e.2 Intermediate flux irradiation assessments																		
a. Complete irradiation, DRE-Core Edge(CE) assbly#1	▽		△															
b. Test specimens of DRE-CE-1								▽				△						
c. Analyze specimen/dosimetry results								▽							△			
d. Interim report, DRE-CE-1 findings												▽			△			
e. Complete irradiation, DRE-CE-2	▽															△		
f. Test specimens of DRE-CE-2																	▽△	
g. Analyze specimen/dosimetry results																	▽△	
h. Interim report, DRE-CE-2 findings																	▽△	
i. Continue irradiation DRE-CE-3	▽																	△
3.e.3 High flux irradiation assessments																		
a. Complete irradiation, DRE-In Core (IC) assbly#1															▽	△		
b. Test specimens of Dre-IC-1															▽	△		
c. Analyze specimen/dosimetry results															▽	△		
d. Interim report, DRE-IC-1 findings															▽	△		
e. Complete irradiation,DRE-IC-2,DRE-IC-3, DRE-IC-4																	▽△	
f. Test specimens, DRE-IC-2, DRE-IC-3, DRE-IC-4																	▽	△
g. Analyze specimen/dosimetry results																	▽	△
3.e.4 Neutron spectrum calculation/determination															▽	△		
3.e.5 Final Report																	▽	△
REPORT SUMMARY															△	△	△△	△

Figure 4.11 Milestone Statement and Schedule for Subtask 3e

4.6 Subtask 3f Variable Radiation Sensitivity

4.6.1 Objective

This subtask is directed to the experimental isolation and qualification of combined alloying element and residual element effects on the 288°C radiation embrittlement resistance of pressure vessel steels. Research materials are plates from laboratory melts of A 302-B or A 533-B steel. Impurity elements investigated are Cu, P, Sn, Sb and As; alloying elements investigated individually and in conjunction with Cu level are Ni, Mn, Mo and Cr.

4.6.2 Background

The detrimental effects of a high copper content and a high phosphorus content on the resistance of reactor vessel steels and welds to 288°C radiation embrittlement is well established. The primary impetus to the current study was the recent experimental confirmation of a nickel and copper content interaction through which the detrimental effect of copper is enhanced significantly. The interaction is believed primarily responsible for the high radiation sensitivity levels exhibited by the high copper, high nickel content welds of many early production reactor vessels. A likelihood of contributions from other elements acting in combination is suggested by other data and also by computer evaluations of current data banks for both test reactor and power reactor irradiations. Subtask 3f was initiated in 1982 to explore and qualify other suspect interactions.

The subtask has purchased seven laboratory melts of steel. The procedure of multiple casting with specific element additions to the melt between casts was used to obtain four composition variations from each melt. The base composition was A 302-B or A 533-B in each instance. Primary impurity elements varied were copper and phosphorus. Combinations of these two elements (individually or in pairs) with the alloying elements nickel, chromium, manganese and molybdenum form the main composition matrix. The matrix provides other element variations, including tin, arsenic and antimony, but on a second priority basis.

Relative radiation sensitivity is being ascertained from the radiation-induced change in C_v notch ductility and tensile properties produced by 2×10^{19} n/cm^2 ($E > 1$ MeV) at 288°C. The thrust of Subtask 3f is the development of key information upon which further refinements to Regulatory Guide 1.99 can be confidently based. By design, the results will also help guide studies of annealing and reirradiation behavior described above. As stated earlier, this subtask provides test materials and I-condition information for Subtasks 1b and 3a.

4.6.3 Plan of Action

The necessary experimental steps for completion of the original subtask plan are shown schematically in Fig. 4.12. At the commencement of the current program, 16 of the 28 plates had been irradiated and evaluated for relative notch ductility change by 2×10^{19} n/cm^2. C_v specimens of eight additional plates had also been irradiated but the reactor assembly remained unopened. Accordingly, completion of the Variable Radiation Sensitivity (VRS) series requires the testing and evaluation of C_v specimens from one reactor assembly (VRS-3)

(subelement 3.f.2), the 288°C irradiation and testing of C_v specimens of four plates and also the 288°C irradiation and testing of tensile specimens of all 28 plates (subelement 3.f.3).

The plan for the remaining neutron exposures is to use a multiple-capsule assembly capable of irradiating both specimen types simultaneously. Some revisions to the standard MEA assembly design are required and will be made in early 1984. All experimental phases should be completed by early 1985. Findings from the four reactor assemblies comprising the VRS series will be issued in three reports for simplicity (see subelements 3.f.1 and 3.f.4).

4.6.4 Milestones

The schedule of milestones for this subtask if given in Fig. 4.13.

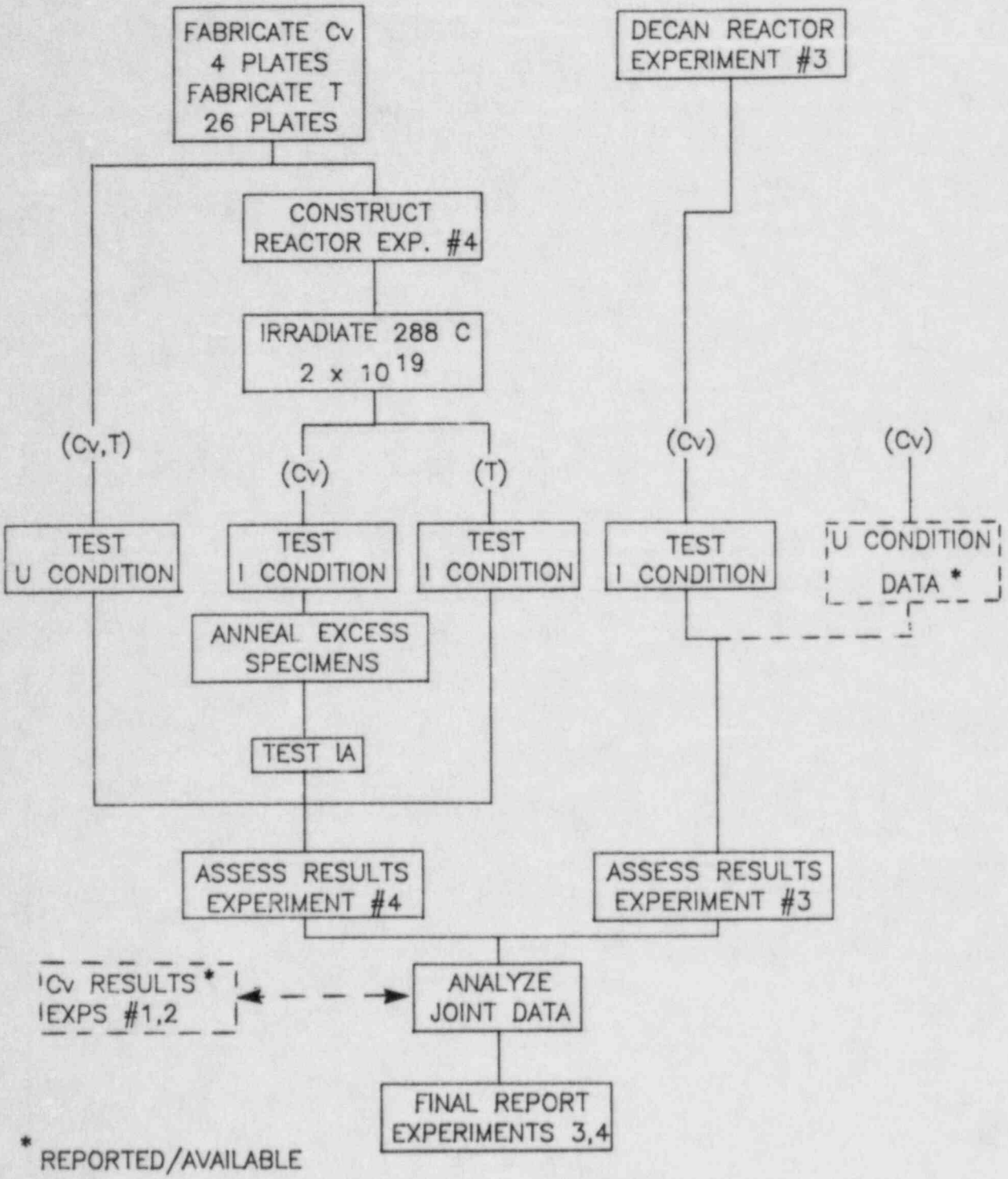

Figure 4.12 Flow Diagram for Subtask 3f: Variable Radiation Sensitivity. Capsule irradiations in this subtask are designated as Variable Radiation Sensitivity (VRS) Series.

MILESTONE STATEMENT AND SCHEDULE

Subtask 3f Variable Radiation Sensitivity

CY84

MILESTONE	FY84									FY85						FY 86	FY 87	Beyond FY87
	J	F	M	A	M	J	J	A	S	O	N	D	2	3	4			
3.f.1 Interim report, findings for VRS Series Assemblies 1 and 2					▽			△										
3.f.2 VRS Series Assembly 3																		
a. Test specimens (Cv, I-condition)					▽			△										
b. Analyze specimen/dosimetry results					▽						△							
c. Interim report, VRS-3 findings										▽		△						
3.f.3 VRS Series Assembly 4																		
a. Cut/machine specimens	▽		△															
b. Construct VRS-4			▽		△													
c. Irradiate VRS-4						▽	△											
d. Test specimens of VRS-4 (Cv, tensile)										▽			△					
e. Analyze specimen/dosimetry results									▽				△					
f. Letter report, VRS-4 findings													▽	△				
3.f.4 Final Report, Subtask 3f														▽	△			
REPORT SUMMARY								△				△		△		△		

Figure 4.13 Milestone Statement and Schedule for Subtask 3f

4.7 REFERENCES

4.1 F. A. Smidt, Jr., and J. A. Sprague, "Property Changes Resulting from Impurity Defect Interactions in Iron and Pressure Vessel Alloys," in ASTM STP 529, American Society for Testing Materials, 1973, pp. 78-91.

5.0 BUDGETARY ASSUMPTIONS

The budgetary assumptions on which this issue of the four-year plan are based are given in this chapter. The four-year program budget is given in Table 5.1.

Table 5.1 Budgetary Assumptions by Contract Year

CY	YEARLY BUDGET ($K)
1	1739
2	1630
3	1982
4	1953

The budget for each contract year (1984-1987) by task and subtask is presented in Table 5.2.

Table 5.2 Program Cost by Contract Year (CY)

TASK		SUBTASK	CY 1 1984	CY 2 1985	CY 3 1986	CY 4 1987
1. FRACTURE MECHANICS	1a.	Cladding Fracture	131	162	124	37
	1b.	C_v-K_{Ic} Correlation	140	78	58	75
	1c.	Warm Prestress	38	56	75	21
	1d.	K_{Ic} Curve Shift	110	89	116	46
	1e.	Piping Fracture	187	206	218	206
	1f.	HSST 4th Irradiation	60	0	0	0
	TOTAL	TASK 1	666	591	591	385
2. ENVIRONMENTAL CRACKING	2a.	S-N Curves	145	142	248	219
	2b.	Environmentally-Assisted Fatigue	180	136	73	0
	2c.	Crack Geometry	77	103	222	352
	2d.	Cladding Fatigue	13	36	48	50
	2e.	Mechanisms	83	80	92	79
	2f.	Total Fatigue	0	20	42	70
	2g.	Cumulative Damage	46	40	57	54
	2h.	ICCGR	23	25	18	20
	TOTAL	TASK 2	567	582	800	844
3. RADIATION SENSITIVITY	3a.	High-Temperature Annealing	103	75	117	98
	3b.	Composition Effects on Annealing	80	64	93	35
	3c.	Irradiation Damage Mechanisms	62	126	143	144
	3d.	IAR Phase 2	76	45	0	34
	3e.	Dose Rate	99	97	227	413
	3f.	Variable Radiation Sensitivity	86	50	11	0
	TOTAL	TASK 3	506	457	591	724
	PROGRAM TOTAL		**1739**	**1630**	**1982**	**1953**

NRC FORM 335 (11-81)

U.S. NUCLEAR REGULATORY COMMISSION

BIBLIOGRAPHIC DATA SHEET

1. REPORT NUMBER (Assigned by DDC)
NUREG/CR-3788 , Vol. 1
MEA-2047

4. TITLE AND SUBTITLE (Add Volume No., if appropriate)
Structural Integrity of Light Water Reactor Pressure Boundary Components
Four-Year Plan 1984-1988

2. (Leave blank)

3. RECIPIENT'S ACCESSION NO.

7. AUTHOR(S)

5. DATE REPORT COMPLETED
MONTH: April YEAR: 1984

9. PERFORMING ORGANIZATION NAME AND MAILING ADDRESS (Include Zip Code)
Materials Engineering Associates, Inc.
9700-B George Palmer Highway
Lanham, MD 20706

DATE REPORT ISSUED
MONTH: September YEAR: 1984

6. (Leave blank)

8. (Leave blank)

12. SPONSORING ORGANIZATION NAME AND MAILING ADDRESS (Include Zip Code)
Division of Engineering Technology
Office of Nuclear Regulatory Research
U. S. Nuclear Regulatory Commission
Washington, D. C. 20555

10. PROJECT/TASK/WORK UNIT NO.

11. FIN NO.
B8900

13. TYPE OF REPORT
Technical

PERIOD COVERED (Inclusive dates)
1984-1988

15. SUPPLEMENTARY NOTES

14. (Leave blank)

16. ABSTRACT (200 words or less)

This document is the first in a series intended to provide an up-to-date statement of the four-year plan for the program, "Structural Integrity of Light Water Reactor Pressure Boundary Components," which is being conducted by Materials Engineering Associates, Inc. (MEA). This program consists of engineering and research in fracture, fatigue and radiation sensitivity of nuclear structural steels and weldments and addresses many of the key uncertainties in the margin of safety in operating nuclear plants. All tasks are integrated to focus on structural integrity of LWR pressure boundary components. The approach centers on an experimental characterization of nuclear grade steels and an assessment of fracture and fatigue behavior under conditions of a nuclear environment, so investigation of irradiated materials is a key element of each task. Experimental studies are supported by analytical models and investigation of the mechanisms responsible for the observed behavior. Data developed in the program will provide the basis for recommendations for the ASME Boiler and Pressure Vessel Code and ASTM test methods, and revisions to NRC Guides.

17. KEY WORDS AND DOCUMENT ANALYSIS

17a. DESCRIPTORS

J Integral - R Curve; Low Upper Shelf; Elastic-Plastic Fracture; Nuclear Pressure Vessel Steels; Corrosion Fatigue; Stress Corrosion Cracking; Piping Steels; Load Ratio Effects; A 533-B Steel; Postirradiation Heat Treatment; Radiation Embrittlement; Notch Ductility; Embrittlement Relief; Annealing; Temperature Effects; Orientation Effects

17b. IDENTIFIERS/OPEN-ENDED TERMS

18. AVAILABILITY STATEMENT
Unclassified

19. SECURITY CLASS (This report)
Unlimited

21. NO. OF PAGES

20. SECURITY CLASS (This page)
Unlimited

22. PRICE
$

NUREG/CR-3788 Vol. 1

STRUCTURAL INTEGRITY OF LIGHT WATER REACTOR PRESSURE BOUNDARY COMPONENTS

SEPTEMBER 1984